In Vitro Prediction of Inherent Cellular Radiosensitivity

Kathleen Ann Smit

Thesis submitted in compliance with the requirements for the degree of
Master Technologiae (Biomedical Technology)
to the Faculty of Applied Sciences, Cape Technikon

Department of Biomedical Technology
Faculty of Applied Sciences
Cape Technikon

Cape Town, 2005

Supervisor: **Dr. K. Meehan**

Co-supervisor: **Dr. J.P. Slabbert**

I declare that this is my own work.

It is being submitted for the degree of

Master Technologiae (Biomedical Technology)

to the Cape Technikon, Cape Town.

It has not been submitted before for any other degree or examination

at any University of Technology or tertiary institution.

The work was undertaken at the Faculty of Applied Sciences,

Cape Technikon ;

Radiobiology Laborotory, iThemba LABS, Faure and

the Department of Radiobiology, University of Stellenbosch.

The opinions and conclusions drawn are not necessarily those of the Cape Technikon.

K Smit

Kathleen Ann Smit

19 April 2005.

Date

Acknowledgements

The completion of this manuscript brings to a close a chapter in my life made possible by the efforts of many individuals and institutions. I would like to take the opportunity to acknowledge their contribution and express my gratitude.

My sincere appreciation to the management of the Cape Technikon for awarding a bursary for the period of the study as well as to the management and staff at the iThemba LABS for providing a well equipped laboratory and access to both neutron and gamma radiation facilities.

To my Head of Department, Professor Colleen Wright and the National Health Laboratory Service (NHLS) for granting me a period of study leave to attend the congresses at which I was able to present my work as well as do the essential laboratory work.

Dr. Kathy Meehan, my supervisor, thank you for sharing your knowledge with me and for affording me the opportunity to enter the world of research. Your guidance, encouragement and continued enthusiasm exposed me to new methodologies broadening my knowledge and skills. Your insight in identifying and securing funding for this project from the National Research Fund and Thuthuka program is truly appreciated.

I am truly indebted to Dr. Kobus Slabbert, my co-supervisor, from the Radiation Biophysics Laboratory at the iThemba LABS, Faure for his unending patience and hours of teaching me the principles of radiobiology. I have learned so much from you. Your authority and excellence in the field made this project possible making your contribution greatly appreciated.

Particularly deserving of my gratitude is the Department of Radiobiology, University of Stellenbosch for allowing the use of the laboratory even in the wee hours of the morning. Here especially to Dr. Tony Serafin for your encouragement and help in making up reagents and to Dr. John Miggie for endless hours trying to help me get my head around a flow cytometer.

It was a special honour to meet Professor Nigel Crompton and my gratitude to him for sharing his valuable expertise and for finding the population of apoptotic cells!

I would like to thank Mr. Timothy Sebeela from the iThemba LABS, Mr Henry Neetling from the Faculty of Applied Sciences Cape Technikon, Mrs. Dee Blackhurst from UCT medical school and Mr. Christo Muller from the University of Stellenbosch for their technical assistance.

My colleaque-friends Ester and Jolene and my co-student Annemarie who helped in innumerable ways, providing valuable suggestions support and encouragement, thank you so much. Also to Professor Peter Wrantz my previous Head of Department, who never failed to encourage and show an interest in the work I was doing.

To my family who often found themselves without a cook, thank you for giving me space and time to think and to Stuart, who discovered his hidden housekeeping talents, my love and appreciation. To my daughters Bernadette and Michaela life is a journey not a destination, may you never stop learning.

Dedicated to the Upliftment and

Empowerment of Women

Ipsa scientia protestas est

Cicero (106-43 B.C)

Knowledge itself is power

Table of Contents

List of Figures.

List of Tables.

Abbreviations

α	alpha
β	beta
γ	gamma
$\bar{D}$	mean inactivation dose
μg	microgram
μl	microlitre
μSv/h	*microsievert per hour*
AI	apoptotic index
bp	base pairs
Bq	Bequerel
Ci	Curie
DMSO	dimethyl sulfoxide
DEVD	amino acid sequence Asp-Glu-Val-Asp
Co	cobalt
DSB	double strand break
EDTA	ethylenediaminetetra-acetic acid
FITC	fluorescein isothiocyanate
FLICA	fluorescence inhibitor of caspases
kb	kilobase
LET	linear energy transfer
LMPA	low melting point agarose
L-Q	linear quadratic
M	molar
mA	milliampere
mg	milligram
ml	millilitres
mM	millimolar
NMPA	normal melting point agarose
PAP	Papanicolaou

PARP	poly-ADP-ribose polymerase
PBS	phosphate buffered saline
PBS	phosphate buffered saline
pCi	picoCurie
PE	plating efficiency
PI	propidium iodide
PS	phosphadtidyl serine
RBE	relative biological effectiveness
rem	röntgen-equivalent-man
SF	surviving fraction
SSB	single strand breaks
TUNEL	terminal deoxynucleotidyl transferase dUTP nick end labelling
V	volts
V/cm	volts per centimetre
v/v	volume per volume

Summary

The principal objective in irradiating tumours is to permanently inhibit their reproductive ability. More than half of all malignancies are primarily treated with radiation but tumours of different histologies differ greatly in response to radiotherapy as well as individual patients displaying great variability in response to treatment. The need for reliable assays predicting tumour and normal tissue response to radiation is therefore a prime objective of clinical oncology. The requirement of such a test would be that it would relate to clinical outcome i.e. the possibility of recurrence of disease or of tumour control as well as indicating whether the treatment should be administered more aggressively or not. These are important factors that, if known, could be used as part of the treatment planning in radiotherapy and selection of best therapy modality.

The colony forming clonogenic assay has been shown to be a reliable reflection of a cells ability to maintain reproductive integrity after radiation exposure. In this study it has successfully been used to demonstrate the surviving fraction of cells but has the limitation of cells needing to process the ability to form colonies. Cells from primary tumours do not readily form colonies and may display poor anchorage making this assessment of radiosensitivity in the clinic less desirable. These data are presented together with unpublished data obtained using the micronucleus assay. Micronuclei frequency (MNF) varies in different cell types with test doses and provides a

means to rank the cell in terms of response to radiation. In normal cells a linear inverse correlation exits between MNF and cell survival. However, MNF does not rank malignant cells according to their intrinsic survival to radiation displaying a weak correlation between MNF and cell survival. This could be due to ploidy in malignant cells that affords the cell the ability to generate micronuclei and yet survive making the application of this assay as a predictive assay unreliable.

Single-cell gel electrophoresis is an assay in which cells do not have to be clonogenic or display good anchorage and was examined as a potential radiosensitivity test. The validity of the test was assessed by the exposure of cells to gamma and neutron radiation. The assay reflected these differences in a dose response manner as well as reflecting the differences in ionisation densities (high and low LET) of the two radiation modalities. The use of this assay may prove to be advantageous in predictive testing.

The tendency for a cell to undergo apoptosis is cell type specific and it is thought that the level of radiation-induced apoptosis may be a reflection of its inherent radiosensitivity. Apoptosis is time and dose dependent and varies in each biological system. The presence of apoptotic cells is measured by various endpoints depending upon which event in the apoptotic process is evaluated. Activation of executioner caspases 3 and 7 is an earlier event and was evident after irradiation. DNA fragmentation, measured by flow cytometry (TUNEL) and regarded as a late event, was induced as a function of both

gamma and neutron radiation. Morphologic examination by fluorescent microscopy revealed characteristic features of radiation-induced apoptosis reflected in a dose response manner. Furthermore, a proportionally higher percentage of neutron radiation-induced apoptosis was observed suggesting that DNA fragmentation examined morphologically may be a suitable parameter to reflect radiosensitivity.

Cell cycle analysis confirmed that CHO-K1 cells responded as expected to radiation exposure. These cells are p53-mutated and showed a build up in G_2 by 36 hours post irradiation. However by 48 hours post irradiation the cells appeared to recover returning to a near normal distribution throughout the cell cycle.

The observation of giant cell formation appears to be a feature of genomic instability in p53 mutant cells and is facilitated by radiation exposure. This process appears to provide a mechanism for double-strand DNA repair within the cells, providing a possible alternative pathway used by p53 mutant cells, including tumour cells, to survive high doses of radiation.

PARTS OF THIS THESIS PUBLISHED IN PEER-REVIEWED PUBLICATIONS

1. Smit, K.A., Slabbert, J.P. and Meehan, K. 2004. *The Intrinsic Radiosensitivity of Chinese Hamster Ovary Cells (CHO-K1) using the Clonogenic and Micronuclei Assays.* **Med.Tec.SA.** 18 (1), 3-4
2. Smit, K.A., Slabbert, J.P. and Meehan, K. 2005. *Response of CHO-K1 cells to Gamma and Neutron radiation as measured by single-cell gel electrophoresis (SCGE).* Submitted to **Mutation Research**
3. Smit, K.A., Slabbert, J.P. and Meehan, K. 2005. Morphological Evaluation of Apoptotic Response in CHO-K1 Cells. Submitted to **Med. Tec. SA**

PARTS OF THIS THESIS PRESENTED AT THE FOLLOWING CONFERENCES

1. **SAAPMB 43rd Congress:** 10-13th June 2003, iThemba LABS, Somerset West.
   Poster presentation titled: ***Response of CHO-K1 cells to Gamma and Neutron radiation as measured by single-cell gel electrophoresis (SCGE)***
   Smit, K.A., Slabbert, J.P. and Meehan, K.
2. **Stellenbosch University Academic Year Day:** 12-14th August 2003, Medical School, Tygerberg Campus
   Poster presentation titled: ***Response of CHO-K1 cells to Gamma and Neutron radiation as measured by single-cell gel electrophoresis (SCGE)***
   Smit, K.A., Slabbert, J.P. and Meehan, K.
3. **FSASP 44th Annual Conference with SASCC:** 2004 Stellenbosch
   Poster/ Oral presentation titled: ***Single-Cell Gel Electrophoresis (SCGE) as a measure of Radiosensitivity***
   Smit, K.A., Slabbert, J.P. and Meehan, K.
4. **SAAPMB 44th Congress:** 21-23rd September 2004, Johannesburg
   Poster presentation titled: ***Morphological Characterisation and analysis of ^{60}CO gamma and p(66/Be) neutron radiation-induced apoptosis in CHO-K1 cells***
   Smit, K.A., Slabbert, J.P. and Meehan, K.
5. **Environmental Mutagen Society 35th Congress:** 2-6 October 2004, Pittsburgh
   Poster presentation titled: ***Single-Cell Gel Electrophoresis (SCGE) as a measure of Radiosensitivity***
   Smit, K.A., Slabbert, J.P. and Meehan, K.

Chapter 1

Introduction and Literature Review

We stand upon the intellectual shoulders of those medical giants of bygone days and, because of the help they afford us, we are able to see a little more clearly than they were able to.

Claude Bernard, 1937

1.1 Radiation and Radioactivity

Natural or background radiation is the largest source of ionising radiation to man, with radon responsible for more than half of the average annual effective dose (Dainiak, 2002). On average an individual is exposed to approximately 3.5 millisievert (mSv) annually while occupational exposures have a recommended annual limit of 50 mSv (Van Rooyen and Meyer, 1995). The deposition of energy by ionising radiation in the target matter is a radiochemical event which leads to altered target molecules and subsequent enzymatic reactions which together determine the eventual effect of the radiation on the organism (Frankenberg-Schwager, 1989). Features of ionising radiation that influence the biological response are the quality, half-life, dose rate and dose of the radiation with dose being most significant for predicting the effect on tissue in the body (Dainiak, 2002). The biological

consequences of this absorption may however not become evident immediately and may appear years later (Finch, 1997).

Radioactivity is the alteration of the nuclei of radioactive atoms together with the emission of radiation in the form of particles or waves and can be natural or induced (Samarin, 2001). The goal of radioactivity is to produce a stable, non-radioactive element and to create equilibrium in the parts of radioactive substances. During this process there is emission of alpha particles, beta particles or gamma radiation. The absorption of energy from radiation may lead to excitation or ionisation. Excitation is the raising of an electron to a higher energy level without actual ejection of the electron. Ionising radiation is radiation that, when possessing sufficient energy, can eject one or more orbital electrons from an atom or molecule (Hall, 2000). The most important feature of ionising radiation is a localised release of a large amount of energy, which can be classified into electromagnetic or particulate radiation.

1.1.1 Electromagnetic Radiation

Gamma (γ) and x-rays are forms of high-energy electromagnetic radiation but differ by the method of production. Radioactive isotopes emit gamma rays whereas x-rays are produced extranuclearly by accelerating the electrons to high energies that impact on targets of tungsten or gold. Gamma and x-rays can also be referred to as streams of photons containing a certain amount of energy. The fundamental difference between ionising and non-ionising radiation is the size of these individual packets of energy and not the total energy involved. Heat and mechanical energy is absorbed evenly and

uniformly whereas photon energy (gamma rays) is deposited in the cells of living things unevenly and in discrete packets, capable of breaking chemical bonds and resulting in biological change. In photons the spatial distribution of the ionising events are well separated and are said to be sparsely ionising. For this reason these radiation qualities are referred to as low LET radiation as the energy transferred per unit length of the tract is low.

1.1.2 Particulate Radiation

Neutrons (*n*) possess the greatest penetrating ability and are uncharged particles that cannot be accelerated. The mass of a neutron is expressed as 1 atomic mass unit (a.m.u.) that is equivalent to 1.66×10^{-27} kg and are approximately 1840 times heavier than an electron. They are the products of nuclear reactions or as in the case of the p(66)/Be neutron beam at iThemba LABS, are produced by the reaction of 66 MeV protons on a 19.6mm thick beryllium target, resulting in maximum neutron energy of 64.15MeV (Van Rooyen and Meyer, 1995). Neutrons interact with atomic nuclei of the absorbing material and set heavier nuclear fragments, α-particles or protons into motion causing further ionisations. In biological systems neutrons deposit energy as high linear energy transfer (LET) and interact with hydrogen, which is the most abundant atom in tissue (Hall, 2000).

Protons carry a positive charge and have a mass almost 2 000 times that of an electron. When entering tissue, protons are stopped abruptly and deposit their energy and induce ionisations in an area referred to as the Bragg peak (Dainiak, 2002).

Alpha radiation (α) is nuclei of helium atoms. Emission is by the atoms of radioactive elements like radium, plutonium and uranium and is a major source of natural background radiation. Alpha particles have a large mass and due to the positive $^{(+2)}$ charge carried, interact intensely with negative electrons of atoms and particles near the track of the alpha particle are intensely ionised. Although α-radiation is unable to penetrate the outer layer of skin it is defined as a radiation of high ionisation density. The major health hazard posed by alpha radiation is the fact that particles can be ingested or inhaled exposing the internal tissue to its strong ionising effects whereas although gamma rays penetrate human skin and tissue their ionising effect (dose equivalent) is less than that of an alpha particle by a factor of 20.

Beta radiation (β) consists of electrons emitted from an atom during radioactive decay or by accelerating electrons to high energies by using a betatron or linear accelerator. This application is widely used in cancer therapy. Beta particles do not exist in the nucleus but are created in this process of decay whereby a neutron converts to a proton to emit an electron. The β^- particle carries a negative $^{(-1)}$ charge and has a lower mass than the α-particle enabling it to move faster, increasing penetrating ability in tissue, to a depth of about 5mm. The interaction of β^- particles with the negative electrons of atoms is less intense than α-particles and only ionises ±100 000 ion pairs per cm where the α-particle produces 10 million ion pairs per cm. The β+ particle is a positive electron and produces the same ionisation density as it travels through matter, however at the end of its path it will have lost most of its energy and combines with a negative electron producing two gamma

photons known as annihilation photons which in turn cause further ionisation (Van Rooyen and Meyer, 1995).

Heavy charge particles are nuclei of elements that have had some or all of the planetary electrons stripped from them. The radiation–induced effects from highly energetic, heavy, charged particles known as HZE particles are a serious challenge to astronauts during extended space travel (Kennedy *et al.*, 2004), examples of which are GeV/n iron ions or high-energy (80 Mev/u) 20 Ne^{10+} ions (Qiu *et al.*, 2003).

1.1.3 Units of Measurement

Measuring radioactivity in living organisms and matter is the basis of dosimetry. Physical measurements of individual dose are made using a whole body dosimeter and dosimeters used for evaluating dose in materials and surrounding environment.

The unit for expressing dose of radiation absorbed in living tissue is the Gray (Gy) where 1Gy = 1 joule of radiation energy absorbed per kilogram of tissue.

The measurement of ionisation in air or the unit of exposure is referred to as the roentgen (R) and has been replaced by the coulomb per kilogram. In most cases one roentgen in air is nearly equal to one gray in tissue.

The Rad (radiation absorbed dose) is defined as 100 ergs deposited per gram of tissue and has been replaced by the Gray, which is the SI unit for dose where 1 Gy = 100rads and 1 rad = 1 centigray (cGy).

The dose equivalent of a given type of radiation is expressed as Sievert (Sv), previously the roentgen equivalent in man (Rem) where 1 Sv = 100 Rem. Dose equivalent is determined by the dose of the radiation expressed in Gray, multiplied by a quality factor based of the RBE of that radiation. This means that 1 Sv is that amount on radiation, roughly equivalent in relative biological effectiveness (RBE), to 1 Gy of gamma radiation.

Equivalent doses of different types of radiation do not produce the same biological effect. This is due to the different patterns in the deposition of energy at a microscopic level. Usually the biological effectiveness of a test radiation is expressed as a comparison with 250 KeV x-rays. The relative biological effectiveness (RBE) is the ratio of the doses of the 250KeV x-rays and the test radiation needed to create an equal level of biological damage. The factors that would determine relative biological effectiveness would be the radiation quality, dose per fraction, dose rate and the biological system or endpoint used.

To measure radioactivity, the number of atoms undergoing radioactive decay must be determined per unit time and this quantity was called one Curie (Ci). This has now been replaced by the Bequerel (Bq) and represents that quantity of the element in which there is one atomic disintegration per second. (1 Bq= 2.7×10^{-11} Ci; 1 Ci = $3,7 \times 10^{10}$ Bq or 37 GBq)

Ionising radiation beams are characterised in terms of their linear energy transfer (LET), which refers to the energy transferred per unit length of the track in the absorbing material (Dainiak, 2002). The unit for measuring this

quantity is kiloelectron volt per micrometer (keV/μm) of unit density material.

1.1.4 Absorption of Radiation

Ionising radiation displaces electrons from atoms and changes their physical state causing the atoms to become electrically charged or ionised. All charged particles are directly ionising, indicating that they are able to disrupt the atomic structure of the matter through which they pass and bring about chemical and biological changes. Electromagnetic radiations (x- and γ-radiation) are indirectly ionising, as they do not produce the damage to the matter through which they pass themselves but rather deposit their energy in such as way as to produce fast moving charged particles.

When radiation is absorbed in biological matter it may interact with the atoms (direct action) of the target itself that in turn become ionised and lead to biological change. Alternately the radiation may interact with other atoms in the cell, often water, (indirect action) producing free radicals that are able to damage the critical targets.

Neutrons predominantly interact with the nuclei of the absorbing material. Protons set in motion by the absorption of neutrons are heavy, densely ionising particles, in contrast to the light, negatively charged particles set in motion by gamma absorption. The density of ionisation tracts for neutrons account for the differences in biological effects as well as the fact that direct action of radiation is the dominant feature of neutron radiation.

1.2 Biological Effects of Radiation

The response of an organism to the products of radiation is approximately 10^{-6} seconds to many years following the exposure.

R.M.Sutherland, 1987.

1.2.1 Deterministic and Stochastic Effects

Ionising radiation causes various types of damage to the DNA molecule and human survival is dependent on the integrity of the genome. This is why there is an immediate response to any cellular DNA damage by numerous biochemical pathways whose purpose it is to repair damage and minimise mutations (Li *et al.*, 2001). When this damage is not repaired effectively it may cause the defective cell to loose its ability to reproduce, or it may result in the cell remaining viable proceeding to the next mitotic division effectively passing on the mutation to its progeny. These two pathways have profound consequences. When an organism looses a significant amount of cells, the organ affected by the loss may show impaired function. The dose causing this harm has to be above a certain threshold dose and when this is reached the probability of harm increases and the severity of harm increases with dose above this point. This is defined as a deterministic effect. If however the cell survived the dose but retained a mutation the probability of carcinogenesis and hereditary effects increases with dose but the severity of the cancer or

hereditary defect is not dose-related. This effect is referred to as stochastic.

1.2.2 Radiation and The Cell Cycle

In order to procreate a cell undergoes cell division best described as a cycle of events through which it passes and is repeated by each successive generation (Figure 1.1). Some cells do not divide at all when mature while others complete a cycle every 16 to 24 hours (Martinez, 1995). Briefly, during interphase the quantity of DNA in the nucleus doubles as each chromosome replicates itself exactly. Prophase begins with a thickening of the chromatin and is completed by each chromosome possessing a centromere from which the arms of the chromosomes extend as well as the assimilation of the nuclear-plasm and cytoplasm. During metaphase the chromosomes centralise and the centromeres divide enabling the chromosomes to migrate to the poles during anaphase. Once at the poles, the chromosomes begin to uncoil during telophase with the reappearance of the nuclear membrane and nucleoli.

After every division telomeric DNA is lost. After 40 to 60 divisions the telomeres in human cells shorten resulting in vital DNA sequences being lost. At this point the cell cannot divide anymore and become senescent. Cancer cells have the ability to evade this problem by activating the enzyme telomerase (Sun *et al.*, 2004). Telomerase is a reverse transcriptase and continuously rebuilds the chromosome end, immortalising the cell. Cells in tissue culture are able to divide beyond the normal limit as a result of telomere stabilisation and the activity of telomerase. Practically all human tumour cell lines and about 90% of human cancer biopsy specimens, exhibit telomerase

activity that is not present in normal cells (Roninson, *et al.*, 2001).

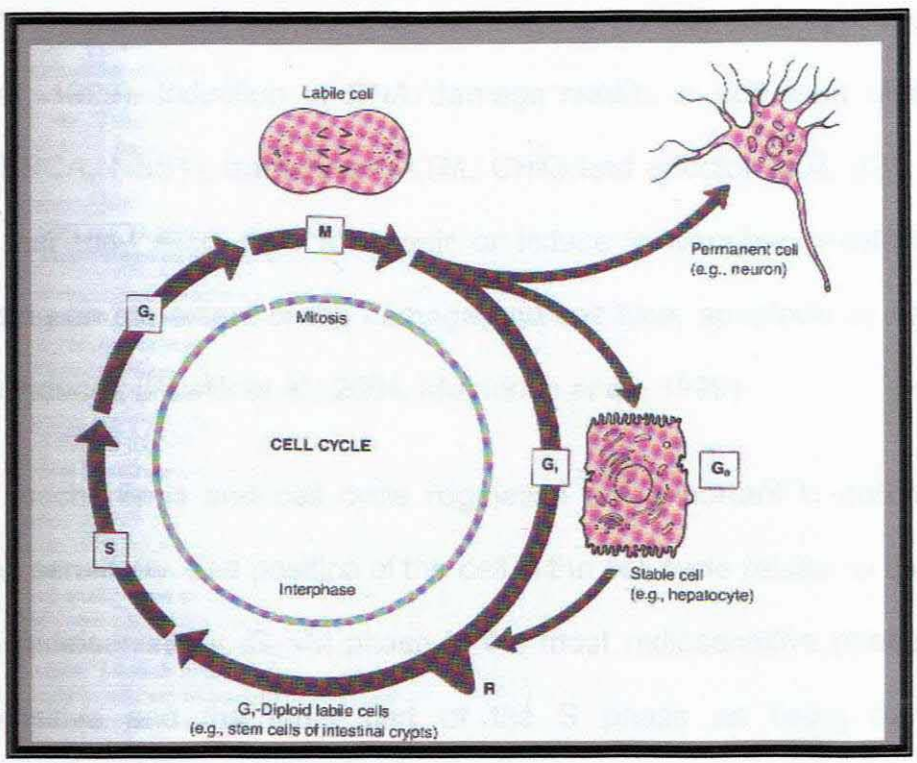

Figure 1.1: *The cell cycle. Labile cells undergo continuous replication. In G_1 they perform their own specialised activity and if they pass the restriction point (R) they are destined to a new round of division. A phase of DNA synthesis (S) follows leading to a gap phase G_2 and then on to mitosis. Stable cells take up their specialised functions and do not undergo mitosis unless stimulated (G_0). Other permanent cells become terminally differentiated and cannot re-enter the cell cycle. (Rubin and Faber, 1987,in Essential Pathology, 2nd Ed)*

As a cell progresses through the cell-cycle checkpoints it has to ensure that all biochemical events are completed before progression to the following phase is permitted. The tumour suppressor protein, p53 is involved in DNA damage cell cycle checkpoints and its importance in tumorigenesis is emphasised by the fact that this gene is mutated in about 50% of human cancers (Jongmans

and Hall, 1999).

Mammalian cells undergo cell cycle arrest when exposed to ionising radiation and activate numerous pathways to maintain the genetic integrity (Jongmans and Hall, 1999). Induction of DNA damage results in activation of sensor (RAD, BRCA, NBS1), transducer (ATM, CHK) and effector (p53, p21, CDK) genes that may allow time for repair or induce irreversible growth arrest. Depending on the extent of the damage and cell type, apoptosis or necrosis may be induced (Pawlik *et al.*, 2004, Mustonen *et al.*, 1999).

Repair mechanisms and cell cycle regulation are important in determining radiation sensitivity. The position of the cell in the cell cycle relates to the cell's relative radiosensitivity, G_2 -M phase is the most radiosensitive phase, G_1 – less sensitive and the latter part of the S phase as being the most radioresistant.

1.2.3 Radiation Induced DNA Strand Breaks

Two systems are vitally important for genome integrity, DNA repair and apoptosis. Cells unable to repair DNA accumulate damage and those defective in apoptosis survive with excess damage and replicate damaged DNA causing mutations leading to carcinogenesis (Bernstein *et al.*, 2002).

The amount of unrepaired DNA double strand breaks in cells has been correlated to cell killing in eukaryotic cells (Frankenberg-Schwager, 1989), however other authors reported no correlation (Olive *et al.*, 1994).

In a study conducted by Schwartz and co-workers (1988), single strand DNA

induction and repair was not found to be an important factor in the radiation response of human tumour and normal cell lines but the rate at which DNA double strand breaks are repaired was a significant contribution to radioresistance.

Radiation deposits energy in the target within about 10^{-19} and 10^{-14} seconds and in eukaryotic cells results in each gray (1 Gy) absorbed producing about 10^5 ionisations per cell (Frankenberg-Schwager, 1989), which cause about 2000 single strand breaks and about 40 double strand breaks in the DNA as well as other DNA damage (Lewanski and Gullick, 2001). Double strand breaks (DSBs) are the most critical effect of ionising radiation. These are repaired with the least efficiency and are best correlated with cell killing and mutagenesis. Densely ionising, high linear energy transfer (LET) types of radiation (fast neutrons, alpha particles and heavy ions) are biologically more effective than low-LET radiation (gamma rays, X-rays and electrons). Compared with low-LET radiation, neutrons are more lethal per unit dose and induce more chromosome aberrations. It is proposed that the slow repair of double strand breaks plays an important role in neutron radiation lethality (Mustonen *et al.,* 1999). This is verified by the energy deposition pattern of high-LET radiation which is thought to result in clustering of a substantial number of damaged sites in a small volume of cellular DNA, called locally multiply damaged sites (LMDS) (Mustonen *et al.*, 1999). Therefore the type of radiation and the energy of the radiation, decides the nature of the interaction with the absorbing biological matter.

1.2.4 Radiation Induced Chromosome Aberrations

Ionising radiation is one of very few agents that induce direct DNA breakage (Albertini *et al.*, 2000; Sachs *et al.*1997), often resulting in double strand breaks which are known to lead to chromosome-type and chromatid-type chromosomal aberrations (Bryant, 1997). Besides double strand breakage, these structural aberrations may be induced by other mechanisms like the replication of DNA on a damaged template or the inhibition of DNA synthesis. When the cell is irradiated early in interphase, before duplication of chromosomal material, a break in a single strand of chromatin is induced. This will cause the replicating chromosome to duplicate itself during the DNA synthesis (S) phase that follows and replicate the break. This aberration is evident at the next mitosis as an identical break in the corresponding area of a pair of chromosomes. If the dose of radiation is given later in interphase i.e. after DNA replication and the chromosome consists of two strands of chromatin, the aberration produced is the referred to as a chromatid aberration, as the break occurs in a single chromatid arm after replication, leaving the opposite arm of the same chromosome undamaged.

When there is damage to the chromosomal sub-structure or the mitotic spindle the cell may undergo abnormal division resulting in a change in the number of chromosomes and is described as a numerical aberration. Both structural and numerical aberrations are visualised by metaphase spreads or by using fluorescence in situ hybridisation (FISH) where whole chromosome painting (WCP) is a means of analysing aberration formation to quantify radiation induced chromosomal changes (Knehr *et al.*, 1996). Cytogenetic

methods used to study cells during metaphase have shown a close correlation between chromosome aberrations and cell killing (Jones *et al.*, 1994).

Micronuclei are chromatin masses appearing in the cytoplasm resembling nuclei. These remnants occur as a result of intact chromosomes or chromosome fragments lagging behind at anaphase. When present in cells micronuclei represent structural and/or numerical chromosome aberrations occurring during mitosis (Fenech *et al.*, 1999; Leal-Garza *et al.*, 2002).

Types of chromosomal aberrations are numerous but formation of dicentrics; rings and anaphase bridges are lethal formations. A dicentric involves an interchange between two separate chromosomes after a break occurs in each early in interphase, and the sticky ends of the separate chromosomes join (Figure 1.2A). This is then replicated in S phase, resulting in a chromosome with two centromeres (dicentric) and a fragment with no centromere (acentric). The formation of a ring occurs after a break is induced in each arm of a single chromatid and the sticky ends rejoin to form a ring (Figure 1.2B). An anaphase bridge results from a break in both chromatids of the same chromosome after they have replicated. The sticky ends then rejoin incorrectly to form a sister union. At anaphase when the two sets of chromosomes move to opposite poles the section of chromatin between the two centromeres is stretched across the cell between the poles, preventing the separation into two new daughter cells, resulting in the reproductive death of the cell (Figure 1.2C).

Two important non-lethal chromosomal changes are symmetric translocations

and small deletions. A symmetric translocation is a break in two chromosomes where broken ends are exchanged between the two. Translocations are associated with human malignancies. Small deletions result from two breaks in the same arm of the same chromosome, leading to loss of genetic information. This loss may translate into the deletion of a tumour suppressor gene culminating in malignant change (Figure 1.2, insert).

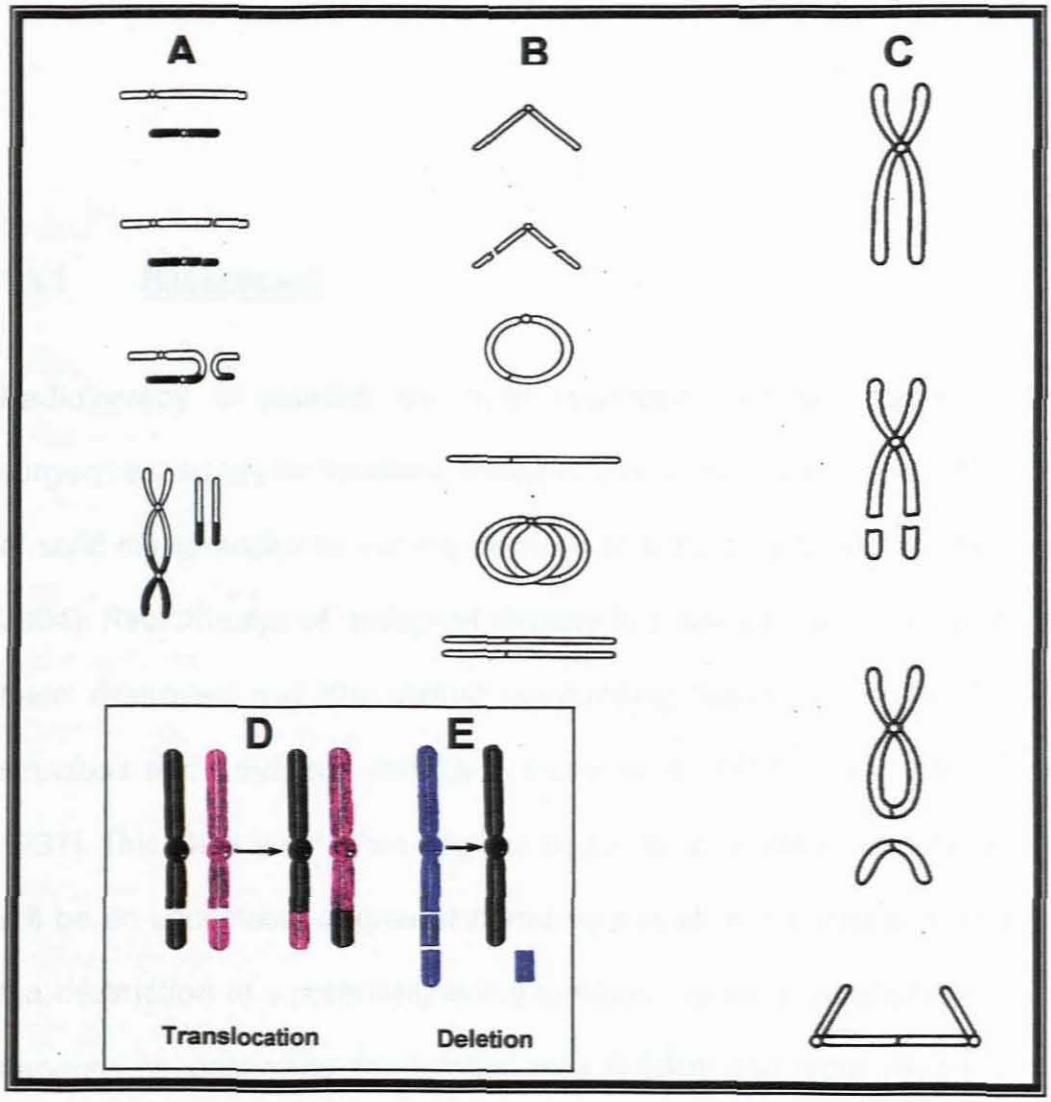

Figure 1.2: *Diagram showing chromosome aberrations induced by radiation.* ***A)*** *The steps in the formation of a dicentric induced prior to replication. The break occurs in two separate chromosomes with the sticky ends joining forming an interchange between the two. After replication one chromosome has two centromeres.* ***B)*** *Ring formation occurs when breaks in both arms of the same chromosome are induced. The sticky ends join and a ring forms.* ***C)*** *An anaphase bridge occurs post replication where breaks occur in each chromatid of the same chromosome. Incorrect joining results in a sister union. At the next anaphase the accentric fragment is lost while the centromere goes to each pole the chromatid will be stretched between the poles. Daughter cells cannot separate and this aberration may be lethal.* ***Insert****: Radiation produces a break in two different prereplicating chromosomes resulting in a* ***D)*** *translocation or a deletion* ***E)****. This is not necessarily lethal but may activate an oncogene (Hall, 2000: 5th ed. Philadelphia: Lippincott, Williams and Wilkins).*

1.3 Radiotherapy and Radiosensitivity

Improvements in the therapeutic ratio can come from either reduction in normal tissue injury or an increase in the effectiveness of tumor treatment.

Simon Kramer, MD

1.3.1 Background

Radiotherapy is possibly the most important treatment for cancer after surgery, especially for localised diseases and is used to treat virtually all types of solid malignancies to varying degrees of success (Pawlik and Keyomarsi, 2004). Radiotherapy of malignant disease is successful when the tumour has been destroyed and the normal surrounding tissue has suffered minimal structural and functional damage (Levine *et al.*, 1995; Rubin and Siemann, 1987). This ideal is not often attained and a compromise exists whereby there will be an acceptable degree of permanent residual damage in exchange for the destruction of a potentially lethal tumour. The radio-curability of a tumour depends on destroying the tumour cells quicker and more readily than the normal tissue for the equivalent dose absorbed or to focus the radiation source in such a way as to differentiate between the dose absorbed by the tumour and that absorbed by normal tissue.

Radiation kills cells and it is established that as the dose increases, more cells are destroyed leading to a calculated dose that can completely eradicate the tumour. The normal tissue and organs that have different tolerance doses however drive this curability. If patients that would show severe reactions to treatment could be identified the benefits would translate in an increase in treatment dose to others that could potentially lead to a 20% increase in tumour control rates for those levels of tolerability currently accepted (West and Hendry, 1992).

Tumours of different histologies differ in response to radiotherapy (West, 1995). Lymphomas and seminomas respond well but others such as melanomas and osteosarcomas appear more radioresistant. It has also become apparent that the intrinsic radiosensitivity of the cell plays a role in this radioresponsiveness of the tumour. Fertil and Malaise (1981) showed that there is a correlation in the ability to control certain types of tumours and the radiosensitivity of cell lines derived from these different tumour types. Deschavanne and Fertil (1996) built a scale of radiosensitivity according to cell type and found consistent differences in radiosensitivity between human cell types *in vitro*. Studies on animal tumour models have shown that by measuring the surviving fraction at 2 Gray (SF_2) *in vitro*, the response to irradiation *in vivo* can be predicted. This naturally led to the hypothesis that individual tumour radiosensitivity could predict response to radiotherapy. Cervical tumours treated with radiotherapy alone were followed up for a 2-year period and measurements of SF_2 were shown to be predictive for patient response (West *et al.*, 1993). Tumour radiosensitivity was classified as

radiosensitive ($SF_2 < 0.40$) and those displaying radioresistance ($SF_2 > 0.40$) as measured using a soft agar clonogenic assay. Patients whose tumours displayed SF_2 values below the average of 0.40 had substantially higher local tumour control and survival than those whose tumours were found to be more radioresistant.

1.3.2 Radiation Cytology

Radiotherapy is the non-surgical treatment of choice for all stages of cervical carcinoma (Levine *et al.,* 1995). Radiation may be effective in the treatment of tumour cells but results in changes in the epithelium which may be transitory (acute) or which may persist (chronic) for the lifetime of the patient. The cytomorphological features of the acute changes associated with radiation are large squamous epithelial cells or macrocytes, vacuolisation that may contain ingested neutrophils, cells or debris, severe inflammatory response with epithelial regeneration and repair. Chronic radiation changes are the result of DNA damage induced by radiation in the benign mitotically active cells and may persist for years or even be present for life. These changes are similar to the acute changes with the presence of macrocytes that take on pleomorphic cell shapes, however the inflammation and repair usually disappears.

Cytology provides a useful mechanism for detecting persistent or recurrent cancer in patients who were diagnosed with cervical carcinoma. In addition the detection of post radiation dysplasia particularly within three years of radiation, may indicate a poor prognosis. The occurrence and progression of post radiation dysplasia can be radiation-induced and/or due to human

papilloma virus (HPV) tumourigenesis which carries a poor prognosis (Gupta *et al.*, 1982).

Radiation-induced macrocytic changes in both epithelium and mesenchymal cells can mimic those seen in HPV infections, carcinoma and even sarcoma (Figure 1.3). Bi-nucleation and multinucleation are common with increase in cytoplasmic and nuclear volumes retaining the nuclear-cytoplasmic ratio. Papanicolaou smears taken on follow up of cervical cancers often show a linear decline in the malignant cell population pending the end of radiotherapy (Ng, 2003). This decline in numbers is evident within a week after commencement of therapy and usually disappears completely after a month of completion of therapy.

Assessment of smears 6 to 8 weeks post therapy providing no evidence of a good radiation reaction may be a poor prognostic factor (DeMay, 1996). Cytological parameters of poor host response are the presence of haemolysed red blood cells and necrotic polymorphonuclear leucocytes that may indicate severe local tissue injury and lack of repair suggesting poor treatment outcome. By contrast, infiltration of lymphocytes, stromal cells and multinucleated giant cells suggest an ongoing healing process. It has been demonstrated histologically that an infiltration of Langerhans cells after radiotherapy is associated with a significantly better 5-year survival rate (Nakano *et al.*, 1989).

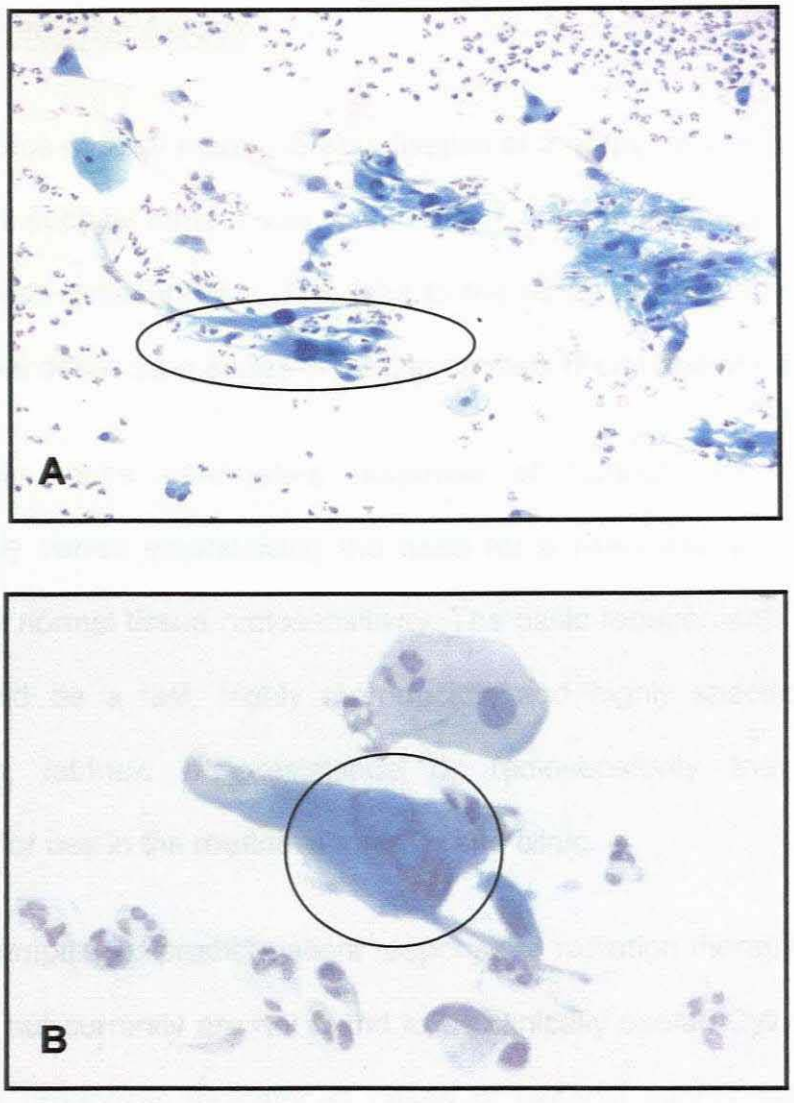

Figure 1.3: *Photomicrographs of Papanicolaou stained cervical smears taken from a 65-year-old patient who presented with a Stage IIIb carcinoma and treated with radiotherapy. The cytomorphologic features of the cells in* ***A*** *(x100 magnification) are easily confused with those of a sarcoma. Note the significant inflammatory infiltrate in the background of the smear. In* ***B*** *(x400 magnification) extensive vacuolisation and giant cell (macrocyte) formation evident after radiotherapy. An acute inflammatory response is present in the background of the smears.*

1.3.3 Predictive Assays

In the absence of tailor made individualisation of therapy, radiotherapists have used factors such as tumour size, tissue origin, differentiation and proliferation rate to access radiocurability. This lead to the range of prescribed estimated tumour lethal doses for a series of human cancers (Fertil and Malaise, 1981).

Even within these parameters response of tumours to treatment is considerably varied emphasising the need for a rapid assay for assessing tumour and normal tissue radiosensitivity. The basic requirements for such an assay would be a fast, highly reproducible and highly specific assay for determining intrinsic radioresistance or radiosensitivity that could be applicable for use in the routine laboratory and clinic.

Assays attempting to predict patient response to radiation therapy have been developed but currently are not found to be clinically useful. Cytology can be used as a prognostic indicator in cases of cervical cancer but only after radiation has been administered. The need to have knowledge of the cellular response of the tumour as well as the normal tissue to radiation prior to radiotherapy is required.

Broadly, predictive assays can be categorised into those assessing cellular radiosensitivity and those that assess factors influencing the cells response to radiation (Peters *et al.,* 1986; Peters and McKay, 2001). These have been applied to assess the effects of human exposure to ionising radiation and other clastogenic agents and the following have been selected for discussion.

The clonogenic survival assay is thought to be the gold standard as it measures the reproductive ability of the cell that cannot be assessed by apoptosis or micronuclei formation. Micro-nucleation is a cellular response to DNA damaging agents.

The alkaline version of the single cell gel electrophoresis assay or comet assay is also a genotoxic endpoint, detecting DNA damage. At pH > 13 single and double strand breaks as well as alkaline labile sites are expressed.

Apoptosis is also a cellular response to DNA damage. Spontaneous apoptosis reflects chromosomal instability (Duchaud *et al.*, 1996) and radiation induced apoptosis is a form of radiation-induced cell death. As chromosomal instability increases so does radiosensitivity (Guo *et al.*, 1998).

Assessment of radiation-induced apoptosis using flow cytometry reveals information regarding the redistribution of cells in the cell cycle and provides added insight into the cellular kinetics of the biological system evaluated.

1.3.3.1 The Colony Assay

Clonogenic assays have been used to measure the clonogenic cell survival and to quantify the cellular response to anticancer agents as well as radiation (Puck and Marcus, 1956). This is expressed as microscopic colonies formed by the replication of a single cell which when counted give an indication of the reproductive integrity of that cell. Cells used in these assays are usually taken from established cell lines and not directly from human tumour biopsy specimens as these do not grow readily and have a poor plating efficiency.

The cell survival curve reflects the relationship between dose and the percentage of cells surviving that dose. The surviving cell can be described as one that has retained its reproductive integrity and is able to proliferate indefinitely to produce a large clone or colony and is therefore referred to as clonogenic. Reproductive death is the end point measured with cells cultured *in vitro*. This is of relevance to tumour radiotherapy, as the successful elimination of the tumour only needs to render the cells incapable of division and metastasising. More radio-resistant cell types will display higher levels of survival than radiosensitive cell lines.

1.3.3.2 Micronuclei (MN)

Micronuclei (MN) arise in cells from chromosomal fragments that lag behind in anaphase and are excluded in the daughter nuclei. The cytokinesis-block micronucleus assay has been a method suggested for the prediction of radiosensitivity (Fenech and Morley, 1985; Lee *et al.*, 2000). It is generally thought that radiosensitive cell lines are more likely to develop radiation - induced micronuclei and that these micronuclei are an expression of the cells radiosensitivity.

Adding Cytochalasin B inhibits the formation of the microfilament ring that narrows the cytoplasm between the daughter nuclei blocking the cells during cytokinesis (Fenech *et al.*, 2003). This helps maintain a stable MN frequency in cultures with different kinetics. The assay is easy and fairly rapid to perform and holds the distinct advantage that the cells do not have to be clonogenic.

1.3.3.3 The Single-Cell Gel Electrophoresis Assay (SCGE)

This assay, also called the comet assay, was originally developed in 1984 by Östling and Johanson, and under neutral electrophoretic conditions could detect DNA damage, particularly DNA double strand breaks. Singh *et al.*, (1988) modified the technique and introduced an alkaline version (pH>13) allowing detection of single strand breaks and alkali-labile sites. The greatest advantage is that data can be collected at the level of the individual cell and a small sample size is required. The technique has become a method for studying DNA damage induced by radiation. It is a sensitive and rapid assay, able to identify different types of strand breaks in individual cells. The DNA damage can also be quantified on an individual cell basis using the parameters of tail length, tail moment and tail inertia. The last two express migrations of the various DNA fragments forming the tail and their relative amounts of DNA. DNA repair capacity of individual cells after radiation exposure can be analysed, leading to the potential for estimation of individual radiosensitivity. The damaged cells are visualised and scored by the DNA migration from the nucleus forming the comet shape, hence the name 'comet assay.

1.3.3.4 Apoptosis

Apoptosis has become a subject of interest to those involved in the treatment of tumours. It is a process of programmed cell death by which the cell is able to trigger its own death and is controlled by gene expression. This can be induced in response to damage by radiation or other cytotoxic agents.

Programmed cell death is a range of death cascades with classical apoptosis at one end extending to necrosis at the other (Ashe and Berry, 2003). A multitude of highly regulated, interconnected pathways exist between these two points that can be subdivided according to various classification systems such as the intrinsic and extrinsic, mitochondrial and death receptor, p53 dependent and independent and caspase dependent and independent pathways. Each of these pathways begins with an initiation of apoptosis that leads to a common commitment phase. Beyond the point of commitment there is a divergence of execution phases.

It is thought that the tendency of a cell to undergo apoptosis when exposed to radiation could be a reflection of its radiosensitivity (Zhivotovsky *et al.*, 1999). Apoptosis is a biological endpoint and when determining the response of tissue to radiation therapy, the most important endpoint for radiosensitivity is cell death (Crompton, 1998). Using the terminal deoxynucleotidyl transferase (TdT) dUtp nick end-labelling (TUNEL) assay on paraffin-embedded tissue Sheridan *et al.* (1999), concluded that a high apoptotic index in adenocarcinomas of the cervix might reflect a high radiosensitivity leading to a favourable prognosis. In squamous carcinoma of the cervix however, a high apoptotic index may indicate high hypoxia and not high radiosensitivity possibly leading to a poor prognosis.

Cells from haematopoietic tumour lines can progress through the entire apoptotic process in 4-6 hours after treatment, whereas in those of epithelial or fibroblastic origin apoptosis can be induced after 24 hours with a much longer duration (Del Bino *et al.*, 1999). The calculated apoptotic index (AI)

taken as a snapshot of this event does not truly reflect the total percentage of apoptosis in a studied cell population. Smolewski *et al.* (2002) proposed to estimate the cumulative apoptotic index (CAI) using a FLuorescent Inhibitor of CAspases (FLICA). This labels the cell with FLICA and arrests the process of apoptosis, which would normally culminate in the disintegration of the cell. The CAI is then measured at predetermined time points by flow cytometry.

Relatively early in the apoptotic cascade phosphatidylserine (PS) relocates from the inner to the outer phospholipid layer of the cell. Annexin V binds to the externalised phosphatidylserine and the number of apoptotic cells in a certain population can be assessed using a flow cytometer. With the addition of propidium iodide this assay enables the discrimination between apoptotic and necrotic cells (Hertveldt *et al.*, 1997).

Caspase activation especially the effector caspases 3 and 7 are thought to execute the apoptotic program (Zörnig *et al.*, 2001). Molecular detection for the active form of caspases 3/7 can be measured by flow cytometry using a suitable substrate linked to a fluorescent complex (Ormerod, 2001). Alternately, as in this study, the complex can be read by a spectrofluorimeter where the amount of fluorescence is proportional to the amount of caspase activity present in the sample.

Molecular analyses of apoptosis are specific to certain biochemical changes occurring in the apoptotic cell. A microscopic evaluation should therefore accompany any study, as the morphologic appearance of apoptotic cells is specific and distinctive (Allen *et al.*, 1997; Vermes *et al.*, 2000; Ormerod, 2002).

1.4 Aims of the Study

Radiotherapy is central to the management of a number of human cancers, either as an adjuvant or primary treatment modality (Ng, 2003). The knowledge that cellular radiosensitivity and patient response to radiation varies significantly has led to a collective attempt to develop predictive assays. This term is defined as a laboratory test capable of predicting the response of tumor and/or normal tissue to radiotherapy on the basis of their radiobiological characteristics (Peters and McKay, 2001). The benefits of this understanding would assist in choosing the best therapy modality and resolve current uncertainties in the planning phase of radiotherapy. To relate the predictive test to clinical outcome would address the lack of knowledge regarding recurrence of disease, tumor control and whether the tumour requires more aggressive treatment by increased dose.

Treatment of radioresistant disease has seen the introduction of particle therapy and high cost carbon ion facilities. The knowledge and understanding of chemotherapy versus/combined radiotherapy, new particle types e.g. protons versus photons and photons versus neutrons/carbon ions would be enormously beneficial. Furthermore an independent test would bring better rational to clinical trials as the patient data accumulated present too many variables.

At present the radiotherapy-planning regime depends on the relative radiosensitivity of the tumour in relation to the dose limiting normal tissue. Most predictive assays on normal tissue have assessed radiosensitivity of

skin fibroblasts and lymphocytes (Dickson *et al.*, 2002; Dikomey *et al.*, 2003; Ozsahin *et al*, 1997).

Repair, apoptosis and micro nucleation are cellular responses to damage induced by radiation that ultimately affects clonogenicity. An understanding of the inter relationship between assays and cell survival may lead to better appreciation of the mechanisms underlying cellular response to radiotherapy. Assays requiring high doses are clinically irrelevant as most treatment is administered at low dose per fraction typically 2 Gy for gamma and 1.1 –1.7 Gy for neutron radiation.

In view of these limitations this study aimed to validate and standardise assays for assessing radiation-induced damage using various endpoints. Chinese hamster cell lines (CHO-K1, CHO-WBL and CHL) are commonly used around the world in genotoxicity tests for cytogenetic damage (Hu *et al.*, 1999). These are adherent, non-haematopoietic, benign mammalian cells and the Chinese hamster ovary cell line CHO-K1 has been used throughout this study.

High linear energy transfer (LET) radiation induces greater damage than low LET radiation. The unique opportunity to assess neutron radiation-induced damage has been made possible due to the close proximity to the iThemba Laboratory for Accelerator Based studies, Somerset West. The response of CHO-K1 cells to graded doses 0, 2, 4, 6, 8, 10 and 12 Gy of ^{60}Co γ-radiation as well as to doses of 0, 1, 2, 3, 4, 6 and 8 Gy p(66/Be) neutron radiation allowed both quantitative and qualitative assessment of the different

endpoints. The aims of the study were as follows:

- To determine CHO-K1 cells' ability to retain reproductive integrity in response to 0,2,4,8 and 12 Gy ^{60}Co γ-radiation using the clonogenic assay. To investigate the relation between micronuclei and surviving fraction.

- To evaluate initial damage induced by ^{60}Co γ- and p(66/Be) neutron radiation using the Comet assay. To establish a dose response curve as well as demonstrate the ability of the end point to differentiate between the two radiation modalities.

- To evaluate apoptosis as a cellular response to ^{60}Co γ- and p(66/Be) neutron radiation assessed using fluorometric, flow cytometric and morphological classification. To establish a dose response curve and relative biological effectiveness for apoptosis. To validate each endpoint, Caspase 3/7 activity, DNA fragmentation and morphological characterisation of apoptosis in terms of the ability of each to differentiate between the two radiation modalities. To evaluate the effect of radiation on the distribution of cells in the cell cycle.

- To standardise the above endpoints in terms of the adherent CHO-K1 cell line.

- To evaluate these endpoints as potential predictive assays *in vitro* for patient response to radiotherapy and to investigate the possibility of introducing such assays into the clinical setting.

1.5 References

Albertini, R.J., Anderson, D., Douglas, G.R., Hagmar,L., Hemminki,K., Merlo,F., Natarajan, A.T., Norppa, H., Shuker, D.E.G., Tice, R., Waters, M.D. and Aitio, A. 2000. IPCS guidelines for the monitoring of genotoxic effects of carcinogens in humans. **Reviews in Mut.Res. (Special issue)** 463(2), 111-172

Allen, R.T., Hunter, W.J., Agrawal, D.K. 1997. Morphological and Biochemical Characterization and Analysis of Apoptosis. **J. Pharm. and Toxicol. Meth.** 37, 215-228

Ashe, P.C. and Berry, M.D. 2003. Apoptotic signalling cascades. **Prog. in Neuro-Psychopharm. Biol. Psych.** 27, 199-214

Bernstein, C., Bernstein, H., Payne, C.M. and Garewal, H. 2002. Review. DNA repair/pro-apoptotic dual-role proteins in five-major DNA repair pathways: fail-safe protection against carcinogenesis. **Mutat. Res.** 511, 145-178

Bryant, P.E. 1997. DNA damage, repair and chromosomal damage. **Int. J. Radiat. Biol.** 71(6), 675-680

Crompton, N.E.A. 1998. Programmed cellular response to ionising radiation damage. **Acta Oncologica** 37, 129-142

Dainiak, N. 2002. Haematological consequences of exposure to ionising radiation. **Exper. Hemat.** 30, 513-528

Del Bino, G., Darzynkiewicz, Z., Degraef,C., Mosselmans, R., and Galand, P. 1999. Comparison of methods based on Annexin V binding DNA content or TUNEL for evaluating cell death in HL-60 and Adherent MCF-7 cells. **Cell Prolif.** 32, 25-37

DeMay, R.M. 1996. Radiation Cytology. In: **The Art and Science of Cytopathology.** ASCP Press:Chicago, 118-120

Deschavanne, P.J. and Fertil, B. 1996. A review of human cell radiosensitivity *in vitro.* **Int.J. Radiat. Oncol. Biol. Phys.** 34 (1), 251-266

Dickson, J., Magee, B., Stewart, A. and West, C.M.L. 2002. Relationship between residual radiation-induced DNA double-strand breaks in cultured fibroblasts and late reactions: a comparison of training and validation cohorts of breast cancer patients. **Radiother. Oncol.** 62, 321-326

Dikomey, E., Borgmann, K., Brammer, I. and Kasten-Pisula,U. 2003. Molecular mechanisms of individual radiosensitivity studied in normal diploid human fibroblasts. **Toxicology** 193, 125-135

Duchaud, E., Ridet, A., Stoppa-Layonnet, D., Janin, N., Moustacchi, E. and Rosselli, F. 1996. Deregulated apoptosis in ataxia telangiectasia: Association with clinical stigmata and radiosensitivity. **Cancer Res.** 56 (6), 1400-1404

Fenech, F. and Morely, A.A. 1985. Solutions of the kinetic problem in the micronucleus assay. **Cytobiol.** 43, 233-246

Fenech, M., Chang,W.P., Kirsch-Volders,M., Holland.N,. Bonassi,S. and Zeiger,E. 2003. HUMN project: detailed description of the scoring criteria

for the cytokinesis-block micronucleus assay using isolated human lymphocyte cultures. **Mut. Res.** 534, 65-75

Fenech, M., Holland, N., Chang, W.P., Zeiger, E. and Bonassi,S. 1999. The HUman MicroNucleus Project – An international collaborative study on the use of the micronucleus technique for measuring DNA damage in humans. **Mut. Res.** 428, 271-283

Fertil, B. and Malaise, E. 1981. Inherent cellular radiosensitivity as a basic concept for human tumour radiotherapy. **Int. J. Radiat. Oncol. Biol. Phys.** 7, 621-629

Finch, S.C. 1997. Leukemia: lesions from the Japanese experience. **Stem Cells.** 15 (Suppl 2), 135-139

Frankenberg-Schwager,M. 1989. Review of repair kinetics for DNA damage induced in eukaryotic cells *in vitro* by ionising radiation. **Radiother.Oncol.** 14, 307-320

Guo, G.Z., Sasai, K., Oya, N., Takagi,T., Shibuya, K. and Hiraoka, M. 1998. Simultaneous evaluation of radiation-induced apoptosis and micronuclei in five cell lines. **Int. J. Radiat. Biol.** 73(3), 297-302

Gupta,S., Gupta, Y.N. and Sanyal, B. 1982. Radiation changes in vaginal and cervical cytology of the cervix uteri. **J.Surg. Oncol.** 19, 71-73

Hall, E.J. 2000. **Radiobiology for the Radiobiologist.** 5th ed. Philadelphia: Lippincott Williams & Wilkins

Hertveldt, K., Philippe, J., Thierens, H., Cornelissen, M., Vral, A. and De Ridder, L. 1997. Flow cytometry as a quantitative and sensitive method to evaluate low dose radiation induced apoptosis *in vitro* in human peripheral blood lymphocytes. **Int. J. Radiat. Biol.** 71(4), 429-433

Hu,T., Miller,C.M., Ridder,G.M. and Aardema,M.J. 1999. Characterization of p53 in Chinese hamster cell lines CHO-K1, CHO-WBL and CHL: implications for genotoxicity testing. **Mut.Res.** 426, 51-62

Jones, L.A., Clegg, S., Bush, C., McMillian, T. and Peacock, J.H. 1994. Relationship between chromosome abberrations, micronuclei and cell kill in two tumour cell lines of widely differing radiosensitivity. **Int. J. Rad.Biol.** 66, 639-641

Jongmans, W. and Hall, J. 1999. Review. Cellular responses to radiation and risk of breast cancer. **Euro.J.Cancer,** 35(4), 540-548

Kennedy, A.R., Ware, J.H., Guan, J., Donahue, J.J., Biaglow, J.E., Zhou, Z., Stewart, J., Vazquez, M. and Wan, X.S. 2004. Selenomethionine protects against adverse biological effects induced by space radiation. **Free Radic. Biol. Med.** 36(2), 259-66.

Knehr, S. Zitzelberger, H., Braselmann, H., Nahrstedt, U. and Bauchinger, M. 1996. Chromosome analysis by fluorescence *in situ* hybridisation: further indications for a non-DNA-proportional involvement of single chromosomes in radiation-induced structural abberrations. **Int. J. Rad. Biol.** 70(4), 385-392

Leal-Garza, C.H., Cerda-Flores, R.M., Leal-Elizondo, E. and Cortés-Gutiérrez,

E.I. 2002. Micronuclei in cervical smears and peripheral blood lymphocytes from women with and without cervical uterine cancer. **Mut. Res.** 515, 57-62

Lee, T-K., O'Brien, K.F., Naves, J.L., Christie, K.I., Arastu, H.H., Eaves,G.S., Wiley,A.L., Karlsson,U.L. and Salehpour,M.R. 2000. Micronuclei in lymphocytes of prostate cancer patients undergoing radiation therapy. **Mut.Res.** 469, 63-70

Lewanski, C.R. and Gullick W.J. 2001. Radiotherapy and cellular signalling. **The Lancet Oncology** 2, 366-370

Li, L., Story, M. and Legerski, R.J. 2001. Cellular responses to ionising radiation damage. **Int .J .Radiat. Oncol. Biol. Phys.** 49(4), 1157-1162

Levine, E. L., Renehan, A., Gossiel R., Davidson S. E., Roberts S. A., Chadwick C., Wilks D. P., Potten C. S., Hendry, J. H., Hunter R. D. and West, C. M. L. 1995. Apoptosis, intrinsic radiosensitivity and prediction of radiotherapy response in cervical carcinoma. **Radiother. Oncol.** 37(1), 1-9

Martinez-Hernandez, A. 1995. Repair, regeneration and fibrosis. In: Rubin, E. and Farber, J.L., editors. **Essential Pathology.** 2nd ed. Philadelphia: J.B.Lippincott Company, 47-63

Mustonen, R., Bouvier, G., Wolber, G., Stöhr, M., Peschke, P. and Bartsch, H. A. 1999. Comparison of gamma and neutron irradiation on Raji cells: effects on DNA damage, repair, cell cycle distribution and lethality. **Mutat. Res.** 429, 169-179

Nakano, T., Oka, K., Arai, T., Morita, S. and Tsunemoto, H. 1989. Prognostic significance of Langerhans' cell infiltration in radiation therapy for squamous cell carcinoma of the uterine cervix. **Arch. Path. Lab. Med.** 113, 507-511

Ng, W-K. 2003. Mini-Symposium: Iatrogenic Pathology. Radiation-associated changes in tissues and tumours. **Curr. Diag. Path.** 9, 124-136

Olive, P.L., Banath, J.P. and Macphail, H.S. 1994. Lack of correlation between radiosensitivity and DNA double-strand break induction or rejoining in six human tumour cell lines. **Cancer Res.** 54, 3939-3946

Ormerod, M.G. 2001. Review. Using flow cytometry to follow the apoptotic cascade. **Redox Report,** 6(5), 275-287

Ormerod,M.G. 2002. Investigating the relationship between the cell cycle and apoptosis using flow cytometry. **J. Immun. Meth.** 265, 73-80

Östling, O and Johanson, K.L. 1984. Microelectropheretic study of radiation-induced DNA damage in individual mammalian cells. **Biochem. Biophys. Res. Commun.** 123(1), 291-8

Ozsahin, M., Ozahin,H., Yuquan,S., Larsson, B., Wurgler, F.E. and Crompton, N.E.A. 1997. Rapid assay of intrinsic radiosensitivity based on apoptosis in human CD4 and CD8 T-lymphocytes. **Int.J.Radio.Onco.Bio.Phys.** 38(2), 429-440

Pawlik, T.M. and Keyomarsi, K. 2004. Role of cell cycle in mediating sensitivity to Radiotherapy. **Int. J. Rad. Oncol. Biol. Phys.** 59(4), 928-942

Peters, L.J., Brock, W.A., Johnson, T., Meyn, R.E., Tofilon, P.J. and Milas, L. 1986. Potential methods for predicting tumor radiocurability. **Int. J. Radiat. Oncol. Biol. Phys.** 12, 459-467

Peters,L. and McKay, M. 2001. Predictive Assays: Will they ever have a role in the Clinic? **Int.J.Rad.Onco.Biol.Phys.** 49(2), 501-504

Puck, T.T & Marcus, P.I. 1956. Action of X-rays on mammalian cells **J. Exp. Med.** 103, 653-666

Qiu, L-M., Li, W-J., Pang, X-Y., Gao, Q-X., Feng, Y., Zhou,L-B. and Zhang, G-H. 2003. Observation of DNA damage of human hepatoma cells irradiated by heavy ions using comet assay. **World. J. Gastroenterol.** 9(7), 1450-1454

Roninson, I.B., Broude, E.V. and Chang, B-D. 2001. If not apoptosis, then what? Treatment-induced senescence and mitotic catastrophe in tumor cells. **Drug Resistance Updates.** 4, 303- 313

Rubin, P. and Siemann, D. 1987. Principles of radiation oncology and cancer radiotherapy. In: **Clinical Oncology for Medical Students and Physicians: A Multidisciplinary Approach.** 6th edition. American Cancer Society.

Sachs, R.K., Chen, A.M. and Brenner, D.J. 1997. Review: Proximity effects in the production of chromosome aberrations by ionising radiation. **Int. J. Rad. Biol.** 71(1), 1-19

Samarin, A. 2001. Absorption and biological effects of ionising radiation. atse.org.au/publications/occasional/occ-samarin.htm ATSE 4, 1-9

Sheridan, M.T., Cooper, R.A., West, C.M.L. 1999. A high ratio of Apoptosis to proliferation correlates with improved survival after radiotherapy for cervical adenocarcinoma. **Int. J. Rad. Oncol. Biol. Phys.** 44(3), 507-512

Singh, N.P., Mc Coy, M.T., Tice, R.R. and Schneider, E.L. 1988. A simple technique for quantitation of low levels of DNA damage in individual cells. **Exp. Cell Res.** 175 (1), 184-191

Smolewski,P., Grabarek, J., Lee, B., Johnson,G. and Darzynkiewicz, Z. 2002. Kinetics of HL-60 Cell entry with TNF-α or Camptothecin Assayed by the Stathmo-Apoptosis method. **Cytometry** 47, 143-149

Sun, B., Huang, Q., Liu, S., Chen, M., Hawks, C.L., Wang, L., Zhang, C. and Hornsby, P.J. 2004. Progressive loss of malignant behaviour in telomerase-negative tumorigenic adrenocortical cells and restoration of tumorigenicity by human telomerase reverse transcriptase. **Cancer Res.** 64(17), 6144-6151

Sutherland, R.M. and Mulcahy, R.T. 1987. Basic principles of Radiation Physics, In: Rubin P., Bakemeier, R.F. and Krackov, S.K. Eds. **Clinical Oncology** 6th ed. American Cancer Society, Inc., 40-46

Schwartz, J.L., Rotmensch, J., Giovanazzi,S., Cohen,M.B. and Wechselbaum, R.R. 1988. Faster repair of DNA double-strand breaks in radioresistant human tumour cells. **Int.J.Radiat.Oncol.Biol.Phys.** 15, 907-912

Van Rooyen, T.J. and Meyer, B.R. 1995. Training course for radiation workers at the National Accelerator Centre, Faure, South Africa.

Vermes, I., Haanen, C. and Reutelingsperger, C. 2000. Flow cytometry of apoptotic cell death. **J. Immun. Meth.** 243, 167-190

West, C.M.L. and Hendry, J.H. 1992. Intrinsic radiosensitivity as a predictor of patient response to radiotherapy. **Br. J. Radiobiol.** 24, 146-152

West, C.M.L., Davidson,S.E., Roberts,S.A. and Hunter,R.D. 1993. Intrinsic radiosensitivity and prediction of patient response to radiotherapy for carcinoma of the cervix. **Br.J. Cancer** 68, 619-823

West, C.M.L.1995. Invited Review: Intrinsic radiosensitivity as a predictor of patient response to radiotherapy. **Br. J. Radiobiol.** 68, 827-837

Zhivotovsky, B., Joseph, B. and Orrenius. 1999. Minireview: Tumor radiosensitivity and apoptosis. **Exper. Cell Res.** 248, 10-17

Zörnig, M., Hueber, A-O., Baum W. and Evan,G. 2001. Review. Apoptosis regulators and their role in tumorigenesis. **Biochimica et Biophysica Acta** 1551, F1-F37

Chapter 2

The Clonogenic Assay and Cell Survival Curve

Including

The Micronucleus Assay

Many factors affect tumor response to radiotherapy.
These include the Rs of radiobiology:
Radiosensitivity, Repopulation, Reoxygenation, Repair, Recruitment, Resorption and Redistribution.

Nigel Crompton et al.,1997

2.1 Introduction

The objective of curative radiotherapy is to attain local tumor control by destroying clonogenic tumour cells and keeping injury to normal surrounding tissue to a minimum (Baumann *et al.,* 2003). Even when clinical prognostic factors such as tumor histology and grade, size and site are assessed, the severity of normal tissue as well as tumor response to radiotherapy varies significantly between patients (Andreassen *et al.,* 2002).

To evaluate inherent cellular radiosensitivity, single-cell plating techniques are considered the standard for evaluating clonogenic cell survival and cellular response to anticancer agents and radiation (Rockwell and Kallman, 1973; Deschavanne and Fertil, 1996). Fertil and Malaise (1981), found significant variations in radiosensitivities of tumors evaluated within each histologic group and demonstrated that radiosensitivity may vary with DNA characteristics of

the tumor cells. A correlation of the intrinsic radiosensitivity of the tumor cell lines with the radiocurability of related tumor groups was reported. The first *in vitro* survival curve for mammalian cells irradiated with x-rays was of cervical carcinoma cells (HeLa) reported by Puck and Marcus (1956). Survival curves have contributed greatly to the understanding of radiobiology. By correlating the *in vitro* radiosensitivity of the cell lines developed from human tumors with the clinical responsiveness of tumors of the same histological classification, a means to interpret and determine cellular intrinsic radiosensitivity was established. Deschavanne and Fertil (1996) reviewed data documenting the radiosensitivity of about 700 cell lines *in vitro* and described a scale of radiosensitivity for human cells.

Also called the colony assay, the clonogenic assay determines a cells' ability to retain reproductive integrity in response to exposure to radiation or other genotoxic agents. To overcome the fact that cells taken from fresh specimens do not maintain their reproductive integrity for more than a few weeks, established cell lines are used extensively in experimental radiobiology. Cell lines are developed from cells taken from biopsies, grown in culture and repeatedly reseeded.

The assay necessitates a cell to pass through a number of post treatment mitoses to form a visible, viable colony of fifty or more cells. A cell that has attained this has proved its clonogenic ability and is scored as a survivor. The systematic loss of this ability as a function of radiation is described by means of the dose-survival curve.

The success of the assay is dependent on calculating the fraction of cells surviving a particular radiation dose. Due to seeding error and cellular characteristics the number of colonies counted does not necessarily correlate with the number of cells seeded. The plating efficiency (PE) is therefore calculated as the percentage of cells seeded that grew into colonies. Taking the PE into account the surviving fraction (SF) of the cells may be calculated. An estimate of cell survival is obtained when this is repeated at different dose points. As the dose increases it is necessary to seed more cells as the survival will be predictably lower.

This data is then plotted on a log-linear scale, with the dose plotted as linear and the surviving fraction plotted as logarithmic. At low doses of low linear energy transfer (LET) sparsely ionising radiation, the curve begins by demonstrating surviving fraction as an exponential function of dose where at higher doses the curve starts to bend. This quality of low LET radiation is best described by the linear-quadratic model and data are expressed as $S=\exp(-(\alpha D + \beta D^2))$, where S is the fraction of cells surviving a dose D and α and β are coefficients. This model proposes that there are two components to cell killing by radiation, one that is proportional to dose (αD) and the other that is proportional to the square of the dose (βD^2). The α-value represents lethal damage and determines the initial slope of the survival curve. The β coefficient represents the reparable damage and forming part of the quadratic component causes the curve to bend at higher doses. Importantly, the α/β ratio is the dose at which these two components of cell killing are equal (αD =

βD^2).

All mammalian cells display similar survival curves. There is an initial shoulder, which displays variability in magnitude, followed by a straightening on the log-linear plot.

Micronuclei appear in mitotic cells and are chromosomal fragments or whole chromosomes that are excluded from the main daughter nuclei during nuclear division (Fenech *et al.,* 1999). Micronuclei containing chromosomal fragments are the result of direct DNA breakage, replication on a damaged template or inhibition of DNA synthesis (Albertini *et al.,* 2000). Increased frequencies of micronucleated cells are a biological indication of genotoxic damage and are induced by agents that cause chromosomal breakages (clastogens) and those that affect the spindle apparatus (aneugens) (Majer *et al.,* 2001). The addition of Cytochalasin-B blocks cytokinesis and cells that have undergone mitosis are distinguished by the appearance of two or more nuclei in the same cytoplasm (Fenech and Morely, 1985).

The tendency of a cell line or lymphocytes to undergo micronucleation is expressed as the micronuclei frequency (MNF) or the micronucleation index.

2.2 Materials and Methods

2.2.1 Cell lines and maintenance

Chinese Hamster Ovary cells (CHO-K1) were kindly provided by iThemba LABS and were cultured in monolayers in T25 culture flasks and incubated at 37°C in a 5% carbon dioxide humidified atmosphere in air. Cells were maintained in alpha minimal essential medium (α-MEM) completed with 10% fetal calf serum, 10μg/ml streptomycin and 10μg/ml penicillin. Media and chemicals were purchased from Sigma (South Africa).

2.2.2 Cell survival assay

CHO-K1 cells were taken from growing stock cultures and prepared as single cell suspensions by trypsination, which caused cells to round up and detach from the surface of the culture flask. Alpha minimal essential medium (α-MEM), completed with 10 % foetal calf serum, was added to stop the tripsinisation. An estimate of cell numbers per unit volume was quantified using a haemocytometer. Serial dilutions of known cell numbers were made and plated in petri dishes according to expected survival to ensure that about 200 colonies per petri dish (Corning, New York) could be counted. Samples were incubated for one hour after plating to allow cells to settle. Cell samples were exposed to doses of 0; 2; 4; 8 and 12 Gy ^{60} Co γ-irradiation and incubated for 7 days (168 hrs) to allow colony formation.

Following incubation, colonies were fixed with glacial acetic acid, methanol and water in a ration of 1:1:8 (v/v/v), stained with a solution of 0.01% Amido

Black. Colonies containing more than 50 cells were enumerated. The plating efficiency (PE) was defined as the fraction of colonies to the number of cells plated in the control samples. Surviving fraction was defined as the number of colonies counted divided by the number of cells seeded multiplied by the PE as follows:

$$SF = \frac{\text{Colonies counted}}{\text{Cells seeded x (PE/100)}}$$

Data was plotted on a log-linear scale where dose was plotted as linear and the surviving fraction as logarithmic.

2.2.3 Micronucleus Assay

The micronucleus assay was performed as a pilot study in the iThemba laboratory and is presented in this study as unpublished data.

Approximately 5 x 10^4 CHO-K1 cells were plated into a 30mm petri dish containing a coverslip. Following gamma irradiations of 0; 1; 2; 3; 4 and 5 Gy, Cytochalasin-B was added to each sample at a final concentration of 2μg/ml. Cytochalasin-B interferes with mitosis and yields bi-nucleated cells. Cells were incubated for 24 hours and fixed using 3:1 methanol:acetic acid. The cells adherent to the coverslips were stained using Acridine Orange, mounted in Gurr buffer (pH 6.8) and visualized using a fluorescent microscope equipped with FITC filter set. Micronuclei were scored as separate from the main nucleus having a diameter not greater than a third of the main nucleus. The number of micronuclei in 500 bi-nucleated cells was counted.

2.3 Results and Discussion

2.3.1 Clonogenic Assay

The clonogenic ^{60}Co-gamma survival curve generated for CHO-K1 cells is presented in Figure 2.2. The graph displays an initial shoulder, which is followed by a straightening on the log-linear plot, in accordance with survival curves of mammalian cells. Colonies consisting of 50 or more cells were enumerated (Figure 2.1) and the mean cell survival per dose point was calculated, corrected for plating efficiency as demonstrated in Table 2.1.

Table 2.1: *Table demonstrating plating efficiency and SF values measured in triplicate on two different occasions. Data corrected for plating efficiency (PE) is also presented.*

TEST	DOSE (γ)	SURVIVING FRACTION			CORRECTED FOR PE		
	Gy	1	2	3	1	2	3
1	0	0.906			1.00		
	2	0.696	0.681	0.640	0.768	0.751	0.706
	4	0.210	0.270	0.230	0.231	0.298	0.253
	8	0.058	0.058	0.052	0.064	0.064	0.057
	12	0.004	0.004	0.005	0.004	0.004	0.005
2	0	0.810			1.00		
	2	0.590	0.510	0.860	0.728	0.630	1.06
	4	0.245	0.256	0.260	0.302	0.320	0.321
	8	0.022	0.038	0.024	0.027	0.100	0.030
	12	0.001	0.0015	0.0014	0.001	0.001	0.002

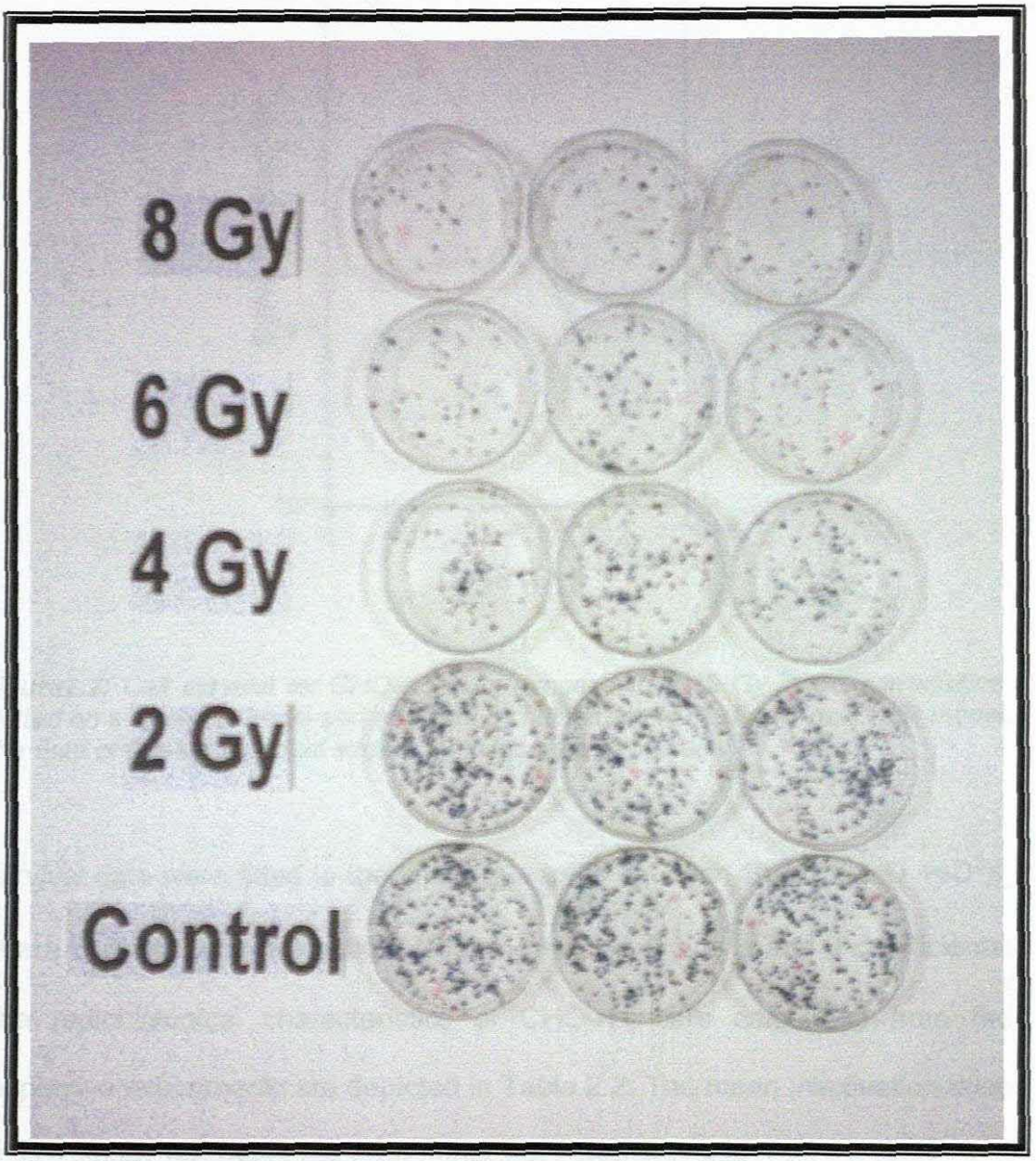

Figure 2.1: *Colonies obtained with Chinese Hamster Ovary cells (CHO-K1) cultured in vitro. Petri dishes were seeded with known amounts of cells and subjected to 0, 2, 4, 6 and 8 Gy ^{60}Co-γ irradiation. Cell samples were cultured for 7 days demonstrating surviving colonies decreasing with increasing dose.*

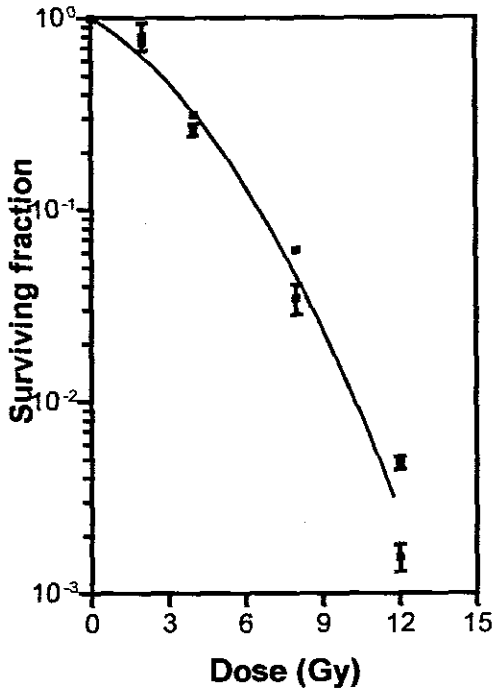

Figure2.2: *Cell survival for CHO-K1 cells exposed to 2-12 Gy ^{60} Co γ Irradiation, plotted on a log-linear scale and obtained by fitting data to the linear-quadratic model. The data of two independent experiments have been pooled.*

Survival data were fitted to the linear quadratic equation $S=\exp(-(\alpha D + \beta D^2))$, where S is the survival fraction, following a dose D and α and β coefficients. The radiobiological characteristics of CHO-K1 cells calculated from the respective experiments are depicted in Table 2.2. The mean inactivation dose or $\bar{D}_\gamma$ values represent the area under the curve and was 3.25 ± 0.44 Gy and 3.23 ± 0.77 Gy respectively. By comparing this data with that of Slabbert *et al.*, 2000, who reported mean inactivation dose in the range of 1.65 - 4.35 for the numerous cell lines studied, CHO-K1 cells falls within the 75 percentile of this range. From this the relative radioresistance of the CHO-K1 cells is demonstrated.

Table 2.2: *The radiobiological characteristics of CHO-K1 cells exposed to ^{60}Co γ-irradiation, where α = lethal damage; β=reparable damage and $\bar{D}$= mean inactivation dose.*

Experiment	$\alpha \pm SE$ (Gy^{-1})	$\beta \pm SE$ (Gy^{-2})	$\bar{D}_\gamma$	SF_2
1	0.20 ± 0.03	0.02 ± 0.003	3.25 ± 0.44	0.742
2	0.15 ± 0.04	0.03 ± 0.003	3.23 ± 0.77	0.806
Mean	0.175 ± 0.025	0.025 ± 0.005	3.24 ± 0.01	0.774 ±0.032

The mean inactivation dose is a one-dimensional parameter reflecting the average cell response and may thus underestimate the differences in radiosensitivity between cell lines. α-Values that quantify the initial slope of the curve are a more sensitive parameter for indicating differences in radiosensitivity.

Comparing the α-values ranging from 0.09 – 0.55 Gy^{-1} presented by Slabbert *et al.*, (2000), and that of 0.18 Gy^{-1} calculated for the CHO-K1 cells, it is interesting to note that the smaller the α-coefficient, the greater the relative radioresistance displayed by the cell to gamma radiation i.e. a smaller α-coefficient translates into a less steep survival curve.

Within each experiment the parameters display little variation although a variation is evident on repetition as indicated in Table 2.1. In order to reduce variation within an experiment, a single dilution route is followed with replicates plated from one dilution. This does not reflect the uncertainties associated with the experiments that are addressed when the experiment is repeated and as a result small error bars are observed (Figure 2.2). In order to achieve the most quantitative results four dose points and a control are set

up in triplicate. In an attempt to address counting variation as well as to better quantify the response to radiation the dilution is performed on untreated cells.

An important observation is that the α-coefficient, indicating non-reparable damage and the β-coefficient, representing reparable damage, are co-variant. As the α-value increases the corresponding β-value decreases. As a result of this the $\bar{D}$ values remain similar. This is in accordance with Steel *et al.*, (1989), who reported that radioresistance does not correlate with the lack of reparable damage.

The r^2 value reflects to goodness of fit and a mean value of 0.97 was calculated using Graph Pad Prism software.

2.3.2 Micronucleus Assay

CHO-K1 cells were subjected to ^{60}Co-γ radiation at doses of 1; 2; 3; 4 and 5 Gray. At least 500 bi-nucleated cells were evaluated for each dose and the number of micronuclei in each enumerated (Figure 2.3). The frequency of micronuclei formations in bi-nucleated CHO-K1 cells increased in a gradual manner (r^2 = 0.997) with radiation dose (Figure 2.4).

A linear-quadratic expression fitted to the experimental observations yielded an α-value of 76.1 $\pm$ 4.7 Gy^{-1} and a β-value of 1.1 $\pm$ 1.1 Gy^{-2}. This is data from a single experiment. Larger variations in alpha and beta values obtained from micronuclei frequency data are expected as the dose range over which the data is generated is much smaller than that of survival curves. As the reparable component of radiation damage is not reflected in a statistically significant manner by the micronuclei data, it is concluded that a simple linear relationship exists between physical dose and cell damage using this endpoint. Within the range of doses used, the rate of micronuclei induction per unit dose appears to be constant and as such reflect in full cellular damage by ionising radiation.

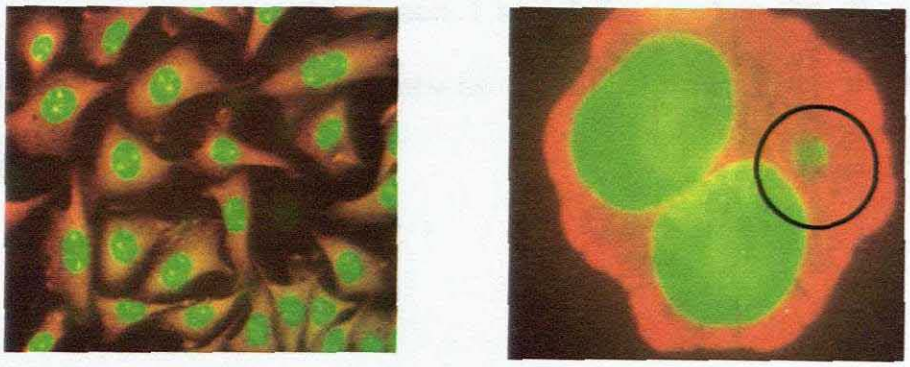

Figure 2.3: *Photomicrographs of CHO-K1 cells stained with Acridine Orange and visualised using a fluorescence microscope. In the circle a micronucleus is demonstrated in a bi-nucleated cell.*

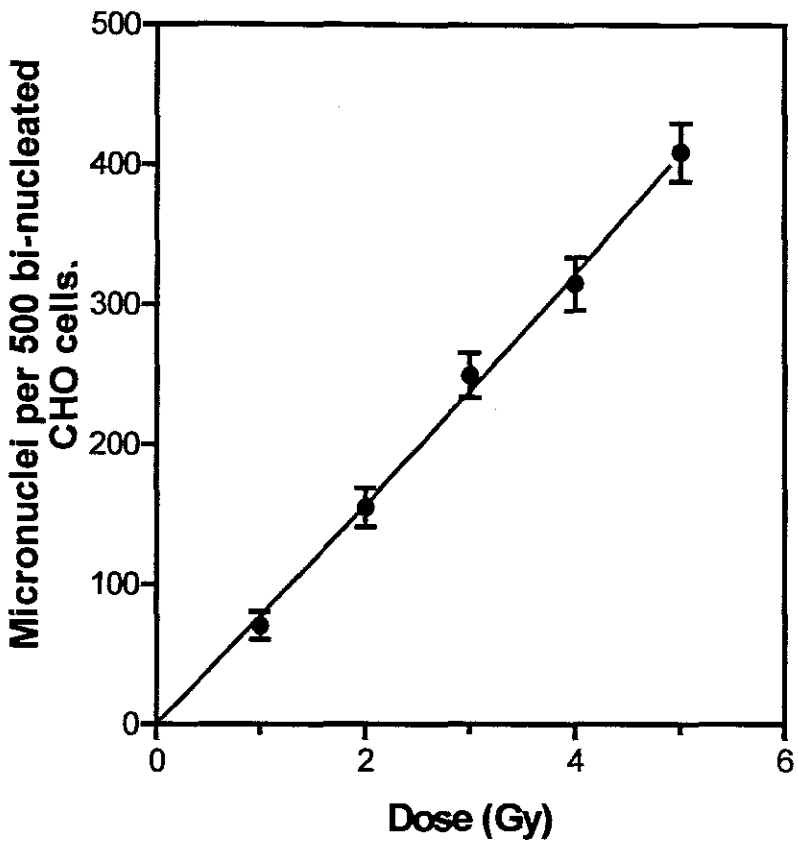

Figure 2.4: *Micronuclei formations in bi-nucleated CHO-K1 cells following exposures to different doses of Gy ^{60}Co γ irradiation. This is data from a single experiment.*

The relation between micronuclei and surviving fraction is shown in Figure 2.5. For gamma doses of between 1 and 5 Gy used in this study a linear inverse relationship is evident between micronuclei frequency and single cell survival.

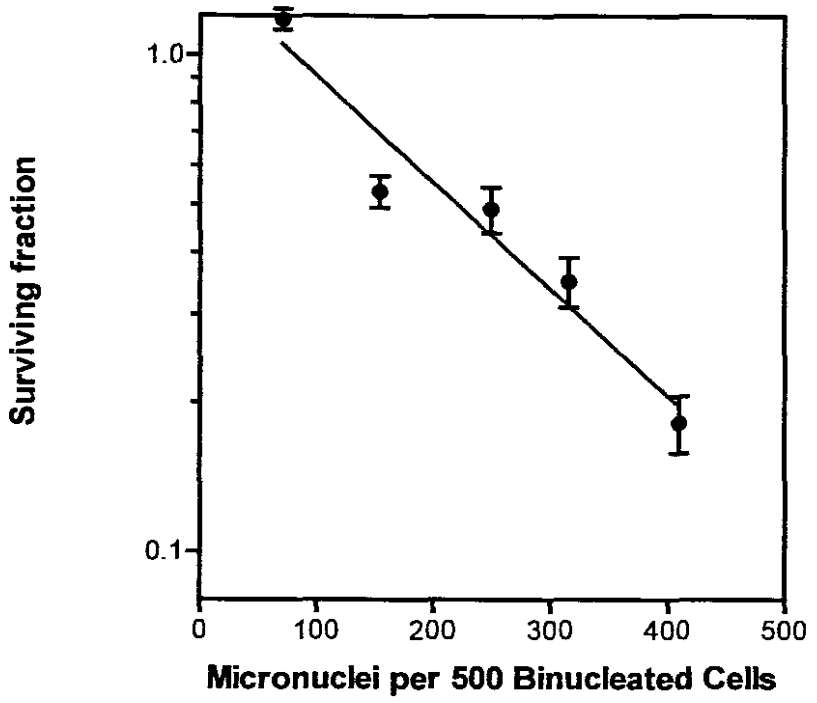

Figure 2.5: *Micronuclei formations in relation to the clonogenic survival of CHO-K1 cells exposed to graded doses of 1 – 5 Gy ^{60}Co γ irradiation.*

2.4 Conclusion

It is concluded that the sensitivity of CHO-K1 cells to ionising radiation can be estimated using both clonogenic survival and micronuclei formations. Both endpoints yield measurable data over a useful dose range and cellular damage can be quantified with reasonable precision. With this in mind it would be most useful to follow the influence of neutron radiation and cell lines varying in radiosensitivity using these endpoints.

2.5 References

Andreassen, C.N., Alsner, J. and Overgaard, J. 2002. Does variability in normal tissue reaction after radiotherapy have a genetic basis – where and how to look for it? **Radioth. Onco.** 64, 131-140

Albertini, R.J., Anderson, D., Douglas, G.R., Hagmar,L., Hemminki,K., Merlo,F., Natarajan, A.T., Norppa, H., Shuker, D.E.G., Tice, R., Waters, M.D. and Aitio, A. 2000. IPCS guidelines for the monitoring of genotoxic effects of carcinogens in humans. **Reviews in Mut.Res. (Special issue)** 463(2), 111-172

Baumann, M., Hölscher,T. and Begg,A.C. 2003. Editorial. Towards genetic prediction of radiation responses: ESTRO's GENEPI project. **Radiother. Oncol.** 69, 121-125

Crompton,N.E.A., Ozsahin,M., Schweizer,P.,Larsson,B. and Luetolf,U.M. 1997. Theory and practice of Predictive Assays in Radiation Therapy **Strahlenther.Onkol.**173(2), 58-67

Deschavanne, P.J. and Fertil, B. 1996. A Review of Human Cell Radiosensitivity *in vitro*. **Int.J.Rad.Onco.Biol.Phys.**34(1), 251-266

Fenech, M., Holland, N., Chang, W.P., Zeiger, E. and Onassi, S. 1999. The Human Micronucleus Project – An international collaborative study on the use of the micronucleus technique for measuring DNA damage in humans. **Mut. Res.** 428, 271-283

Fenech, F. and Morely, A.A. 1985. Solutions of the kinetic problem in the micronucleus assay. **Cytobiol.** 43, 233-246

Fertil, B. and Malaise, E-P. 1981. Inherent cellular radiosensitivity as a basic concept for human tumor radiotherapy. **Int. J. Rad.Oncol. Biol. Phys.** 7, 621-629

Majer, B.J., Laky, B., Knasmüller, S. and Kassie, F. 2001. Review. Use of the micronucleus assay with exfoliated epithelial cells as a biomarker for monitoring individuals at elevated risk of genetic damage and in chemoprevention trials. **Mut. Res.** 489, 147-172

Puck, T.T. and Marcus, P.I. 1956. Action of X-rays on mammalian cells. **J.Exp.Med.**103, 653-666

Rockwell, S.C. and Kallman,R.F. 1973. Cellular radiosensitivity and tumor radiation response in the EMT6 tumor cell system. **Radiat. Res.**53, 281-284

Slabbert, J.P., Theron,T., Zölzer, F., Streffer, C. and Böhm, L. 2000. A comparison of the potential therapeutic gain of p(66)/Be neutrons and d(14)/Be neutrons. **Int. J. Rad. Oncol. Biol. Phys.** 47(4), 1059-1065

Steel, G.G. and Peacock J.H. 1989. Why are some human tumors more radiosensitive than others? **Radiother. Oncol.** 15, 63 - 72

Chapter 3

Single-Cell Gel Electrophoresis (SCGE) Assay

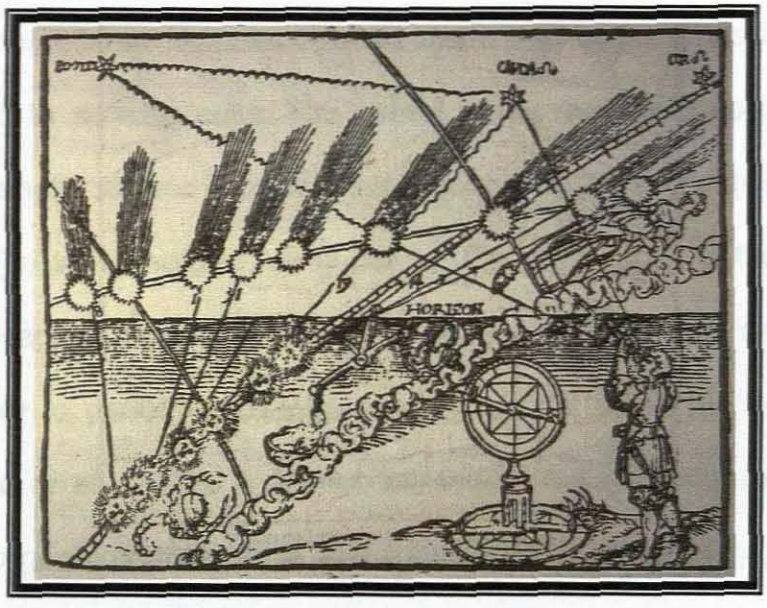

Image published in 1532 by Peter Apian (1495-1552) Professor of Mathematics and Astronomy who discovered that the tail of a comet always pointed away from the Sun.

3.1 Introduction

The earliest attempt at directly measuring DNA strand breaks was made by Rydberg and Johanson in 1978. Östling and Johanson (1984) introduced the single-cell gel electrophoresis assay as a microelectrophoretic technique. Briefly, cells embedded in agarose on a microscope slide are lysed and DNA allowed to unwind enabling it to migrate in an electric field under neutral conditions. DNA is negatively charged and migrates in the direction of the anode, forming the characteristic head and tail that was termed the 'comet assay' (Olive, 1989). Only double strand breaks are detected at a neutral

pH, as base pairing is not disrupted. Singh *et al.,* (1988) introduced electrophoresis under alkaline conditions (pH>13) to detect single strand breaks, alkali-labile sites, DNA-cross-linking and incomplete excision repair sites.

Any eukaryote cell from cultures or fresh tissue may be used, as the assay is not restricted to somatic cells. The comet assay measures damage at the level of the single-cell and resolves heterogeneity within complex populations (Olive, 1999). As a genotoxic assay *per se,* the advantages of the technique are that it is rapid, simple and is sensitive to low levels of DNA damage. The assay is easy to perform, economical and requires small cell numbers per sample (Tice *et al.,* 2000). A further advantage the comet assay has over other *in vivo* genotoxicity tests is that it is not reliant on rapidly proliferating cells.

The application of single-cell gel electrophoresis *in vivo* is reviewed by Hartmann *et al.,* (2003) and includes the detection of genomic damage in marine flat fish (Belpaeme *et al.,* 1998), in murine spermatozoa after exposure to radiation (Haines *et al.*, 2001), as well as tumour hypoxia in breast cancers (Olive *et al.,* 1993b). In environmental studies the comet assay has been used to evaluate the genotoxic effects of fungicides (Lebailly *et al.,* 1997) and contaminants in polluted ground water (Rajaguru *et al.,* 2002) as well as to identify irradiated food (Cerda *et al.*, 1997). The comet assay has been applied in a number of clinical studies (Kassie *et al.,* 2000). Bladder washings of patients with transitional cell carcinomas were evaluated (Mc Kelvey-Martin *et al.,* 1997) and biomonitoring of individuals exposed to low-dose irradiation

(Wojewódzka *et al.*, 1998). Gutierrez *et al.* (1998) monitored damage induced by radiation therapy in thyroid cancer patients.

Radiation-induced damage and repair using the comet assay was used to predict radiosensitivity in tumour cell lines with differing radiosensitivities (McKeown *et al.*, 2003; Boehringer-Wyss *et al.*, 2002; Bergqvist *et al.*, 1998). The difference in cellular radiosensitivity of human fibroblasts has been explained as a reflection of the cells ability to efficiently repair double strand breaks (Würm *et al.*, 1994; Kiltie *et al.*, 1997). In the case of tumour cells, some studies have found a correlation between *in vitro* radiosensitivity and radiation-induced DNA double strand break (DSB) repair (Peacock *et al.*, 1989) while others found no correlation (Olive *et al.*, 1994).

Marples *et al.*, (1998) used the neutral comet assay, to measure the initial and residual radiation-induced DNA DSBs in cervical cancer cell lines. These data demonstrated a significant relationship between the ratio of the initial and residual radiation-induced DNA DSBs and the cellular radiosensitivity of the cells as measured using the clonogenic assay.

The fundamental premise of the alkaline comet assay, which was used in this study, is the migration of DNA in an agarose medium under alkaline unwinding and electrophoresis conditions (Singh *et al.*, 1988; Olive, 1999; Rojas *et al.*, 1999). At a pH> 13 the solution maximises the expression of alkali-labile sites as single-strand breaks. The migration of DNA is reliant on various factors such as the concentration of agarose in the gel, the temperature, pH and duration of unwinding and electrophoresis (Tice *et al.*,

2000; Hartmann *et al.*, 2003).

DNA migration can be visually determined and categorised into different classes or grades (Collins *et al.*, 1993; Lebailley *et al.*, 1997; Godard *et al.*, 2002). Image analysis is often used, where measurement of DNA in the tail, tail length and tail moment are calculated. Tail moment is defined as the product of the distance between the centres of the head and tail, and the proportion of DNA in the tail (Olive, 1999). The use of percentage DNA in the tail gives a clear indication of the appearance of the comet and is linearly related to the DNA break frequency. Although visual scoring is subjective there is a clear relationship between visual scoring and the percentage of DNA appearing in the tail as measured by computer image analysis (Collins *et al.*, 1995).

3.2 Materials and Methods

The response of Chinese Hamster Ovary (CHO-K1) cells to ^{60}Co-γ and p(66/Be) neutron radiation was determined using the comet assay as described by Tice and Vasquez (1999).

3.2.1 Cell line and Maintenance

CHO-K1 cells were grown routinely in monolayers in T25 culture flasks and were incubated at 37°C in a 5% carbon dioxide humidified atmosphere in air. Cells were maintained in alpha minimal essential medium (α-MEM) completed with 10% foetal calf serum, 10-μg/ml streptomycin and 10-μg/ml penicillin. The cells were kindly provided by Dr. Slabbert, iTemba LABS, with media and chemicals purchased from Sigma (South Africa).

3.2.2 Slide preparation and Processing

A 1% normal melting point agarose solution (NMPA) was made up in calcium and magnesium free phosphate buffer. While the NMPA solution was hot, conventional microscope slides were dipped into the solution covering the area up to the frosted end, ensuring an even layer and left to dry completely on a flat surface. A 0.5% solution of low melting point agarose (LMPA) was made up and placed in a water bath to maintain the agarose temperature at 37°C.

Using cell passages below 20, CHO-K1 cells were harvested from confluent cultures by subjecting the monolayer to trypsin for 30 seconds. The trypsin was decanted and the cells incubated for 3 minutes allowing them to round up

and detach from the flask. A single-cell suspension was prepared and an estimate of cell numbers per unit volume was quantified using a haemocytometer and adjusted to yield approximately 1 x 10^6 cells/ml. From this cell suspension 10 µl was mixed with 75 µl of LMPA and gently layered on a slide coated with NMPA. A coverslip was placed on this layer and the slide placed on ice to set. The coverslip was gently removed and 75 µl of LMPA was pipetted over the cell mixture layer. The coverslip was replaced and the slide placed on ice allowing the agarose to set. All slides including the untreated samples were kept on ice and transported to the radiation source.

3.2.3 Irradiation

Cell samples were exposed on slides to ^{60}Co γ-rays at room temperature (~22°C) to doses of 0; 2; 4; 6 and 8 Gy at a dose rate of ~ 0.29 Gy/min. The ^{60}Co γ-source was in a vertical position directed upwards at a source surface distance of 70cm. Slides were placed on a 6mm thick Perspex table (build up) in a 30 x 30 cm^2 field with a 15 cm thick backscatter block of Perspex fixed directly above. A 0.6cm^3 thimble Farmer ionisation chamber was used to confirm the dose at the position of the cells.

Neutron irradiation was conducted with a p(66)/Be neutron vertical beam directed downwards, using a dose rate of 0.35 Gy/min. Slides were placed in a 29 x 29 cm^2 field and a source surface distance (SSD) of 150 cm was used at a gantry angle of 0°, on a 15cm thick backscatter Perspex block. Build up material consisted on 20mm polyethylene. To verify the dose at the position of the cells an 80-cm^3 Far West ionisation chamber and a BNC Portanim current

digitiser was used. Slides were irradiated at doses of 0; 1; 2; 3 and 4 Gy at a dose rate of ~ 0.35 Gy/min. Neutron doses administered were half that of gamma irradiation. The assumption that a relative biological effectiveness (RBE) of approximately 2 applies for neutron radiation ensured that the range of biological damage induced by neutron and gamma radiation would be approximately the same, preventing the dose response curve becoming saturated when using high-LET radiation.

3.2.4 Electrophoresis

Immediately after irradiation slides were placed on ice, coverslips removed and placed in an ice cold freshly prepared lysing solution (2.5M NaCl [146.1g], 100mM Na_2EDTA [37.2g], 10 mM Tris [1.2g], pH 10.0, add fresh 1% Triton X-100, 10% DMSO). The lysis solution was chilled primarily to maintain stability of the gel. Slides were left overnight in the dark at 4°C. After lysis slides were placed in a gel box, side by side in an alkaline electrophoresis buffer (10N NaOH [220g/500ml dist H_20], 200mM EDTA [14.89g/200ml dist H_20], pH>13) and allowed to unwind for 20 minutes. Tice *et al.,* (1991) added 10% DMSO to prevent radical-induced DNA damage related to iron released during lysis of blood in tissue. All preparation was done in reduced light to minimise the possibility of inducing UV damage in the sample.

Immediately after unwinding the slides were electrophoresed for 10 minutes at ~ 0.74 V/cm. The power supply was set at 25 volts and the current adjusted to 300 milliamperes by raising or lowering the buffer level. The unwinding and electrophoresis steps were performed in the dark and on ice keeping the

temperature of the buffer at ~ 4°C. Slides were then coated drop wise with neutralisation buffer (0.4M Tris [48.5g], HCl to pH 7.5), drained and this step was repeated twice, followed by brief exposure to ice cold ethanol and allowed to dry.

3.2.5 Evaluation of DNA damage

Slides were flooded with 75μl of 2μg/ml ethidium bromide and the coverslip replaced. Observations were made at X-400 magnification using a fluorescence microscope equipped with an excitation filter of 515-560 nm and a barrier filter of 590nm. One hundred comets on each slide were visually categorised as belonging to one of four predefined groups according to tail length, using the criteria of Lebailley *et al.,* (1997) as seen in Figure 3.1.

3.3 Results and Discussion

One hundred CHO-K1 cells per slide were scored on at least two slides per dose point.

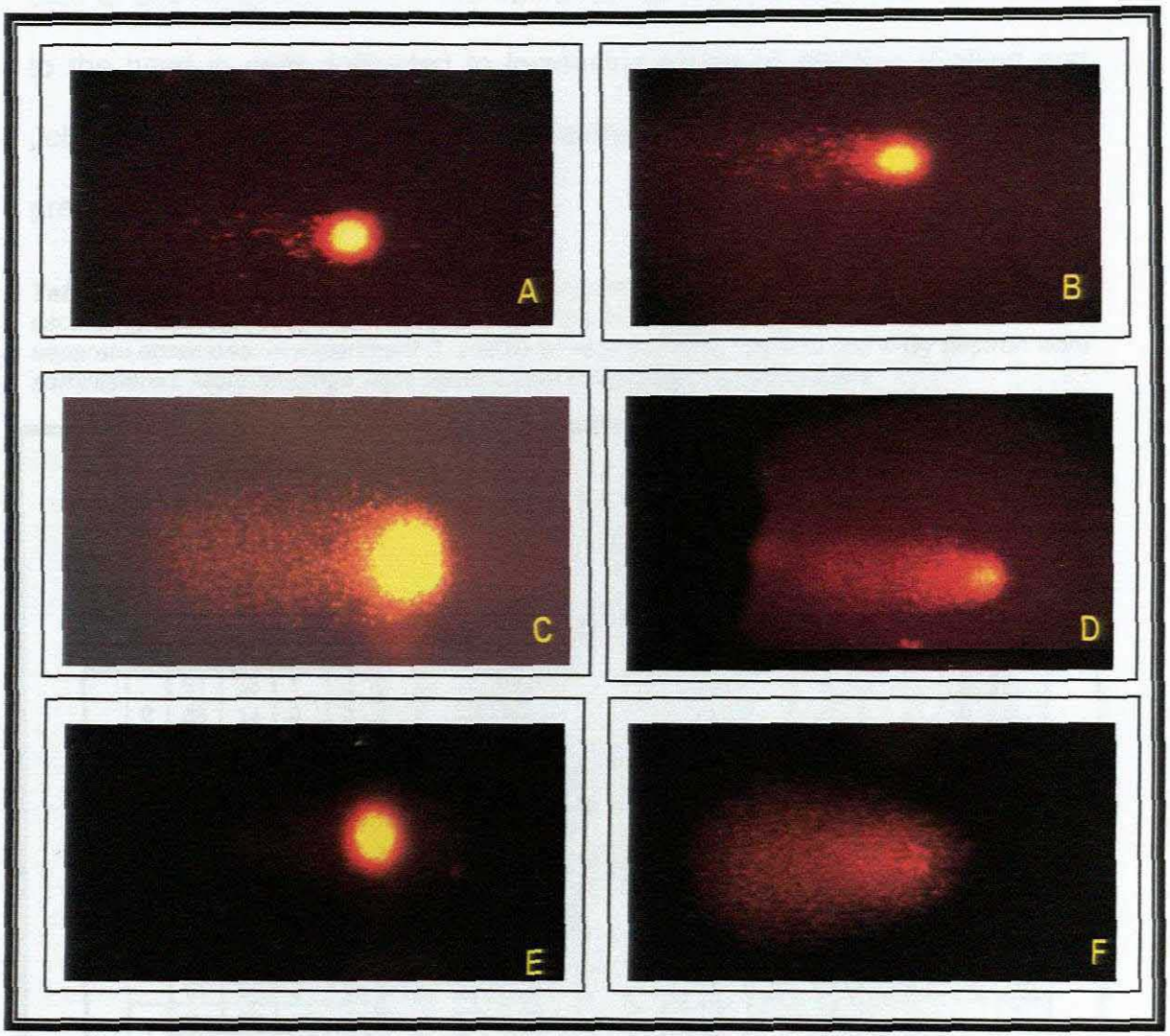

Figure 3.1: *Photomicrographs of CHO-K1 cells after electrophoresis (10min,pH>13), stained with ethidium bromide and visualised using a fluorescent microscope at x400 magnification.* ***A)*** *Grade 1 (undamaged), very little migration,* ***B)*** *Grade 2(slightly damaged)* ***C)****, Grade 3 (damaged) - large amount of DNA is still visible in the brightly stained head with increased tail length;* ***D)*** *Grade 4(highly damaged) cell reflecting progressively more DNA damage as the head stains less brightly and becomes slightly smaller. Migration must be evident in all cells including the control cells (Tice et al., 2000) for electrophoresis to be successful. When images such as these* ***E)*** *are obtained the test is repeated. Images as in* ***F)*** *referred to as 'hedgehogs' or 'ghost' cells by Meintiéres et al., (2003), although observed were not enumerated.*

A differentiation could be drawn between undamaged and slightly damaged cells, placing comets into four categories, undamaged (Grade 1), slightly damaged (Grade 2), damaged (Grade 3) and highly damaged cells (Grade 4). Due to DNA fragmentation, more fluorescence is observed in the tail relative to the head in cells subjected to increasing levels of damage (Östling and Johanson, 1987). The experiments were repeated (x 3) and data obtained are presented below in Table 3.1.

Table 3.1: *Results of the comet assay on CHO-K1 cells exposed to ^{60}Co γ -irradiation at escalating doses of 0; 2; 4 and 6 Gy and 0; 1; 2 and 3 Gy of 66/Be neutron radiation on three separate occasions. In experiment 3, additional doses of 8 Gy gamma and 4 Gy neutron were administered. More readings were taken where more slides were available.*

1

Dose		GRADE			
		1	2	3	4
γ	0	61	38	1	0
		86	14	0	0
		73	24	3	0
	2	36	49	15	0
		31	53	16	0
	4	12	76	9	3
		8	72	16	4
	6	0	11	75	14
		0	15	69	16
n	0	70	20	10	0
		61	36	3	0
	1	29	50	21	0
		33	41	23	3
	2	6	44	48	2
		13	57	26	4
	3	3	16	78	3
		10	21	63	6

2

Dose		GRADE			
		1	2	3	4
γ	0	84	15	1	0
		78	20	2	0
		60	35	5	0
	2	34	55	11	0
		28	55	17	0
	4	7	77	16	0
		10	74	15	1
	6	0	11	60	19
		0	9	79	12
n	0	42	51	7	0
		63	35	2	0
	1	28	64	8	0
		10	42	42	6
	2	6	57	29	4
		11	77	12	0
	3	6	21	58	15
		0	11	81	8
		1	9	81	9

3

Dose		GRADE			
		1	2	3	4
γ	0	66	31	3	0
		60	37	3	0
		65	26	9	0
	2	42	47	12	2
		31	40	28	1
	4	14	54	32	2
		10	66	18	6
	6	0	12	67	22
		0	13	67	21
	8	0	8	36	57
		0	9	46	45
n	0	73	25	1	1
		70	27	4	0
		75	18	8	0
	1	32	50	18	3
		33	55	7	5
	2	11	53	32	7
		31	38	29	2
	3	2	14	64	22
		3	23	43	31
	4	0	4	27	70
		2	19	15	64

The mean distribution of grades per dose point and for each radiation quality was calculated and is shown as stack bars in Figure 3.2. In untreated CHO-K1 cells an average of 70% of comets were grade 1, whereas no grade 1 comets were observed for either 6 or 8 Gy γ-irradiation. A clear increase in DNA damage as a function of dose was seen as no grade 4 comets were observed at 0 and 2 Gy but increased from 3% at 4 Gy and to 51,5% at 8 Gy γ-irradiation.

A similar observation was made when cells were exposed to neutron radiation. An average of 65% of comets were grade 1 in the untreated samples, 3% at 2 Gy and less than 1% at 4 Gy. An increase in DNA damage as a function of dose was seen as no grade 4 comets were observed in the untreated control but increased from 3% at 1Gy, 5% at 2Gy, 12% at 3Gy and substantially to 67% at 4 Gy *n*-irradiation. The increase in the number of grade 4 comets coincided with a decrease in grade 1 comets as the radiation dose increased in both p(66/Be) neutron and ^{60}COγ-radiation.

At the higher doses grades 3 and 4 predominated, indicating more severe damage. For gamma radiation grades 3 and 4 together made up 89% and 92% of the total damage induced at 6 and 8 Gy respectively. This is seen in neutron radiation where grades 3 and 4 together made up 80,5% and 88% of the total damage induced at 3 and 4 Gy respectively.

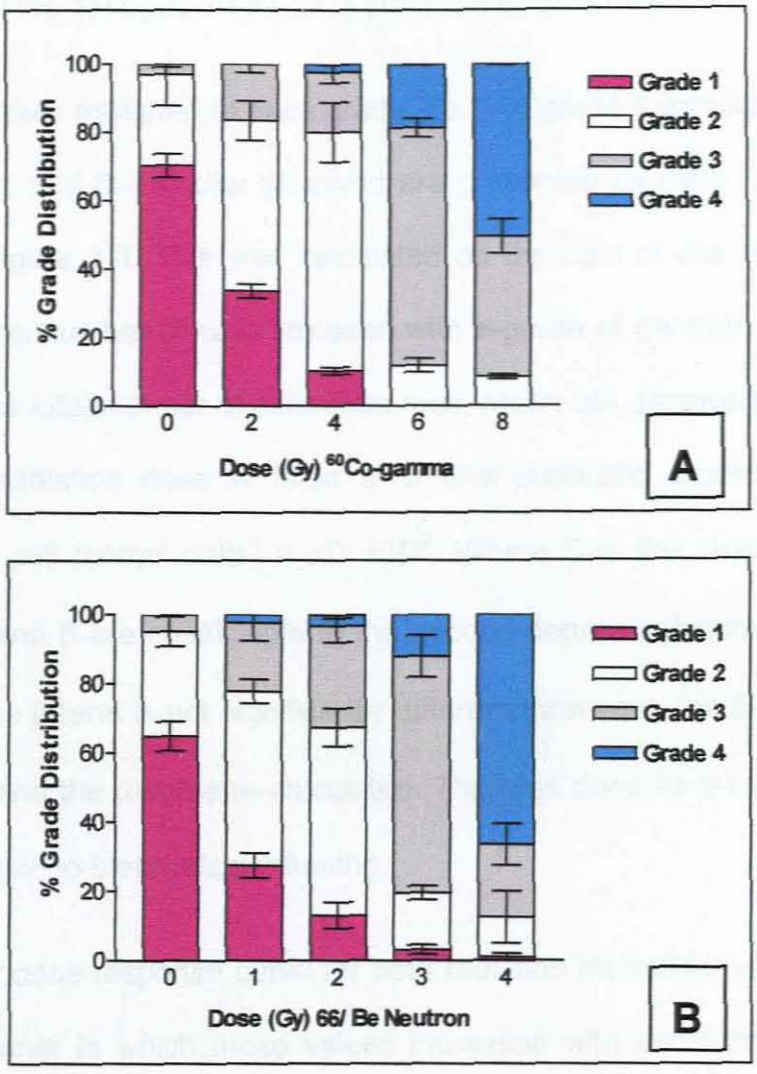

Figure 3.2: *Dose-related distribution of Grades 1 to 4 in CHO-K1 cells post* ***(A)*** *^{60}Co-γ and* ***(B)*** *p(66/Be) neutron irradiation.*

At approximate iso-effective levels the amount of Grade 4 comets increased more in neutrons than photons (gamma). This is consistent with the fact that high LET damage is more discrete, meaning that neutrons leave more cells undamaged yet when imposed the damage is more severe (Ritter *et al.*, 1977; Testard *et al.*, 1997). Using the non-parametric Mann Witney test to compare the comet yield following 2 Gy gamma with 2 Gy neutron irradiation, it is

apparent that the biological damage is significantly different ($p = 0.0263$).

A value was then assigned to each grade, i.e. 1 to grade 1 comets, 2 to grade 2 comets etc. and the results observed are presented as mean cell damage per cell in Figure 3.3. This was calculated as the sum of the products that represents the number of cells (***n***) seen with ***x***-grade of damage (*x = 1 to 4*) divided by the total number of cells examined. Mean cell damage per cell as a function of radiation dose is fitted to a liner-quadratic expression: Mean damage per cell (comet units) = $\alpha D + \beta D^2$. Where D is the physical dose in gray and α and β are coefficients to the second-degree polynomial fit. In the event that the β-term is not significantly different form zero, the β-values were set as zero and the α-value re-calculated. This was done as β-values smaller than zero have no biophysical meaning.

A significant dose response curve for both radiation modalities was observed and the manner in which these values increased with escalating dose was gradual ($r^2 = 0.96$ for gamma radiation and $r^2 = 0.85$ for neutron radiation).

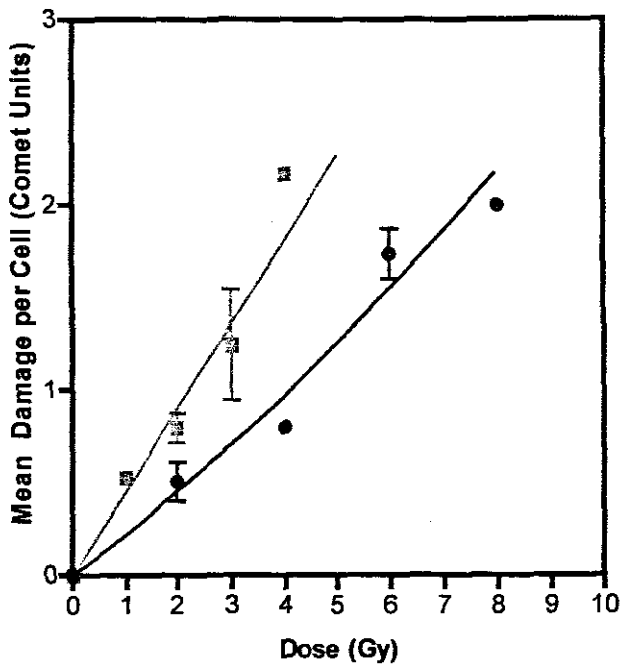

Figure 3.3: *Graphic representation of the Mean Cell Damage (MCD) per cell plotted as a function of p(66/Be) neutron (■) and ^{60}Co γ-radiation (●) induced in CHO-K1 cells.*

When cells were exposed to between 1 and 4 Gy p(66/Be) neutron radiation results obtained were highly significant from zero ($p < 0.0001$) and data fitted a linear response using the expression; Mean Damage per Cell = αD. This is expected as low-LET $^{60}COγ$-radiation results in a linear quadratic response while the high-LET neutron radiation follows a linear response. The comet assay therefore is able to detect increasing levels of radiation damage as well as reflect the changes in the ionisation densities.

For ^{60}CO γ-radiation, a linear quadratic expression fitted to these data generated α - values ranging from 0.13 – 0.21 Gy $^{-1}$(Table 3.2). The same parameter measured for neutron radiation reflected α - values ranging from 0.37 - 0.42 Gy $^{-1}$.

Table 3.2: *The inactivation parameters for CHO-K1 cells exposed to ^{60}Co γ and p(66/Be) neutron irradiation. RBE was determined as the ratio of doses needed to induce a mean cell damage value of 1.5. (α= lethal damage; β= reparable damage and RBE =Relative Biological Effectiveness)*

Experiment	Radiation	α ± SE (Gy^{-1})	β ± SE (Gy^{-2})	RBE
1	Gamma	0.13 ± 0.09	0.03 ± 0.02	1
	Neutron	0.42 ± 0.002	-	1.72
2	Gamma	0.15 ± 0.07	0.02 ± 0.02	1
	Neutron	0.37 ± 0.01	-	1.54
3	Gamma	0.21 ± 0.1	0.01 ± 0.01	1
	Neutron	0.42 ± 0.1	0.03 ± 0.02	1.77

The mean α-value (0.21 Gy^{-1}) for ^{60}CO γ-radiation is almost half that of p(66)/Be neutron (0.45 Gy^{-1}) and this data reflects the greater lethal damage induced by neutron radiation. It is also noted that for ^{60}CO γ-radiation the α - and β - values are co-variant, meaning that as the α - value increases the β-value decreases. This is consistent with the fact that a given amount of radiation energy absorbed in a cell is divided between forming lethal (intratrack-) damage and reparable (intertrack-) damage.

For both neutron and gamma rays the dose responses measured are highly significant. In each instance the standard errors associated with each of the dose response parameters are smaller than the estimate. Furthermore, the 95% confidence interval for the parameter that increases in a linear manner with dose (α-value) and represents the slope of the line is not smaller than zero for both neutrons (0.45 Gy^{-1} ranging from 0.38 – 0.53) as well as for gamma irradiation (0.21 Gy^{-1} ranging from 0.13 – 0.29). It is concluded that the formation of comets is a real response to radiation energy absorbed and not a phenomena that happens by chance as a result of single-cell

electrophoresis.

Cells forming comets with large fan-like tails may be referred to as 'hedgehogs', 'ghost cells', 'clouds' or non-detectable cell nuclei (NDCN) are thought to be cells undergoing apoptosis (Olive *et al.* 1993; Fairbairn *et al.*, 1996; Kizilian *et al.*, 1999; Choucroun *et al.*, 2001; Olive *et al.*, 1993). Cells with the same appearance as apoptotic comets were seen in this study but not enumerated (Meintiéres *et al.*, 2003). It is not clear whether increased DNA fragmentation due to cell death (apoptosis) can result in the generation of false positive results (Hartmann *et al.*, 2003). The assay was performed immediately after irradiation and unlike lymphoid cells, which are exceptionally sensitive to radiation; CHO-K1 cells do not undergo radiation-induced apoptosis as readily (Somosy, 2000). These images have been noted at high doses of gamma radiation under conditions where time intervals were short, making it unlikely for the fragmentation stage to be reached (Testard *et al*, 2000; Tice *et al.*, 2000).

3.4 Conclusion

Cells from tumors of the same origin and pathology can show a wide variation in response to radiation treatment (Bergqvist *et al.*, 1998; West, 1995; Dickson *et al.*, 2002; Baumann *et al.*, 2003). Knowledge of the intrinsic radiosensitivity of a tumor could help produce and optimise radiotherapy protocols for individual patients. Although the clonogenic assay has been the most common method to establish the inherent radiosensitivity of a cell, (West *et al.*, 1993; Fertil and Malaise, 1985; Eastham *et al.*, 1999) to establish a cell

line from each patient is an unlikely proposition.

In this study different levels of cellular damage were reflected by the comet assay in a dose response manner expected from neutrons and photons. These results suggest the value of the comet assay to quantify the radiosensitivity of various cell types. Wada *et al.,* (2003) examined the relationship between cellular radiosensitivity and radiation-induced DNA damage of different cell lines and concluded the comet assay to be a predictive assay for evaluating clonogenic cellular radiosensitivity.

The use of an assay in which cells do not need to be clonogenic as well as one that measures the cells response at the individual level provides an advantageous prospect. The potential for introduction into the clinical setting where patient response to radiotherapy can be predicted remains an attractive option.

3.5 References

Baumann, M., Hölscher,T. and Begg,A.C. 2003. Editorial. Towards genetic prediction of radiation responses: ESTRO's GENEPI project. **Radiother. Oncol.** 69, 121-125

Belpaeme, K., Cooreman, K. and Kirsch-Volders, M. 1998. Development and validation of the *in vivo* alkaline comet assay for detecting genomic damage in marine flatfish. **Mut.Res.** 415,167-184

Bergqvist, M., Brattström, D., Stalberg, M., Vaghef, H., Brodin, O. and Hellmann, B. 1998. Evaluation of radiation-induced DNA damage and DNA repair in human lung cancer cell lines with different radiosensitivity using alkaline and neutral single cell gel electrophoresis. **Cancer Letters** 133(1), 9-18

Boehringer-Wyss, N., Clarkson, S.G. and Allal, A.S. 2002. No benefits of ultrafractionation in two head-and-neck cancer cell lines with different inherent radiosensitivity. **Int.J.Radia.Oncol.Biol.Phys.** 52(4), 1099-1103

Cerda, H., Delincée, H., Haine, H. and Rupp,H. 1997. The DNA 'comet assay' as a rapid screening technique to control irradiated food. **Mut. Res.** 375,167-181

Choucroun, P., Gillet, D., Dorange, G., Sawicki, B. and Dewitte, J.D. 2001. Comet assay and early apoptosis. **Mut. Res.** 478, 89-96

Collins, A.R., Duthie, S.J. and Dobson, V.L. 1993. Direct enzymic detection of

endogenous oxidative base damage in human lymphocyte DNA. **Carcinogenesis** 14, 1733-1735

Collins, A.R., Ai-guo,M. and Duthie,S.J. 1995. The kinetics of repair of oxidative DNA damage (strand breaks and oxidised pyrimidines) in human cells. **Mut. Res.** 336, 69-77

Dickson, J., Magee,B., Stewart,A. and West, C.M.L. 2002. Relationship between residual radiation-induced DNA double-strand breaks in cultured fibroblasts and late radiation reactions: a comparison of training and validation cohorts of breast cancer patients. **Radiother. Oncol.** 62, 321-326

Eastham, A.M., Marples, B., Kiltie, A.E., Orton, C.J. and West,C.M.L. 1999. Fibroblast radiosensitivity measured using the comet DNA-damage assay correlates with clonogenic survival parameters. **Br.J.Cancer.** 79, 1366-1371

Fairbairn, D.W., Walburger, D.K., Fairbairn, J.J. and O'Neil, K.L. 1996. Key morphologic changes and DNA strand breaks in human lymphoid cells: Discriminating apoptosis from necrosis. **Scanning** 18, 407-416

Fertil, B. and Malaise, E.P. 1985. Intrinsic radiosensitivity of human cell lines is correlated with radioreponsiveness of human tumors: analysis of 101 published survival curves. **Int.J.Radiat.Oncol.Biol.Phys.** 11(9),1699-1707

Godard, T., Deslandes, E., Sichel, F., Poul, J-M. and Gauduchon, P. 2002. Detection of topoisomerase inhibitor-induced DNA strand breaks and apoptosis by the alkaline comet assay. **Mut. Res.** 520, 47-56

Gutierrez, S., Carbonell, E., Galofre, P., Creus, A. and Marcos, R. 1998. The alkaline single-cell gel electrophoresis (SCGE) assay applied to the analysis of radiation-induced DNA damage in thyroid cancer patients treated with ^{131} I. **Mut.Res.**413, 111-119

Haines, G.A., Hendry, J.H., Daniel, C.P. and Morris,I.D. 2001. Increased levels of comet-detected spermatozoa DNA damage following *in vivo* isotopic- or X-irradiation of spermatogonia. **Mut.Res.** 495, 21-32

Hartmann, A., Agurell, E., Beevers, C., Brendler-Schwaab, S., Burlinson, B., Clay, P., Collins, A., Smith, A., Speit, G., Thybaud, V and Tice, R.R. 2003. Recommendations for conducting the *in vivo* alkaline Comet assay. **Mutagenesis** 18(1), 45-51

Kassie, F., Parzefall, W. and Knasmüller, S. 2000. Single-cell gel electrophoresis assay: a new technique for human biomonitoring studies. **Mut.Res.** 463, 13-31

Kilizian, N., Wilkins, R.C., Reinhardt, P., Ferrarotto, C. and Mc-Namee, J.P. 1999. Silver stained comet assay for detection of apoptosis. **Biotechniques** 27, 926-930

Kiltie, A.E., Orton, C.J., Ryan, A., Roberts, S.A., Marpels, B., Davidson, S.E., Hunter, R.D., Margison, G., West, C.M.L. and Hendry, J.H. 1997. A correlation between DNA damage and clonogenic measurements of radiosensitivity in fibroblasts from pre-radiotherapy cervix cancer patients. **Int.J.Radiat.Oncol.Biol.Phys.** 39,1137-1144

Lebailly, P., Vigreux, C., Godard, T., Sichel, F., Bar, E., LeTalaër, J.Y., Henry-Amar, M. and Gauduchon, P. 1997. Assessment of DNA damage induced *in vitro* by etoposide and two fungicides (carbendazim and chlorothalonil) in human lymphocytes with the comet assay. **Mut.Res.** 375, 205-217

Marpels, B., Longhurst, D., Eastham, A.M. and West, C.M.L. 1998.The ratio of initial/residual DNA damage predicts intrinsic radiosensitivity in seven cervix carcinoma cell lines. **Br.J.Cancer** 77(7), 1108-1114

McKelvey-Martin, V., Melia, N., Walsh, I.K., Johnston, S.R., Hughes, C.M., Lewis, S.E.M. and Thompson, W. 1997. Two potential clinical applications of the alkaline single-cell gel electrophoresis assay: (1) human bladder washings and transitional cell carcinoma of the bladder; and (2) human sperm and male infertility. **Mut.Res.**376, 93-104

McKeown, S.R., Robson, T., Price, M.E., Ho, E.T.S., Hirst, D.G. and McKelvey-Martin, V. J. 2003. Potential use of the alkaline comet assay as a predictor of bladder tumour response to radiation. **Br.J. of Cancer**, 89, 2264-2270

Meintiéres, S., Nesslany, F., Pallardy, M. and Marzin, D. 2003. Detection of Ghost Cells in the Standard Alkaline Comet Assay is not a good measure of Apoptosis. **Environ. Mol. Mutagen.** 41, 260-269

Olive, P.L. 1989. Cell proliferation as a requirement for development of the contact effect in Chinese hamster V79 spheroids. **Radia. Res.** 117, 79-92

Olive, P.L. 1999. Review. DNA damage and repair in individual cells:

applications of the comet assay in radiobiology. **Int.J.Radiat.Biol.** 75(4), 395-405

Olive, P.L., Banath, J.P. and McPhail, H.S. 1994. Lack of a correlation between radiosensitivity and DNA double-strand break induction or rejoining in six human tumour cell lines. **Cancer Res.** 54, 3939-3946

Olive, P.L., Durand, R.E., Le Riche, J., Olivotto, I. and Jackson, S.M. 1993(b) Gel electrophoresis of individual cells to quantify hypoxic fraction in human breast cancers. **Cancer Res.** 52, 733-736

Olive, P.L., Frazer, G. and Banath, J.P. 1993. Radiation-induced apoptosis measured in TK6 human B lymphoblast cells using the comet assay. **Radiat.Res.** 136(1), 130-136

Östling,O. and Johanson,K.J. 1984. Microelectrophoretic study of radiation-induced DNA damages in individual mammalian cells. **Biochem.Biopys. Res Commun.** 123, 291-298

Östling,O. and Johanson,K.J. 1987. Bleomycin in contrast to gamma radiation induces extreme variation of DNA strand breakage form cell to cell. **Int. J. Radiat. Biol.** 52, 683-691

Peacock, J.M., Eady, J.J., Edward, S., Holmes, A., Mcmillan, T.J. and Steel, G.G.1989. Initial damage and repair as the major determinant of cellular radiosensitivity. **Int.J.Radiat.Biol.** 56, 543-547

Rajaguru, P., Vidya, L., Baskarasethupathi, B., Kumar, P.A., Palanivel, M. and Kalaiselvi, K. 2002. Genotoxicity evaluation of polluted ground water in

human peripheral blood lymphocytes using the comet assay.**Mut.Res.**517, 29-37

Ritter, M.A., Cleaver, J.E. and Tobias, C.A. 1997. High-LET radiations induce a large proportion of non-rejoining DNA breaks. **Nature** 266, 653-655

Rojas, E., Lopez, M.C. and Valverde, M. 1999. Review. Single cell gel electrophoresis assay: methodology and applications. **J. Chromat. B.** 722, 225-254

Rydberg, B. and Johanson, K. 1978. Mammalian cells. In: **DNA repair mechanisms.** Academic Press, New York, pp 465–468

Singh,N.P., McCoy,M.T., Tice,R.R. and Schnider,E.L. 1988. A simple technique for quantification of low levels of DNA damage in individual cells. **Exp.Cell Res.** 175, 184-191

Somosy, Z. 2000. Review. Radiation response of cell organelles. **Micron** 31, 165-181

Testard, I., Dutrillaux, B. and Sabatier, L. 1997. Chromosomal aberrations induced in human lymphocytes by high-LET irradiation. **Int.J. Radiat.Biol.** 72, 423-433

Testard,I. and Sabatier,L. 2000. Assessment of DNA damage induced by high-LET ions in human lymphocytes using the comet assay. **Mut.Res.** 448, 105-115

Tice, R.R. and Vasquez, M. 1999. Protocol for the application of the pH>13

alkaline single cell gel (SCG) assay to the detection of DNA damage in mammalian cells.

Tice, R.R., Agurell, E., Anderson, D., Burlinson, B., Hartmann, A., Kobayashi, H., Miyamae, Y. Rojas, E., Ryu, J-C. and Sasaki, Y.F. 2000. Single Cell Gel/Comet Assay: Guidelines for *In Vitro* and *In Vivo* genetic toxicology testing. **Environ. Mol. Mutagen.** 35, 206-221

Wada,S., Kurahayashi, H., Kobayashi, Y., Funayama, T., Yamamoto, K., Natsuhori, M. and Ito, N. 2003. The relationship between cellular radiosensitivity and radiation-induced DNA damage measured by the comet assay. **J. Vet. Med. Sci.** 64(4), 471-477

West, C.M.L., Davidson,S.E., Roberts,S.A. and Hunter,R.D. 1993. Intrinsic radiosensitivity and prediction of patient response to radiotherapy for carcinoma of the cervix. **Br.J. Cancer** 68, 619-823

West, C.M.L. 1995. Invited Review: Intrinsic radiosensitivity as a predictor of patient response to radiotherapy. **Br.J.Rad.** 68, 827-837

Wojewódzka, M., Kruszewski, M., Iwaneńko, T., Collins, A. and Szumiel, I. 1998. Application of the comet assay for monitoring DNA damage in workers exposed to chronic low-dose irradiation. I. Strand breakage. **Mut.Res.** 416,21-35

Würm, R., Burnet, N.G., Duggal, N., Yarnold, J.R. and Peacock, J.H. 1994. Cellular radiosensitivity and DNA damage in primary human fibroblasts. **Int. J. Radiat. Oncol. Biol. Phys.** 30, 625-633

Chapter 4

Apoptosis Studies

Death? What is the fuss about death, use your imagination, try to visualize a world without death...Death is the essential condition of life, not an evil.

Charlotte Perkins Gilman (1860-1935)

4.1 Introduction

Radiation therapy is the method of treatment for approximately half of all cancer patients (Zhivotovsky *et al.*, 1999). By increasing the radiosensitivity of the tumor cells the potential cure from malignancy can be enhanced, as the major biological factor in radiotherapy failure is radioresistance. Radiosensitivity is however multifactoral but one cellular mechanism on which much research has been focused is the method of killing tumor cells through apoptosis.

A highly controlled and genetically organised programmed cell death (PCD) is evident in all tissues and is part of normal cellular turnover (Blatt and Glick, 2001). Apoptosis is one type of PCD characterised by a sequence of intracellular biochemical pathways accompanied by a particular pattern of

changes in cellular morphology first described by Kerr *et al.* (1972). This process performs the vital function of eliminating abnormal cells, resolving of inflammatory reactions, healing wounds and maintaining homeostasis of tissue and organs by controlling proliferation, growth and differentiation (Ormerod, 2001). At a given time the natural occurrence of apoptosis in normal tissue accounts for less than 2% of the cells. In the liver, for example, under normal healthy conditions about one to five cells per 10 000 hepatocytes are undergoing apoptosis (Brauer, 2003). This may increase in chronic conditions but numbers greater than 10% are rare. Normal physiological processes including involution of the breast after lactation, and shedding of the endometrium during menstruation are the result of hormone-induced apoptosis (Vinatier and Subtil, 1996).

Research done on the nematode *Caenorhabditis elegans* showed that during ontogenesis of the worm, exactly 131 of 1090 cells die by apoptosis, leaving the adult worm with 959 cells (Böhm and Schild, 2003; Keechle and Zhang, 2002). This made it reasonable to deduce that cells die in a genetically programmed manner.

Cells have one of two options when confronted with increasing DNA damage, to repair or to undergo apoptosis. They may switch to cell cycle arrest and repair the damage or may commit to a planned cell death. The ability to control this mechanism appears to be essential in preventing the progression of disease, in effect by not permitting un-repaired damage to lead to mutations and carcinogenesis, apoptosis normally fulfills a protective role. The capability to undergo apoptosis is affected by one of three possibilities, mutation; loss of

pro-apoptotic gene encoding (*p53* and *bax*) and by over expression of genes encoding for suppression of apoptosis (*Bcl-2* or *Bcl-x_L*) (Bernstein *et al.*, 2002). A decreased level of apoptosis could be associated with cancer, autoimmune diseases, viral infections, chemotoxic resistance and lymphoproliferative diseases. On the other hand abnormally high levels of apoptosis could be associated with neurodegenerative disorders, AIDS and Myelodysplastic syndromes (Vinatier and Subtil, 1996). *In vivo* the cells undergoing apoptosis are antigenically modified making them susceptible to phagocytosis by macrophages or surrounding cells avoiding an inflammatory reaction (Harms-Ringdahl *et al.*, 1996). Following the apoptotic insult the process of apoptosis is time dependent. It is dependent on the triggering stimulus and is cell type specific (Shi *et al.*, 2001). By contrast, necrosis is an alternate form of cell death displaying none of these cellular morphological characteristics and occurs rapidly after the insult. It results from trauma or accidental damage affecting large groups of cells and is an unplanned and unstructured process.

4.1.1 Biochemical Events

The field of apoptosis is ever expanding and of interest to many authors making valuable contributions towards revealing the various signal transduction pathways culminating in cell suicide. Apoptosis is an event that requires energy and the cell is metabolically active during the process unlike necrosis in which the cell participates passively (Vermes *et al.*, 2000). It appears, with the exception of a few cell types, that the major biochemical

events (phosphatidylserine translocation and DNA fragmentation) occur in all cells (Allen *et al.*, 1997), irrespective of the eventual pathway followed.

A structural change evident in the plasma membrane is the translocation of phosphatidylserine (PS). The plasma membrane is composed of a number of phospholipids including aminophospholipids (phosphatidylserine and phosphadtidylethanolamine) and choline phospholipids (phosphatidylcholine, sphingomyelin) (Blatt and Glick, 2001). Under normal conditions the cell maintains an imbalance between the phospholipid content of the inner and outer leaflet of the plasma membrane by translocation of PS from the outer to the inner leaflet. However during apoptosis this imbalance is lost, and the presence of PS is equilibrated between the two leaflets, resulting in the exposure of PS on the outer cell surface, triggering phagocytosis of the apoptotic cells *in vivo*. This can be quantified by flow cytometry using the PS-binding protein Annexin-V that binds to the externalised phosphatidylserine.

Transduction pathways are defined as intrinsic and extrinsic, mitochondrial and death receptor (DR), p53–dependent and –independent and the caspase-dependent and –independent pathways (Ashe and Berry, 2003). The process follows a basic route whereby the death-inducing signal is sensed and either the intrinsic or extrinsic signal transduction pathway is activated (Figure 4.1). Each pathway has is own initiation and execution process and is interrelated to other pathways resulting in cellular morphological and biochemical alterations characteristic of apoptosis (Ashe and Berry, 2003; Kiechle and Zhang, 2002).

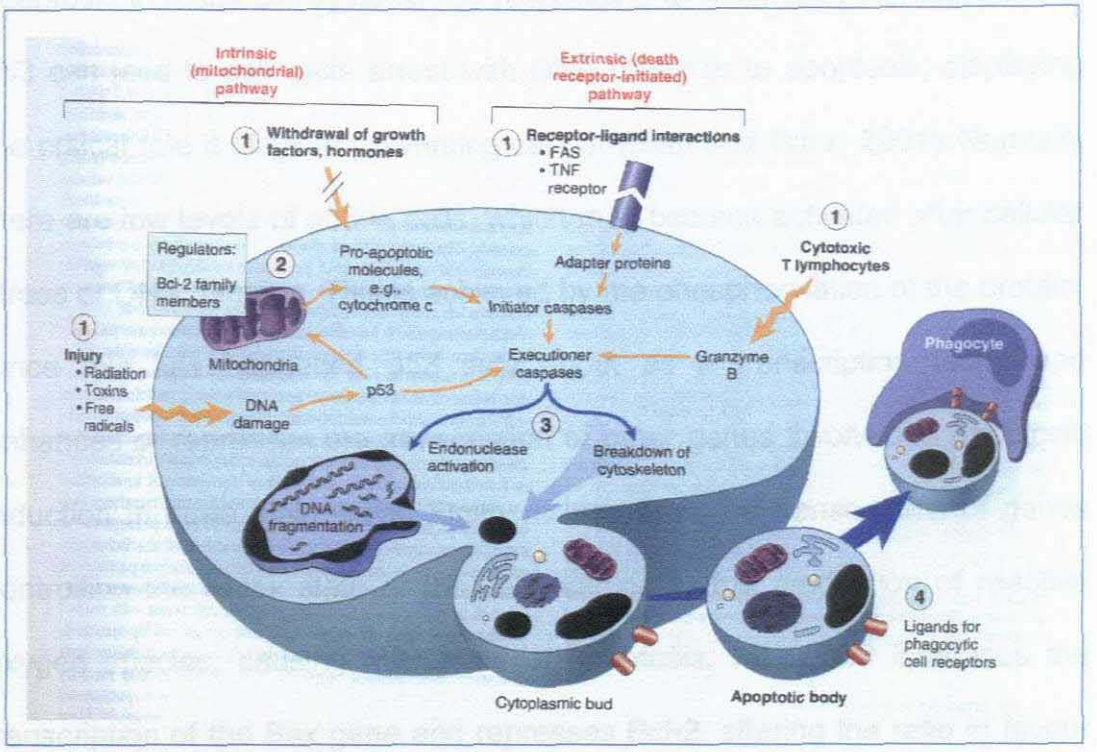

Figure 4.1: *Schematic representation of the mechanisms of apoptosis. The major inducers of apoptosis labelled* ***(1)*** *include specific death ligands, withdrawal of hormones or growth factors and agents such as radiation. Some stimuli for example Cytotoxic T-lymphocytes directly activate caspases while others act via adapter proteins and initiator caspases or due to the release of cytochrome-c by the mitochondria. The Bcl-2 family* ***(2)*** *control the process either by promoting or inhibiting cell death. Executioner caspases* ***(3)*** *trigger endonucleases and proteases that degrade cytoskeletal and nuclear proteins resulting in apoptotic bodies* ***(4)****. These express ligands, which enable uptake by phagocytic cells. (Kumar et al., Pathologic Basis of Disease, 7th Ed., 2005).*

Cancerous cell lineages have been used in research to reveal the apoptotic pathways. One must bear in mind that commonly cancer cells have defective apoptotic mechanisms. The interpretation and application of these data must therefore be done within this context. Within normal cells, cell types of different origins may utilize different suicide pathways (Ashe and Berry, 2003).

Besides these regulatory features, the p53 gene is a further regulator of apoptosis in many cell systems. By responding to a stimulus the activation of p53 can lead to cell cycle arrest with DNA repair or to apoptosis, displaying the critical role it plays in preventing cancer (Blatt and Glick, 2001). Normally there are low levels of p53 in cells, which may become activated after cellular stress or DNA damage. This is achieved by the phosphorylation of the protein. Once this has happened p53 sets about as a transcription factor and enhances or represses the transcription of other genes involved in apoptosis induction in three main ways. Firstly, it increases the transcription of genes controlling the redox state of the cell, leading to the production of reactive oxygen species, causing mitochondrial apoptosis. Next, p53 increases the transcription of the Bax gene and represses Bcl-2, altering the ratio in favour of apoptosis along the mitochondrial pathway. Lastly, p53 also up-regulates Fas receptor transcription making the cell susceptible to apoptosis on contact with Fas ligand (Blatt and Glick, 2001).

4.1.1.1 Caspases

Caspases (Cystein dependent ASPartate cleaving proteASE) are normally present in all cells as inactive pro-enzymes that on activation by proteolysis may engage in enzymatic activity (Vermes *et al.*, 2000, Blatt and Glick, 2001). Caspases are separate from other proteases in that they use a cystein for catalysis and cleave only after aspartic acid residues. They are manufactured as a single polypeptide chain and are inactive zymogens or procaspases. The procaspase has a protease domain and a NH_2 terminal prodomain. This

prodomain varies in length depending on the function the caspase will perform. Prodomains of less than 30 amino acids are found in effector caspases and longer prodomains, more than 100 amino acids, are those of initiator and inflammatory caspases (Ashe and Berry, 2003).

When activated the protease domain of the polypeptide chain is cleaved into a large (20kDa) and small subunit (10 kDa). These two units then dimerize forming a heterodimer; two heterodimers then associate to form a tetramer, which is needed for the active form of caspases (Walker *et al.*, 1994).

The activation of the caspases is often carried out by the caspases themselves, leading to a domino effect of one caspase activating another. A cascade of events is created that leads to the cleavage of macromolecular structures commencing the programmed self-destruction of the cell.

At present 14 caspases are known in mammalian tissue with caspases 11, 13 and 14 not having a human homologue identified yet. (Ashe and Berry, 2003). Caspases can be placed into three categories depending on the substrate specificity for the three amino acids before the aspartic acid. (Blatt and Glick, 2001; Ashe & Berry, 2003) Group I; caspases 1, 4 and 5 are involved in inflammatory processes. Group II; caspases 6, 8, 9 and 10 are referred to as signalling or initiator caspases because they are able to activate other caspases. Finally Group III; caspases 2, 3 and 7 are enzymes known as effector or executioner caspases as they are activated by other caspases. Once these caspases are activated, it appears as if the cell is committed to undergo apoptosis.

Caspases 3 and 7 are key effector caspases (group III), and cleave other caspases as well as targets in the cytoplasm, like cytokeratin 18, and in the nucleus poly(ADP-ribose)polymerase (PARP). Nicholson *et al.,* (1995) mapped the cleavage site of PARP and recognized the tetra-peptide Asp-Glu-Val-Asp (DEVD) as the cleavage site for caspase-3. Using this information, polyclonal antibodies are generated to recognise only the active form of caspase-3. These antibodies are made against an active human caspase-3 fragment and bind to an epitope exposed during activation cleavage of pro-caspase-3. A fluorogenic substrate specific to caspase 3 and 7 may then be used to demonstrate and quantify intracellular caspase activity.

4.1.1.2 DNA-Fragmentation

Kerr *et al.,* (1972), described the cytological changes in a cell undergoing apoptosis which were clearly different from those seen in cells undergoing death by necrosis. Necrosis reflects a pathologic form of injury to which the cells responds in a passive way, whereas there is evidence that apoptosis is a genetically programmed cell death.

In response to an apoptotic stimulus the apoptotic pathway may target the nucleus, resulting in the classic features of chromatin condensation and nuclear fragmentation. DNA undergoes cleavage into fragments of about 180-200bp, which was first observed and described by Wyllie (1980). This cleavage is thought to occur at the linker regions between the nucleosomes and has been shown to be a late event in the apoptotic cascade. These

fragments can be seen on an agarose gel forming the now well-known DNA-ladder and has become the hallmark for identification of apoptosis (Böhm and Schild, 2003). However, internucleosomal DNA fragmentation is not displayed throughout all cell systems and does not always occur during apoptosis (Vinatier and Subtil, 1996;Ormerod, 2001).

The expression of a protein involved in apoptosis can be measured by immunofluorescence, if a suitable antibody is available. Using flow cytometry, multi-parametric measurements can be made on single cells, whereas biochemical measurements e.g. fluorometric assays of caspase 3/7 activity, record the average reading for a population of cells and do not take the heterogeneity of cells into account (Ormerod, 2001). At least 10 000 events are captured enabling correlations to be drawn for example between DNA content and expression of proteins involved in DNA degradation. A DNA histogram reflects the comparative number of cells in G_1/G_0, S and G_2/M phases of the cell cycle as well as the apoptotic population which forms the sub-G_1 peak i.e. the peak just below the G_1 peak (Ormerod, 2002; Shinomiya, 2001; Sgonc and Gruber, 1998).

The action of endonucleases is responsible for the cleavage of DNA into numerous fragments; (Ormerod, 2001) generating a large amount of terminal 3'-hydroxyl (3'OH) ends at the site of these DNA nicks. Unfixed cells can loose these small fragments of DNA and it is therefore important to fix these inside the cell by cross-linking them in paraformaldehyde before fixation in 70% ethanol. By adding the enzyme terminal deoxynucleotidyl transferase (TdT) to the cell sample a FITC-labeled deoxynucleotide triphosphate can be

added in a template-independent manner to the 3'OH ends of either single or double stranded DNA and the fragmented DNA quantified by flow cytometry (Allen *et al.*, 1997).

4.1.2 Morphological Features of Cells Undergoing Apoptosis and Necrosis

Irrespective of the mode of apoptotic induction or cell type, a cell committed to die seems to present with a certain continuity in morphologic features (Allen *et al.*, 1997). There is a clear progression through the process beginning with initiation, execution, disintegration and elimination of the cell. Cell shrinkage is the earliest light microscopic characteristic and occurs roughly at the same time as the nuclear changes. Due to the loss of K+ across the plasma membrane and cleavage of the cytoskeleton the cell becomes smaller and denser. The plasma membranes become convoluted creating surface blebbing seen almost exclusively in culture systems, as the event is too short to be observed *in vivo*.

The earliest ultra structural changes are condensation of chromatin on the nuclear membrane, which then form distinct dark, crescent shaped clumps. These clumps eventually bud from the nuclear membrane and the nucleus undergoes fragmentation. Nuclear material and organelles are enveloped in cytoplasmic membrane bound fragments called apoptotic bodies, which are swiftly phagocytosed *in vivo*, without eliciting an inflammatory response.

An additional morphological feature observed in p53 mutated cell lines e.g. CHO-K1 cells, is the formation of giant cells (Illidge *et al.*, 2000). These

cells display the general cyto-morphological features seen commonly in post radiation smears. These include macrocytic changes with an increase in nuclear and cytoplasmic volumes, abnormal multilobulated nuclei and numerous micronuclei often leading to bizarre cell shapes (Ng, 2003). These features described can be examined by fluorescence (Figure 4.16) or light microscopy (Figure 1.3).

In contrast to apoptosis the morphologic features occurring in a necrotic cell are as a result of ATP depletion. Osmotic barrier loss and the lack of ion-pumping action of the cell membrane results in marked cellular swelling. Disruption of the organelles, leaky mitochondria, and rupture of the cell membrane results in spillage of cellular contents into the surrounding tissue. This elicits an intense inflammatory reaction evident *in vivo* (Brauer, 2003). Chromatin looses structure in a non-specific manner and the DNA degradation is random and in the final stages, it scatters (karyorrhexis) and disappears (karyolysis) (Allen *et al.*, 1997).

Programmed cell death takes many forms, both morphologically and biochemically and examination with multiple biochemical markers at predetermined time points should be used to determine the mechanism of cell death in a particular biological system. Secondary necrosis occurs when apoptotic cells cultured *in vitro* swell and undergo lysis. This terminal stage of cellular death occurs after prolonged periods of incubation where apoptotic cells terminate their metabolism, lose membrane integrity and release their cytoplasmic contents into the culture medium. Cells that initiated apoptosis may exhibit some of the morphological phenotypes associated with necrosis.

4.2 Materials and Methods

4.2.1 Cell Lines and Maintenance

Two cell lines were used in this study.

Chinese Hamster Ovary cells (CHO-K1) were cultured in monolayers in Alpha minimal essential medium (αMEM) completed with 10% foetal calf serum and were kindly provided by Dr. Slabbert, ITemba LABS, Somerset West.

TK 6 cells are a human B lymphoblastoid cell line that was isolated from the lymphoblastoid HH4 line and express wild-type p53 protein. The cells were grown in suspension in RPMI containing 2mM glutamine and 10% foetal bovine serum. The cells were kindly provided by Dr. Antonio Serafin, Department of Radiobiology University of Stellenbosch.

Both cell lines were maintained at 37°C in flasks in a 5% CO_2 humidified atmosphere.

4.2.2 Induction of Apoptosis

4.2.2.1 Irradiation

Cell samples were exposed to ^{60}Co γ-rays at room temperature (~22°C). The ^{60}Co γ-source was in a vertical position directed upwards delivering a dose rate of 0.29 Gy/min at a source surface distance of 70cm. Samples were placed on a 6mm thick Perspex table (build up) in a 30 x 30 cm^2 field with a 15 cm thick backscatter Perspex block fixed directly above. A 0.6cm^3 thimble Farmer ionisation chamber was used to confirm the dose at the position of the

cells.

Neutron irradiation was conducted from a p(66/Be) neutron vertical beam directed downwards, using a dose rate of 0.35 Gy/min. Cell samples were placed in a 29 x 29 cm^2 field and a source surface distance (SSD) of 150 cm was used at a gantry angle of 0°, on a 15cm thick backscatter Perspex block. Build up material consisted on 20mm polyethylene. To verify the dose at the position of the cells an 80-cm^3 Far West ionisation chamber and a BNC Portanim current digitiser was used.

4.2.2.2 Etoposide

Etoposide is a topoisomerase II inhibitor; $C_{29}H_{32}O_{13}$ (VESPESID, Bristol-Myers Squibb Ltd.), which induces DNA strand breaks by an interaction with DNA-topoisomerase II and is a known apoptosis inducing agent. TK 6 cells are characterised by readily undergoing apoptosis and were treated with 20mM etoposide and incubated for 48 hours. This served as a positive control.

4.2.3 Detection of Apoptosis

4.2.3.1 Caspase 3/7 Activity

Measuring caspase-3 and –7 activity was achieved using the Apo-ONE ™ Homogeneous Caspase-3/7 Assay (Promega, USA). The caspase –3/7 substrate rhodamine 110, (z-DEVD-R110), is present as a profluorescent substrate. On cleavage and removal of the DEVD peptides by caspase-3/7 activity and excitation at 499nm, the Rhodamine 110 leaving group becomes intensely fluorescent (DEVD used to describe the amino acid sequence Asp-

Glu-Val-Asp). Cells are seeded in wells in opaque multi-well plates. Fluorescence of each well was measured 4 hours after adding the reagent by a spectrophotometer (Varian Instruments, Australia) at an excitation wavelength of 485 nm and an emission wavelength of 530 nm using Cary Eclipse software. The amount of fluorescent product generated is proportional to the amount of caspase-3/7 activity present in the sample.

4.2.3.2 DNA Fragmentation and Flow Cytometric Analysis

DNA fragmentation was detected using the ApoDirect Kit (BD Biosciences Pharmingen). DNA breaks are labelled using single step staining to identify apoptotic cells by flow cytometry. Terminal deoxynucleotidyl transferase enzyme (TdT) catalyzes a template-independent addition of fluorescein isothiocyanate labeled deoxyuridine triphosphates (FITC-dUTP) to the 3'OH ends of the DNA double or single strand breaks. Propidium Iodide solution for staining total DNA content was included in the kit.

A flow cytometry analysis was performed on a FACSCalibur cytometer (Becton Dickinson) equipped with a 488nm argon laser. Ten thousand events were acquired from each sample and were analysed using the CellQuest program.

A scatter diagram of forward light-scatter versus side light-scatter was obtained as well as DNA histograms, which were also analysed for cell cycle disruption using ModFit software. Dual parameter displays were created as Propidium Iodide (FL-1), fluorescing at 623nm stains for DNA content versus FITC-dUTP (FL-3), fluorescing at 520nm stains for apoptotic cells.

4.2.3.3 Morphologic Measurement of *in vitro* Apoptosis by Fluorescence Microscopy

The measurement of apoptosis *in vitro* was performed as described by Akudugu and Bohm (2001).

A minimum of 500 cells was evaluated per sample. The frequency of apoptotic cells, corrected for spontaneous apoptosis in untreated samples was scored according to criteria described by Mirkovic *et al.,* (1994), and Weil *et al.,* (1996). These included cells displaying a pyknotic, fragmented or crescent-shaped nuclei and overall shrinkage as shown in Figure 4.16. Apoptosis was expressed as the mean (± SD) ratio of apoptotic cells to the total number of cells scored and calculated using Graph Pad Prism software. Giant cells were observed but not enumerated.

4.2.4 Cell Preparation

4.2.4.1 Caspase 3/7 Activity

CHO-K1 cells were harvested from confluent flasks of exponentially growing stock cultures and prepared as single cell suspensions by trypsination, which caused cells to round up and detach from the surface of the culture flask. Alpha minimal essential medium (α-MEM), completed with 10 % foetal calf serum, was added to stop the tripsinisation. An estimate of cell numbers per unit volume was quantified using a haemocytometer. Serial dilutions of known cell numbers were exposed in test tubes to 0; 4; 8 and 12 Gy ^{60}Co gamma

and to iso-effective doses of 0; 2; 4 and 6 Gy neutron radiation, and incubated for 48 and 72 hours at 37°C.

Due to uncertainty regarding the potential overgrowth in the untreated control wells and extensive cell kill in the wells of the higher radiation doses, it was decided to seed according to expected cell kill and doubling time. A duplicate plate was set up for cell counting purposes only and exposed to the same conditions as those in the test plate.

The influence of serum quality and quantity on caspase 3/7 activity was unknown. To address this various percentages of serum in growth medium were incubated with and without cells and read at different time intervals post addition of reagent.

Cell suspensions of approximately 2 x 10^5 cells/ml in a volume of 50μl were prepared. One hundred micro-litres of cell suspension were seeded in triplicate in wells in multi-well plates for each dose point. Simultaneously, 50μl of cell suspension were seeded at the same dose points to determine which amount would result in the required number of cells post incubation. A blank well was set up containing only αMEM.

TK 6 lymphoblastoid cells were prepared according to the instructions included in the kit (Apo-ONE Homogeneous Caspase 3/7 Assay, Promega, USA) for a 96 well plate, 200μl final reaction volume. A single cell suspension was prepared prior to a cell count and centrifuged at 300 rpm for 5min. The supernatant was discarded and the cells resuspended in warm RPMI to a 20 x 10^4 concentration. A hundred micro litres of TK 6 cell suspension previously

treated with 20mM etoposide an incubated for 48 hours, as well as untreated TK 6 cell suspensions (approx. 20 x 10^4 cells), were seeded in triplicate. A blank well was set up containing 100μl of RMPI only.

Preparation and addition of reagent

The reagent included in the kit was added according to instructions supplied in the Apo-ONE Homogeneous Caspase 3/7 Assay (Promega, USA). The substrate and buffer were thawed to room temperature and mixed well followed by diluting the substrate 1:100 with buffer to the desired volume. 100μl reagent was then added to all cell samples, including the blanks, taking care not to cross-contaminate samples or create bubbles. Blank controls are used to measure background fluorescence related to the culture system and bubble interference with the fluorescence reading. Mixing was further enhanced by the use of a plate shaker, incubating at room temperature up to read time. All samples were shielded from light.

4.2.4.2 DNA Fragmentation

One hour prior to radiation, CHO-K1 and TK6 cells were seeded in culture flasks in 10 ml growth medium for each dose point at densities of anticipated cell kill and doubling time. Cells were irradiated in culture flasks at equivalent doses of 0; 4 and 8 Gy p(66/Be) neutron and ^{60}Co γ-radiation, followed by 24, 36 and 48 hours incubation at 37°C.

After incubation, single cell suspensions were prepared and centrifuged in 5ml

polystyrene tubes and the growth medium aspirated. The cells were resuspended in 1% (w/v) paraformaldehyde in PBS at a concentration of 1-2 x 10^6 cells/ml and placed on ice for 45 min in order to permeabilise and fix the cells. This was followed by centrifugation for 5 min, discarding the supernatant and resuspending in 5ml of PBS. The wash was repeated and cells gently resuspended in the residual PBS. Cell concentration was adjusted to 1-2 x 10^6 in ice-cold ethanol, 70% (v/v), mixed gently and incubated at -20°C for one hour (ApoDirect Kit, BD Biosciences, Pharmingen). Centrifuging for 5 min followed, to remove the ethanol without disturbing the pellet. Each tube was resuspended in 1ml of wash buffer (included in ApoDirect kit), centrifuged and supernatant removed. The wash buffer treatment was repeated once to ensure complete removal of the ethanol. Each tube was then resuspended in 50µl of FITC staining solution (BD Biosciences, Pharmingen). Cell samples were incubated overnight at room temperature on a plate rocker. After incubation, 1ml rinse buffer was added and each tube centrifuged for 5 min. The supernatant was removed and the rinse was repeated. After the supernatant was removed, 0,5ml of the PI/RNase staining buffer was added and mixed gently. Cells were incubated for 30 min at room temperature in the dark and analysed within 3 hours. Negative and positive controls for DNA fragmentation were included in the kit and run concurrently in each experiment.

4.2.4.3 Cellular Morphology

A single cell suspension (2 X 10^4) was obtained from exponentially growing CHO-K1 cells and seeded in triplicate in 35mm plastic petri-dishes (Corning, USA) containing 22mm glass coverslips (Chance Propper, England) to a final volume of 2ml. One hour after plating, cells were exposed to 0; 4; 6; 8 and 10 Gy ^{60}Co gamma and p(66/Be) neutron radiation and incubated for 48 hours at 37°C. After incubation treated and untreated cultures were fixed at room temperature (~22°C) in methanol: acetic acid (3:1, v/v) and air-dried.

Staining was performed using the fluorochrome Acridine Orange (AO), which stains nucleic acids presenting DNA as green fluorescence and RNA as red fluorescence. A stock solution consisting of 1.0mg AO ($C_{17}H_{20}N_3Cl$, FW=301.8; Sigma, South Africa) per ml phosphate buffer (Gurr Buffer, pH 6.8) was made up and stored in the dark at 4°C for several months. For staining, 0.4ml of stock solution is added to 40ml of buffer to a final concentration of 10μg Acridine Orange per ml of buffer. The stain was pre-warmed to 37°C as this enhances the interchelation of the fluorochrome and thereby improves the image quality during microscopy. The cell sample was exposed to the staining solution for 2 minutes, washed in warmed PBS, air-dried and the coverslips mounted on slides for microscopy. Morphological characteristics, including giant cell formation were evaluated in 500 CHO-K1 cells per dose point.

4.3 Results and Discussion

4.3.1 Caspase Activity

To establish the influence of serum quantity and quality on caspase 3/7 activity, treated and untreated samples of CHO-K1 cells were incubated for 48 hours post 12 Gy ^{60}Co γ- irradiation. Various percentages of serum in αMEM were simultaneously incubated with and without cells and read at different time points (2, 7 and 16 hours) post addition of reagent as shown in Table 4.1. An explanation of abbreviations is shown in the key below.

Test	Explanation of abbreviation.
10%	Medium + 10% serum, no cells
20%	Medium + 20% serum, no cells
0%	Medium only, no serum, no cells
0	Cells cultured in medium + 10% serum (Control)
r10%	Irradiated (12 Gy) medium +10% serum; no cells
sfree	Cells cultured in serum free media
fresh	Cells irradiated (12 Gy); cultured, replaced with fresh before reading
old	Cells irradiated (12 Gy); cultured, media not replaced

Table 4.1: *Test samples cultured in varying qualities and quantities of αMEM with or without CHO-K1 cells. After 48 hrs incubation caspase 3/7 activity was measured by adding reagent and reading at different time intervals 2, 7 and 16 hrs. Irradiated samples were exposed to 12 Gy ^{60}Co γ-radiation.*

TEST	FLUORESCENCE VALUES WITH OR WITHOUT CHO-K1 CELLS								
	2 hrs			7 hrs			16 hrs		
10%	-3.231	-3.417	-2.656	-1.493	-1.691	-1.574	0.683	-0.889	0.582
20%	0.646	2.372	5.741	5.425	5.243	10.816	9.943	9.846	14.793
0%	0.738	1.422	-1.253	1.471	0.523	-1.601	2.012	0.984	-0.726
0	14.452	13.183	5.747	21.721	18.677	9.444	27.026	24.667	13.661
r10%	1.947	5.063	5.840	-1.036	1.716	2.715	1.212	2.969	5.290
sfree	123.085	146.486	128.397	156.433	168.222	148.719	195.477	195.933	170.730
fresh	121.171	130.591	126.453	295.443	231.180	225.281	468.193	354.225	346.996
old	191.006	209.362	175.367	311.581	304.250	206.387	404.017	379.389	242.534

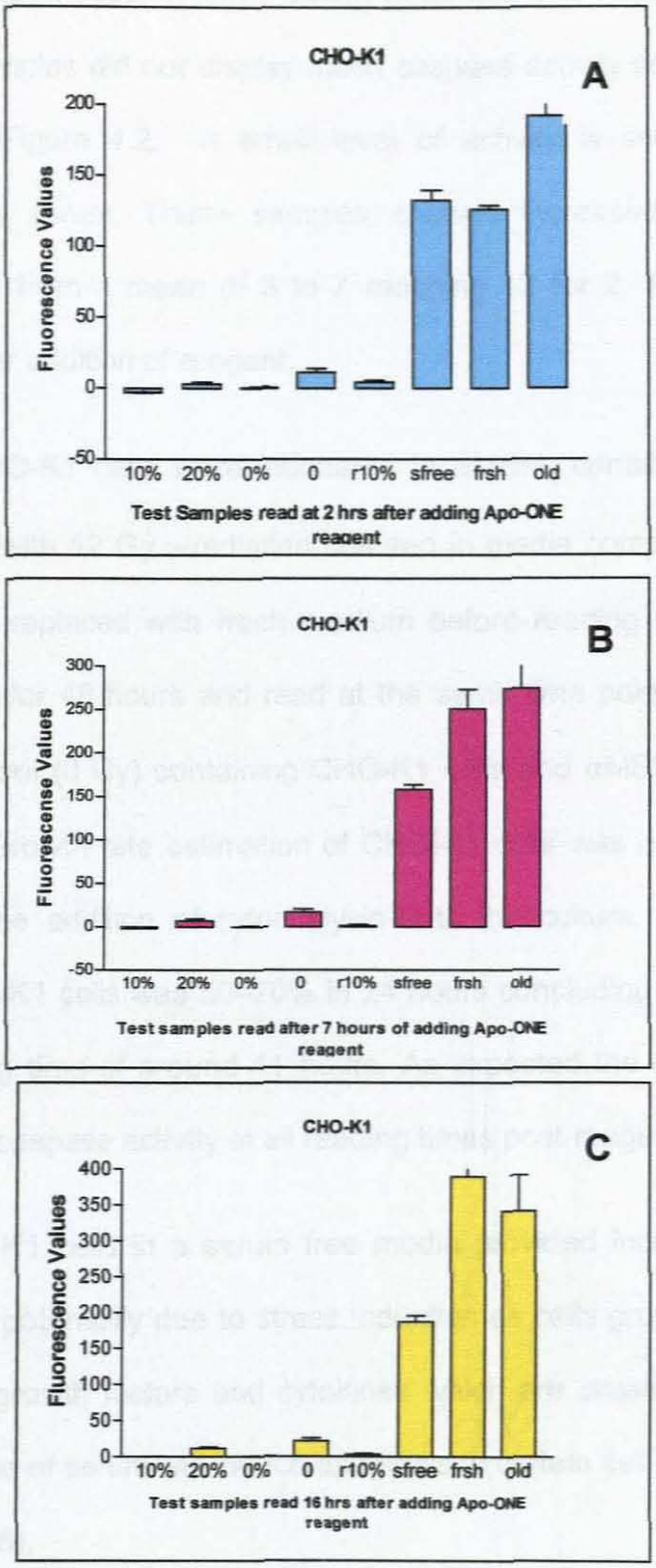

Figure 4.2: *Bar graphs displaying results of test samples with or without CHO-K1* ***(A-C)*** *cells cultured in varying qualities and quantities of αMEM. Caspase 3/7 activity was measured 48 hrs post incubation by adding ApoONE reagent and reading at different time intervals of 2, 7 and 16 hrs. Irradiated samples were exposed to 12 Gy ^{60}Co γ-radiation. An explanation of abbreviations is provided on Pg.98.*

The different percentages of serum added to treated and untreated αMEM in the acellular samples did not display much caspase activity as shown by the bar graphs in Figure 4.2. A small level of activity is seen in samples containing 20% serum. These samples showed increased activity as a function of time from a mean of 3 to 7 reaching 12 for 2, 7 and 16 hours respectively after addition of reagent.

Samples of CHO-K1 cells were incubated in αMEM, containing no serum (sfree); treated with 12 Gy γ-radiation cultured in media completed with 10% serum (old); or replaced with fresh medium before reading (frsh). Samples were incubated for 48 hours and read at the same time points post reagent addition. A control (0 Gy) containing CHO-K1 cells and αMEM (10% serum) was included. Growth rate estimation of CHO-K1 cells was performed in our laboratory by the addition of cytochalysin-B to the culture. The rate of bi-nucleated CHO-K1 cells was 50–70% in 24 hours concluding that these cells have a doubling time of around 11 hours. As expected the control samples (0 Gy) showed caspase activity at all reading times post reagent addition.

Culturing CHO-K1 cells in a serum free media provided increased caspase activity. This is potentially due to stress induction as cells growing *in vitro* are dependent on growth factors and cytokines which are present in the serum and the absence of serum will induce apoptosis in certain cell lines (Al-Rubeai and Singh, 1998).

Replacing culture media with fresh media before reading reduced the measured caspase activity induced by 12 Gy ^{60}CO γ-radiation (frsh). The

readings taken from the samples irradiated by 12 Gy gamma radiation without replacing the media were always higher (old). From these results it was concluded that by not replacing the media with fresh media before addition of reagent, a more representative reflection of total caspase 3/7 activity could be expressed by the cells over the entire culturing period of 48 hours.

Based on these findings it was decided to determine the effect of both ^{60}CO γ- and p(66)/Be neutron radiation on CHO-K1 cells as described above. Two time intervals of 24 and 48 hours were evaluated for both radiation modalities with these data demonstrated in Table 4.2. High doses of gamma (12 Gy) and neutron (6 Gy) radiation, reached maximum values of only 26 and 34 at 24 hours. At 48 hours the level of caspase activity was less than that at 24 hours for gamma radiation. Neutron induced caspase 3/7 activity was marginally higher as seen in Figure 4.3.

TK 6 cells treated with 20mM etoposide for 48 hours reflected caspase 3/7 activity as expected and were used as a positive control.

Table 4.2: *Caspase 3/7 activity induced in CHO-K1 cells exposed to 0; 4; 8 and 12 Gy ^{60}CO γ-irradiation and 0; 2; 4 and 6 Gy p(66/Be) neutron radiation incubated for 24 and 48 hours. Caspase activity was induced in TK6 cells by exposure to 20mM etoposide for 48 hours and used as a positive control.*

CELL	TIME	TYPE	DOSE (GY)	ETOPOSIDE	FLUORESCENCE VALUES				MEAN
CHO-K1	24 hrs	Gamma	0	-	18.749	17.149	17.639	15.121	**17.16**
			4	-	18.090	21.435	22.104	22.880	**21.13**
			8	-	25.821	25.955	26.706	26.996	**26.40**
			12	-	28.211	29.890	31.072	28.699	**29.47**
		Neutron	0	-	27.452	23.357	23.613	23.382	**24.50**
			2	-	24.854	23.659	23.332	21.218	**23.30**
			4	-	22.687	21.541	20.147	23.337	**21.93**
			6	-	29.708	33.699	34.949	36.150	**33.63**
	48 hrs	Gamma	0	-	8.162	9.349	11.569	13.115	**10.55**
			4	-	10.111	12.545	14.190	14.749	**12.90**
			8	-	20.321	17.145	15.783	15.048	**17.07**
			12	-	18.846	20.744	24.225	28.761	**23.14**
		Neutron	0	-	23.160	23.029	23.466	23.032	**23.17**
			2	-	22.461	22.498	19.735	20.492	**21.30**
			4	-	28.859	23.791	25.134	27.222	**26.25**
			6	-	28.420	32.462	31.032	32.190	**31.03**
TK6	-	-	-	20mM	194.699	197.229	200.601	209.203	**200.43**

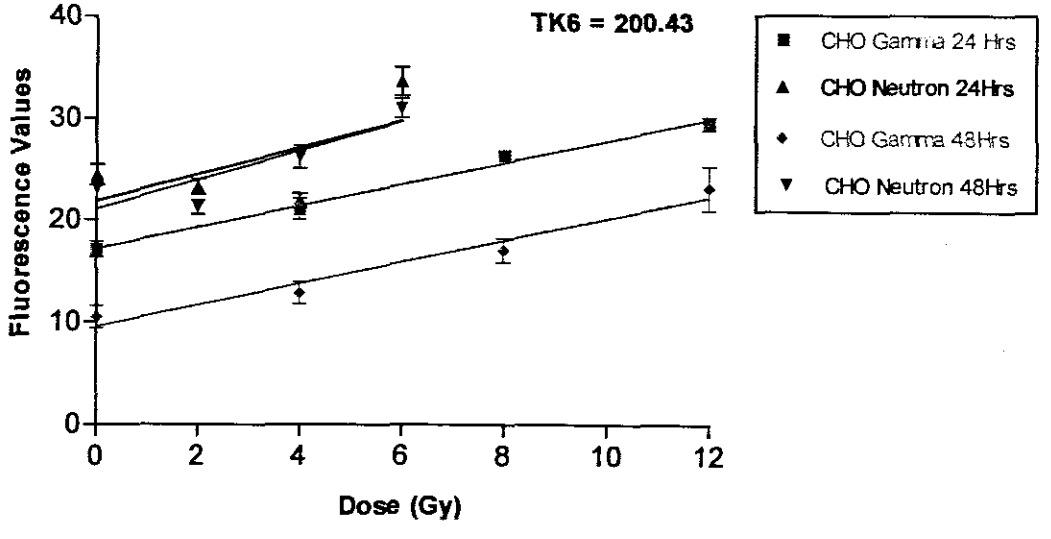

Figure 4.3: *Caspase 3/7 activity measured in CHO-K1 cells at 24 (■) and 48 hours (◆) post 4, 8 and 12Gy ^{60}CO γ-irradiation as well as at 2, 4 and 6Gy, 24 (▲) and 48 hours (▼) post p(66/Be) neutron irradiation. Caspase activity in TK6 cells by 20mM Etoposide for 48 hours was calculated to a mean value of 200.43.*

Although the dose responses are somewhat ineffectual they do deviate significantly from zero ($p < 0,0001$) for both 24 hours ($r^2 = 0.92$) and 48 hours ($r^2 = 0.75$) post gamma irradiation (Figure 4.3). The same applies to the neutron response curves at 24 hours ($p = 0.0148$) and at 48 hours ($p = 0.0001$). This indicates a linear increase in caspase 3/7 activity as a function of increased radiation dose. Low intra-experimental variability (Table 4.2) was reflected by the small error bars shown in Figure 4.3.

The effect of ^{60}CO γ-radiation on CHO-K1 cells was then evaluated at 48 and 72 hours post irradiation at doses of 0; 4; 8 and 12 Gy. TK 6 cells, a human lymphoblastoid cell line that readily undergo apoptosis was exposed to 20mM etoposide for 48 hours and included as a positive control. This data is demonstrated in Table 4.3 and graphically represented in Figure 4.4.

Table 4.3: *Caspase 3/7 activity measured in CHO-K1 cells exposed to 0; 4; 8 and 12 Gy ^{60}CO γ-irradiation and incubated for 48 and 72 hours. Samples of TK 6 were untreated or exposed to 20mM etoposide for 48 hours and used as a positive control for caspase induction.*

CELL	TIME	DOSE (GY)	ETOPOSIDE	FLUORESCENCE VALUES			MEAN
CHO-K1	48 HRS	0	-	-0.148	-0.186	-0.076	**-0.137**
		4	-	0.885	0.292	-0.086	**0.365**
		8	-	7.811	7.676	4.737	**6.741**
		12	-	17.872	30.220	-	**24.046**
	72 HRS	0	-	0.509	1.696	0.035	**0.747**
		4	-	0.534	3.827	0.431	**1.600**
		8	-	11.102	12.423	9.346	**10.957**
		12	-	8.215	12.287	9.778	**10.093**
TK 6	48 HRS	-	CONTROL	6.093	5.376	3.206	**4.892**
		-	20MM	26.893	21.156	20.230	**22.800**

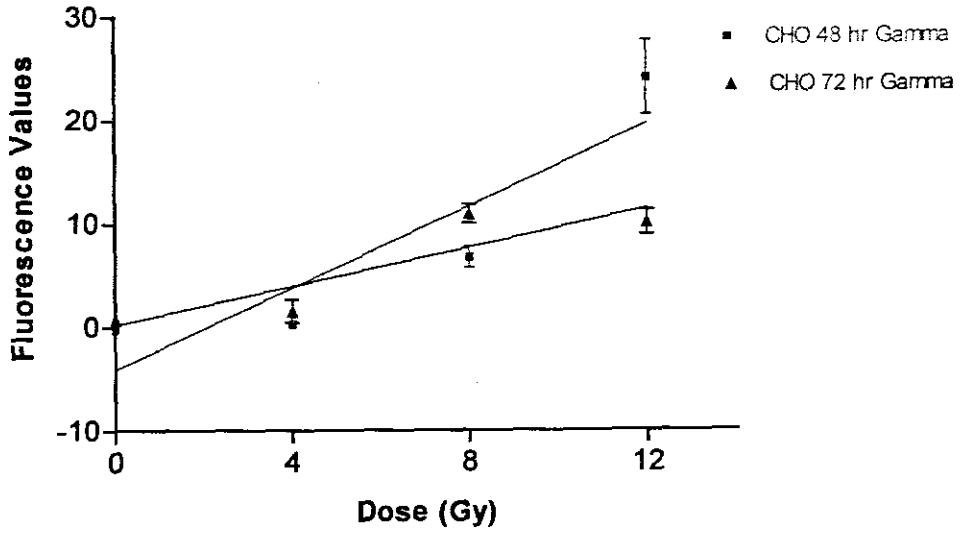

Figure 4.4: *Caspase 3/7 activity measured in CHO-K1 cells at 48 (■) and 72 hours (▲) post 4, 8 and 12 Gy ^{60}CO γ-irradiation.*

The effect of ^{60}CO γ- and p(66/Be) neutron radiation on CHO-K1 cells was then repeated and evaluated 48 hours post irradiation. This data is demonstrated in Table 4.4 and Figure 4.5.

Table 4.4: *Caspase 3/7 activity induced in CHO-K1 cells exposed to 0,4,8 and 12 Gy ^{60}CO γ-irradiation and 0, 4, 6 and 8 Gy p(66/Be) neutron radiation incubated for 48 hours.*

TIME	RADIATION	DOSE	FLUORESCENCE VALUES			MEAN
48 hrs	Gamma	0	48.292	30.691	17.817	**32.27**
		4	211.437	328.052	305.387	**281.63**
		8	308.330	343.255	401.894	**351.16**
		12	542.251	565.705	568.457	**558.80**
	Neutron	0	48.292	30.691	17.817	**32.27**
		4	212.610	268.394	262.534	**247.85**
		6	326.125	409.307	323.868	**353.10**
		8	295.331	347.354	433.023	**358.70**

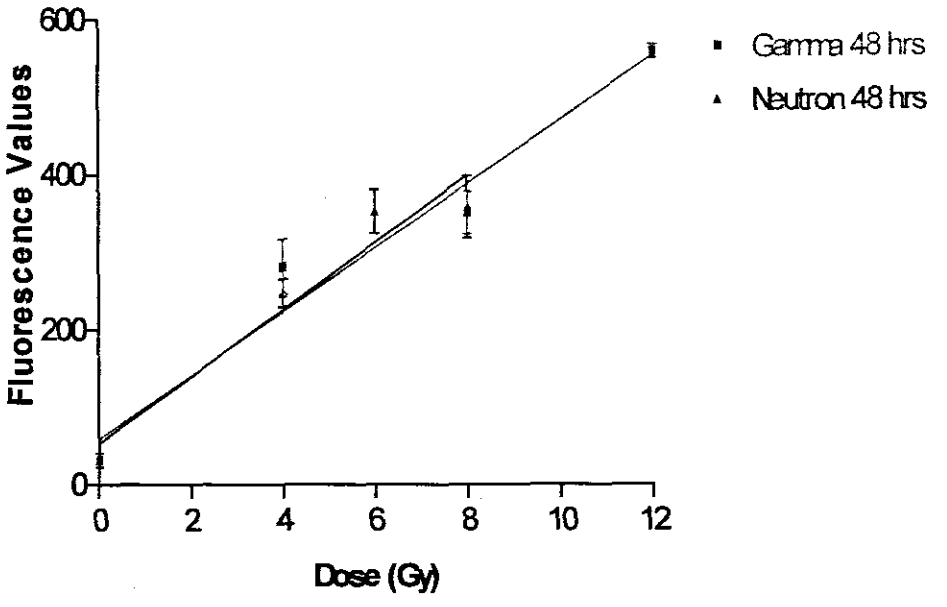

Figure 4.5: *Caspase 3/7 activity measured in CHO-K1 cells at 48 hours post irradiation. Cells were exposed to doses of 4; 8 and 12 Gy ^{60} Co γ- (■) as well as to 4; 6 and 8 Gy p(66/Be) neutron radiation (▲).*

CHO-K1 cells displayed a significant linear dose response for both radiation modalities ($p < 0.0001$) reflecting a goodness of fit as $r^2 = 0.93$ for gamma and 0.87 for neutron radiation.

As readings fluctuated on repeat experimentation data could not be compared and an alternative presentation of the data was to view the readings as a ratio of caspase activity present in treated samples and that in the control samples demonstrated in Table 4.6 for gamma and in Table 4.7 for neutron radiation. This was done only for the 48-hour post radiation readings and represented in Figure 4.6.

Table 4.5: *Ratio representation of fluorimetric readings obtained 48 hours post ^{60}CO γ- radiation in CHO-K1 cells.*

Batch 1						
Dose	**Gamma**				**Mean**	**Ratio**
0	16.1	15.4			15.75	1.00
4	98	91.4			94.7	6.01
8	114.4	125.6			120	7.62
12	158.8	166			162.4	10.31
Batch 2						
0	8.2	9.3	11.6	13.1	9.7	1.00
4	10.1	12.5	14.2	14.8	12.26667	1.26
8	20.3	17.1	15.8	15	17.73333	1.83
12	18.8	20.8	24.2	28.8	21.26667	2.19
Batch 3						
0	48.3	30.7	17.8		32.26667	1.00
4	211.4	328.1	305.4		281.6333	8.73
8	308.3	343.3	401.9		351.1667	10.88
12	542.3	565.7	568.5		558.8333	17.32

Table 4.6: *Ratio representation of fluorimetric readings obtained 48 hours post p(66/Be) neutron radiation in CHO-K1 cells.*

Batch 1						
Dose	**Neutron**				**Mean**	**Ratio**
0	16.1	15.4			15.75	1.00
4	173.1	182.8			177.95	11.30
6	224.9	189.4			207.15	13.15
8	179.1	172.5			175.8	11.16
Batch 2						
0	23.2	23	23.5	23	23.23333	1.00
2	22.5	22.5	19.7	20.5	21.56667	0.93
4	28.9	23.8	25.1	27.2	25.93333	1.12
6	28.4	32.5	31	32.2	30.63333	1.32
Batch 3						
0	48.3	30.7	17.8		32.26667	1.00
4	212.6	268.4	262.5		247.8333	7.68
6	326.2	409.1	323.9		353.0667	10.94
8	295.3	347.4	433		358.5667	11.11

Limited studies are done on radiation-induced caspase activity using adherent rapidly dividing cells measured by the Apo-ONE kit. The wells were seeded according to expected cell kill but the potential for serum deprivation, overgrowth and necrosis in the wells remain a possibility.

Although the dose response curves are still ineffectual there is a marginal increase in caspase 3/7 activity in neutron-irradiated cells as seen in Figure 4.6. Linear trend lines fitted to the data generated a good fit for the gamma fluorescence ratio to dose ($r^2 = 0.97$).

The low level of caspase 3/7 activity in CHO-K1 cells was not unexpected, as Singh *et al.,* (1994) reported that biochemical features of apoptosis were not observed in CHO cells. Fluorometric assessment using biochemical markers for assessing radiation-induced caspase 3/7 activity in CHO-K1 cells proved not to be a good parameter for reflecting cellular damage.

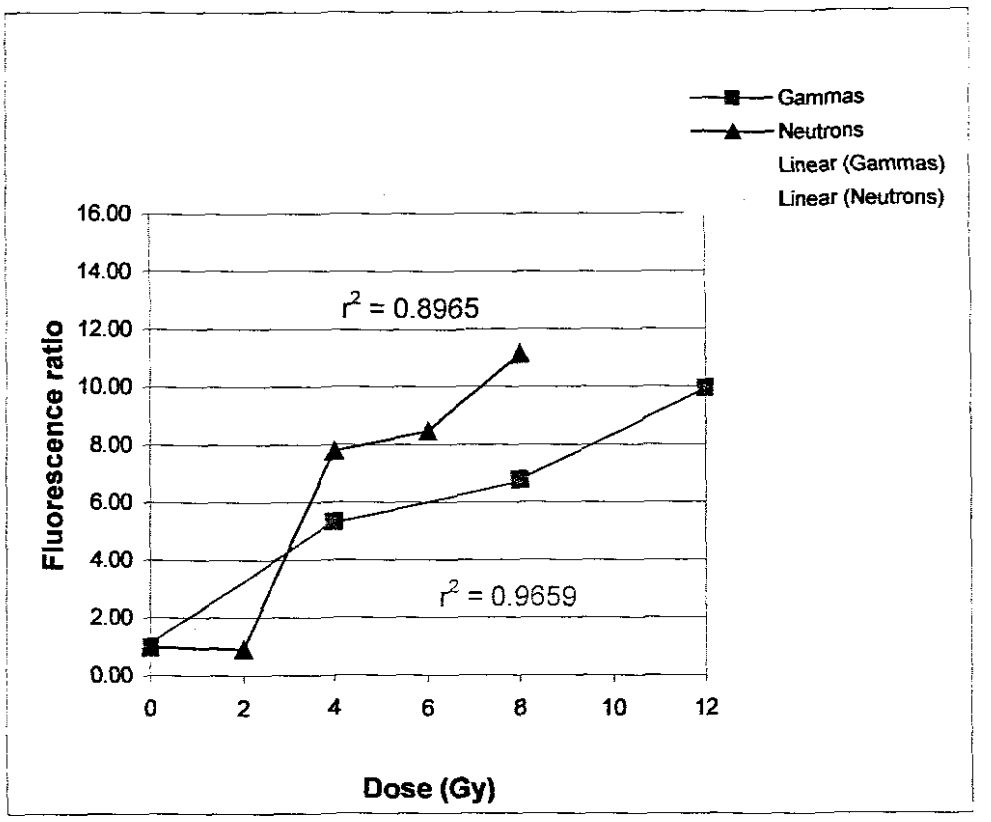

Figure 4.6: *Caspase 3/7 activity 48 hours post radiation represented as the ratio of fluorescence generated in irradiated samples to control samples in each experiment. Dose response curve for p(66/Be) neutron (▲) and ^{60}CO γ- radiation (■) became more evident. The linear trend line fitted to both sets of data provided a good fit for the gamma fluorescence ratios to dose (r^2 =0.97).*

4.3.2 Conclusion

The success of the assay has been established using cells of haematopoietic origin exposed to radiation (Datta, *et al,* 1997), including data generated from our own laboratory on lymphocytes exposed to low doses of ionising radiation (Rossouw, 2004). Limited literature was available as to the use of rapidly dividing adherent cells. The amount of fluorescent product generated expressed in the assay is proportional to the amount of caspase 3/7 activity. The recommended cell amount per well was 2 x 10^4 which is attainable when using quiescent cells (e.g. Lymphocytes) or non-adherent proliferating

cells (e.g. TK 6 cells) as cell numbers can be adjusted when dispensed into wells. Although cell kill was anticipated and CHO-K1 cells were seeded accordingly, the amount of cells in the final reaction after the prolonged incubation time (48 hours) was indeterminate.

Cellular radiation sensitivity was poorly represented by the ineffectual response showing little differentiation between damage induced by neutron and gamma radiation. Lukovic *et al.*, (2003) assessed caspase 3/7 activity cytofluorimetrically in HeLa cells induced by staurosporine and concluded that the activation of effector caspases does not equate to the point of irrevocable cellular commitment to death.

In this study it was noted that caspase 3/7 activity decreased at 48 (Table 4.2) and 72 hours post irradiation (Table 4.3). Fluctuations in readings led to high inter-experimental variation resulting in poor reproducibility. As biological systems differ in response to radiation it would be advantageous to evaluate additional time intervals to determine optimal caspase 3/7 activity in CHO-K1 cells.

This technique showed insensitivity to increase in dose and the different ionising deposition patterns are not reflected by the assay making it unsuitable for cellular radiosensitivity testing.

4.3.3 DNA Fragmentation

The execution phase of apoptosis corresponds to nuclear apoptosis and manifests in the most striking morphology characterised by chromatin condensation and DNA cleavage into high-molecular-weight (HMW) fragments and oligonucleosomes (Lecoeur, 2002). DNA fragmentation into HMW fragments is considered the hallmark of apoptosis and amount and rate at which these fragments are generated is related to the apoptotic agent, duration of stimulus and cell type (Suzuki *et al.*, 2003).

Nuclear apoptosis is mediated through activation of endonucleases that generate DNA fragments with 3'OH termini. The terminal deoxynucleotidyl transferase dUTP-mediated nick end-labelling (TUNEL) assay is more sensitive than agarose gel electrophoresis and has become the method of choice for DNA fragmentation analysis (Crompton *et al.*, 2001; Sheridan and West, 2001; Ormerod, 2001).

Flow cytometric data was generated using the APO-Direct TUNEL Assay (BD Biosciences, Pharmingen, 2001). Forward (FSC) and side (SSC) scattering was first measured. FSC reflects cell size and SSC reflects the intracellular structure or granularity of the cell, making it possible to differentiate the types of cells and to gate for acquisition. Dual parameter displays were created as follows: Propidium Iodide, using FL-1, fluoresces at 623nm and stains for DNA content versus FITC-dUTP using FL-3, fluoresces at 520nm and stains for apoptotic cells. Histograms were created for negative and positive control cells (Figure 4.7) included in the kit and were treated as the test samples with

FITC-dUTP that labels the 3'-hydroxyl-DNA ends in apoptotic cells.

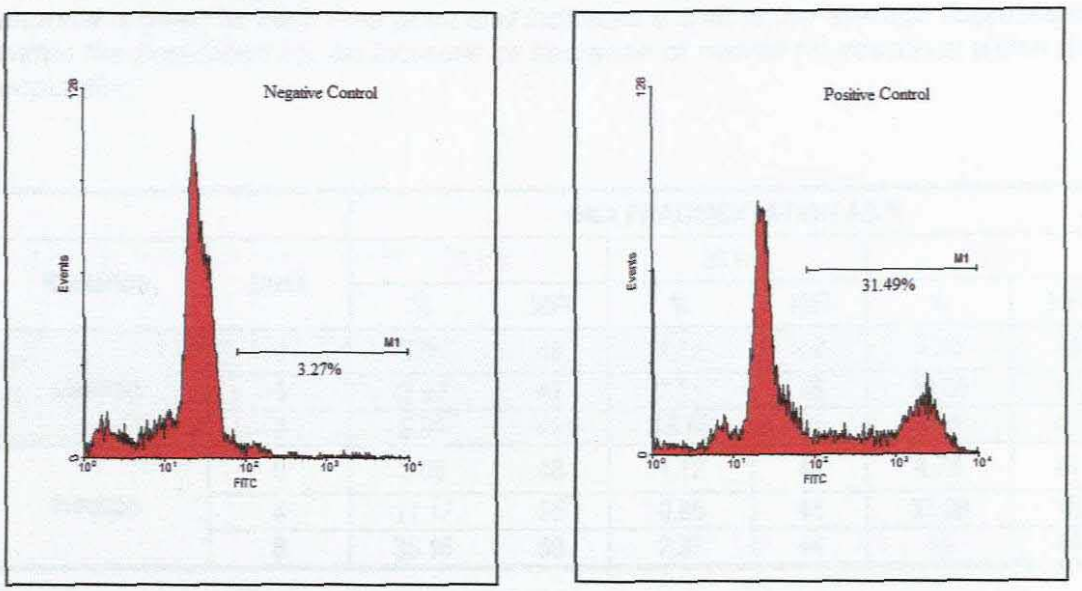

Figure 4.7: *Flow cytometric histograms generated using the APO-Direct negative and positive control cells. The negative control (left) and positive (right) are treated as the test samples with FITC-dUTP that labels the 3'-hydroxyl-DNA ends in apoptotic cells. The presence of apoptotic cells is shown as the population in the positive control displaying FITC increase (M1 gate) as a measure of DNA fragmentation.*

In a similar way the M1-gate was created on the 0 Gy (control) samples and applied to the radiation exposed CHO-K1 cells. The presence of apoptotic cells was shown as the population displaying FITC increase (M1 gate). This gate was applied to all test samples as a measure of DNA fragmentation (Figures 4.8 - 4.10). These data are displayed in Table 4.7, corrected for background apoptosis and presented in Table 4.8. Induction of DNA fragmentation in CHO-K1 cells at 24; 36 and 48 hours post ^{60}CO γ- and p(66/Be) neutron radiation exposed to doses of 0; 4 and 8 Gy are reflected in Figure 4.11.

Table 4.7: *Raw data obtained using the TUNEL assay showing DNA fragmentation values obtained at 24, 36 and 48 hours post p(66/Be) neutron and ^{60}Co γ-radiation at dose points of 0 (control), 4 and 8 Gray. The Mean Fluorescense Intensity(MFI) channel is given at each time point and indicates a shift in the average fluorescence within the population i.e. an increase or decrease of overall fluorescence within that population.*

		DNA FRAGMENTATION AS %					
Radiation	Dose	24 hrs		36 hrs		48 hrs	
		%	MFI	%	MFI	%	MFI
Gamma	0	3.05	48	1.12	44	4.78	44
	4	3.92	47	2.21	45	29.06	45
	8	2.91	46	13.76	47	18.1	47
Neutron	0	3.05	48	1.12	44	4.78	44
	4	11.17	55	0.65	44	33.98	48
	8	35.16	50	2.37	44	16	44

Table 4.8: *Radiation induced DNA fragmentation in CHO-K1 cells as a function of p(66/Be) neutron and ^{60}Co γ-radiation. The data was normalised by subtracting background DNA fragmentation values from those obtained in Table 4.7 and represented graphically in Figure 4 .11 on Page 117.*

		DNA FRAGMENTATION AS %		
Radiation	Dose	24 hrs	36 hrs	48 hrs
Gamma	0	0	0	0
	4	0.87	1.09	24.06
	8	2.91	12.64	13.32
Neutron	0	0	0	0
	4	8.12	0.65	29.20
	8	32.11	0.12	11.22

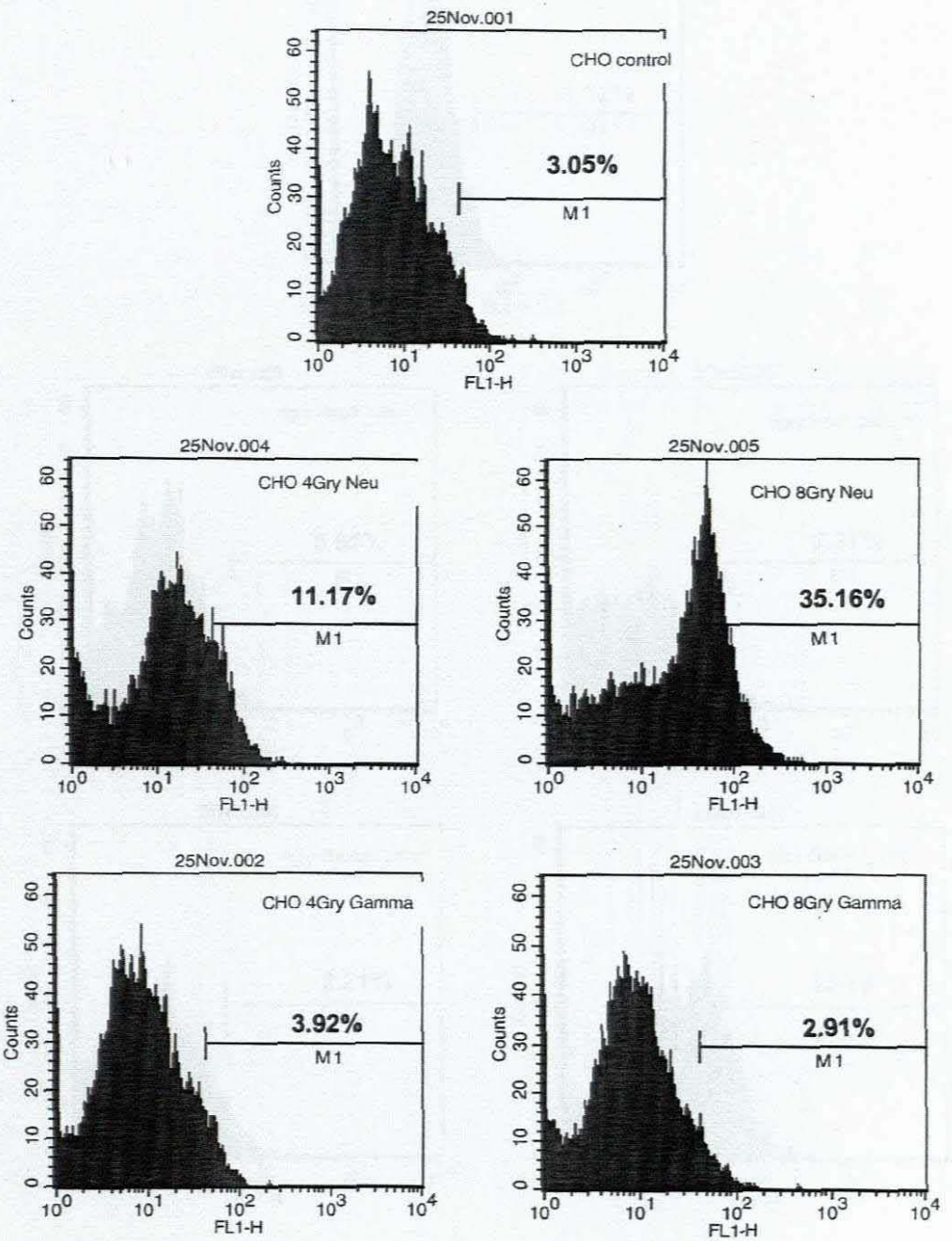

Figure 4.8: *Flow cytometric histograms generated from CHO-K1 cells 24 hours post neutron and gamma irradiation using the APO-Direct TUNEL assay. The presence of apoptotic cells is shown as the population displaying FITC increase (M1 gate).*

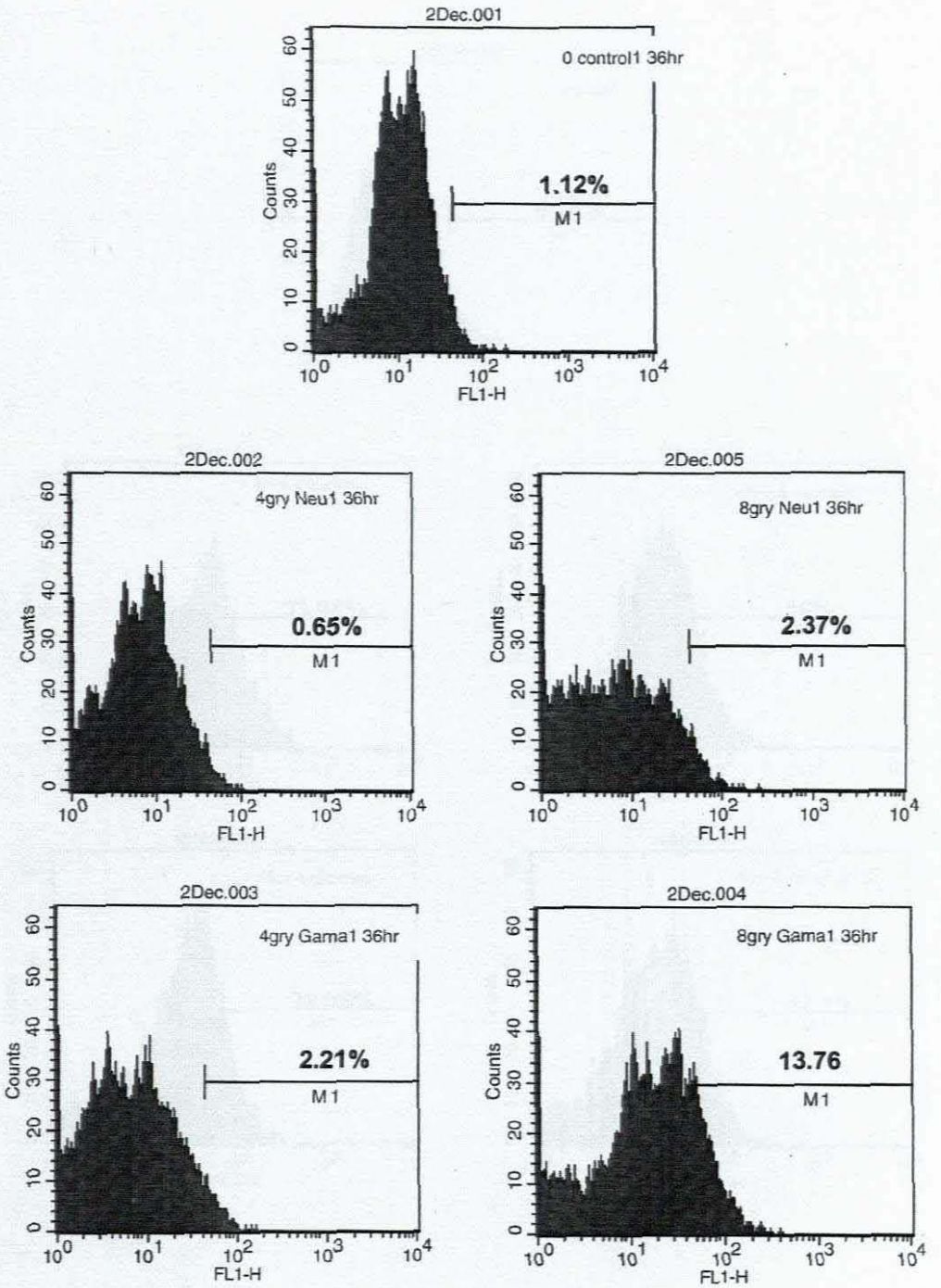

Figure 4.9: *Flow cytometric histograms generated from CHO-K1 cells 36 hours post neutron and gamma irradiation using the APO-Direct TUNEL assay. The presence of apoptotic cells is shown as the population displaying FITC increase (M1 gate).*

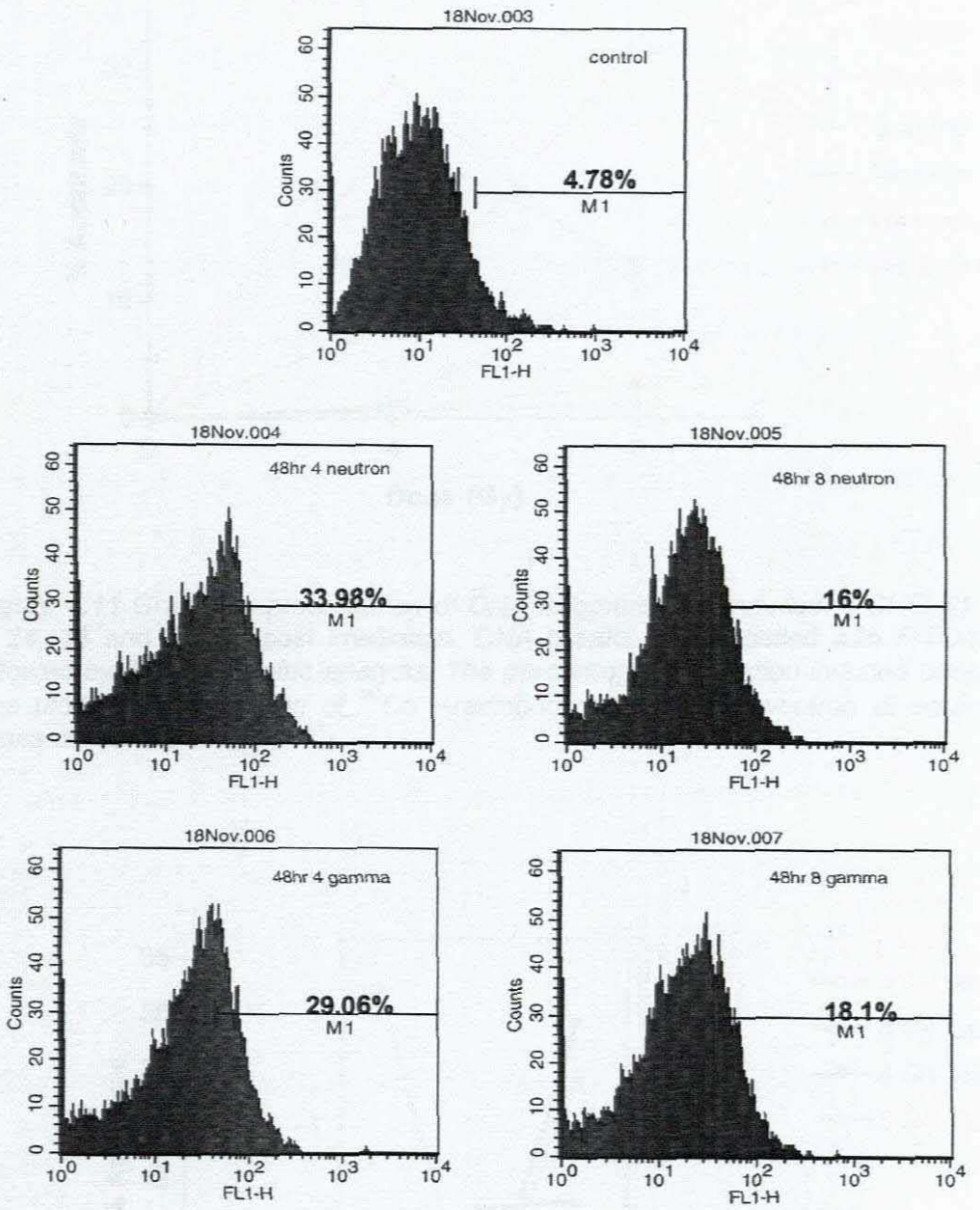

Figure 4.10: *Flow cytometric histograms generated from CHO-K1 cells 48 hours post neutron and gamma irradiation using the APO-Direct TUNEL assay. The presence of apoptotic cells is shown as the population displaying FITC increase (M1 gate).*

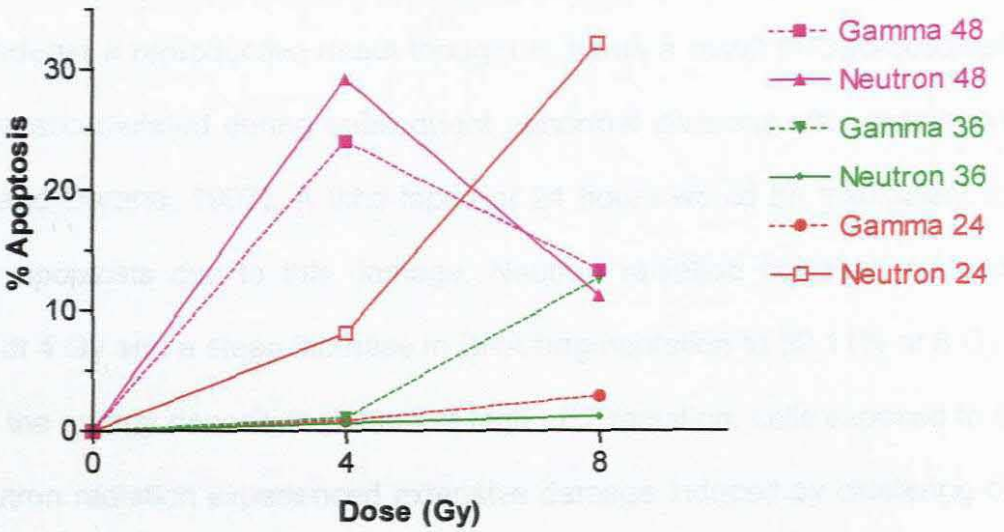

Figure 4.11 *Graphic representation of DNA fragmentation induced in CHO-K1 cells at 24, 36 and 48 hrs post irradiation. DNA breaks were labelled with FITC-dUTP followed by flow cytometric analysis. The percentage of radiation-induced apoptosis was plotted as a function of ^{60}Co γ-radiation and p(66/Be) neutron at equivalent doses of 4 and 8 Gray.*

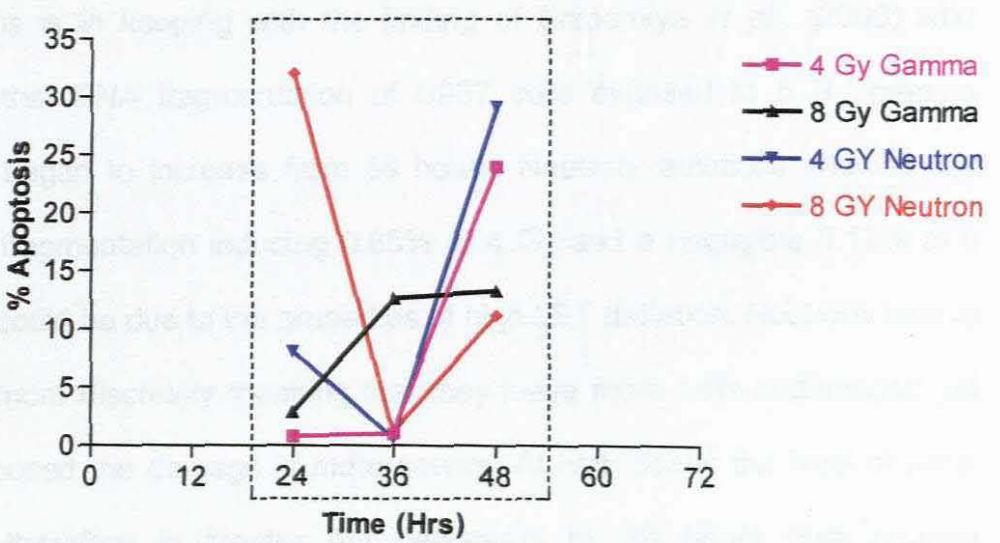

Figure 4.12: *Graphic representation illustrating the influence of time on DNA fragmentation in CHO-K1 cells at 24, 36 and 48 hours post 4 and 8 Gy gamma and neutron irradiation.*

At 24 hrs radiation-induced DNA fragmentation increased negligibly from 0.87% at 4 Gy to 2.91% at 8 Gy. This can be expected as non-haematopoietic cells undergo a reproductive death thought to be as a result of chromosomal damage accumulated during subsequent abnormal divisions after irradiation (Olive and Durand, 1997). A time lapse of 24 hours would be insufficient to display apoptosis due to this damage. Neutron radiation however induced 8.12% at 4 Gy and a steep increase in DNA fragmentation to 32.11% at 8 Gy. Due to the energy deposition pattern of high LET radiation, cells exposed to 8 Gy neutron radiation experienced extensive damage induced by clustering of damaged sites in a small volume of DNA locally multiply damaged sites (LMDS) potentially inducing interphase apoptosis (Mustonen *et al.,* 1999).

DNA fragmentation at 36 hours post irradiation was not significantly induced by either radiation modality, with the exception of the 8 Gy gamma dose which reflected 12.64%. Only 1.09% was induced by 4 Gy gamma radiation (Figure 4.12). This is in keeping with the finding of Shinomiya *et al.,* (2000) who reported that DNA fragmentation of U937 cells exposed to 5 Gy gamma radiation began to increase from 36 hours. Neutron radiations showed low levels of fragmentation inducing 0.65% at 4 Gy and a negligible 0.12% at 8 Gy. This could be due to the properties of high LET radiation. Neutrons induce damage more discretely meaning that they leave more cells undamaged yet when imposed the damage is more severe. At high doses the level of initial damage therefore is greater but decreases by 36 hours post neutron irradiation (Testard *et al.,* 1997).

DNA fragmentation was most notable at 48 hours post radiation for both radiation modalities. At 4 Gy, 24.06% was evident decreasing to 13.32% at 8 Gy gamma irradiation. Neutron radiation-induced DNA fragmentation was 29.2% at 4 Gy, declining at 8 Gy to 11.22%. This is in keeping with a study by Olive *et al.*, (1996) where it was concluded that apoptotic death continued for several days and that the surviving fraction could not be predicted from the fraction of cells undergoing apoptosis measured at a particular time point.

The Mean Fluorescence Intensity (MFI) channel was evaluated at each time interval for each dose point and indicates a shift in the average fluorescence within the population i.e. an increase or decrease of overall fluorescence within that population. These parameters reflected higher values at 24 hours post neutron irradiation but remained similar to the values generated by the control sample at the other time intervals for both radiation modalities (Table 4.7).

4.3.3.1 Cell Cycle Analysis

Eukaryotic cells respond to ionising radiation by inducing cell cycle arrest controlled largely by p53 expression (Datta *et al.*, 1997; Cohen-Jonathan, 1999). Cells with mutated p53 do not arrest in G_1 but do so at the G_2 checkpoint (Illidge *et al.* 2000). Cells undergo apoptotic cell death at various stages of the cell cycle following exposure to ionising radiation. Depending at what stage in the cell cycle radiation death was induced, results in pre- or post mitotic apoptosis (Shinomiya, 2001).

An exponentially growing population of CHO-K1 cells were irradiated in flasks and a normal variation in cell cycle distribution was expected. Redistribution of cells in cell samples responded as demonstrated by the histograms in Figure 4.13. Stacked bar charts in Figure 4.15 indicate a G_2 build up was evident at 36 and 48 hours post irradiation. At 48 hours cells steadily increased in this phase from 18% in the control sample to 26% at 4 Gy and 28% at 8 Gy ^{60}Coγ-irradiation. When exposed to p(66)/Be neutron radiation the cells redistribute more markedly at 4 Gy to 33% and 55% at 8 Gy in the G_2 phase. The TK6 cells indicated increased sensitivity to radiation as expected as they are known to be more radiosensitive and undergo apoptosis readily when exposed to radiation. These cells displayed a well-defined histogram in the control sample with 12% of cells in G_2 progressing rapidly to a build up of 38% at 2 Gy, which increases to 40% at 4 Gy γ-irradiation (Figure 4.14). The key in Figures 4.13 and 4.14 denotes the following:

	Percentage Cellular Debris
	Percentage Aggregates (Doublets etc.)
	Dip G1 – percentage cells in G1 phase
	Dip G2 - percentage cells in G2 phase
	Dip S – percentage cells in S phase

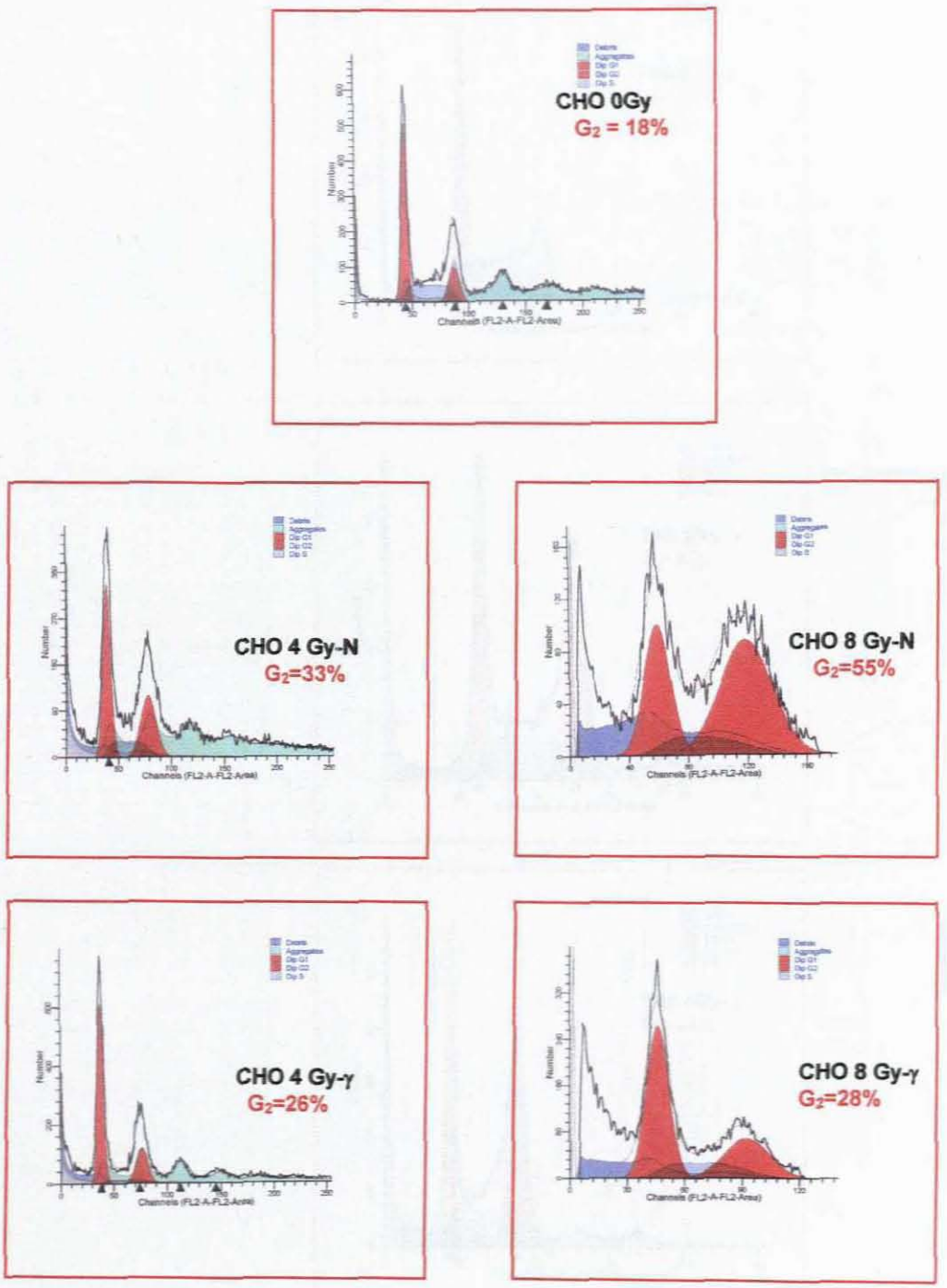

Figure 4.13: *Histograms displaying redistribution of CHO-K1 cells in the cell cycle as a function of $^{60}Co\gamma$- and p(66/Be) neutron radiation, 48 hours post exposure. The X-axis indicates DNA content.*

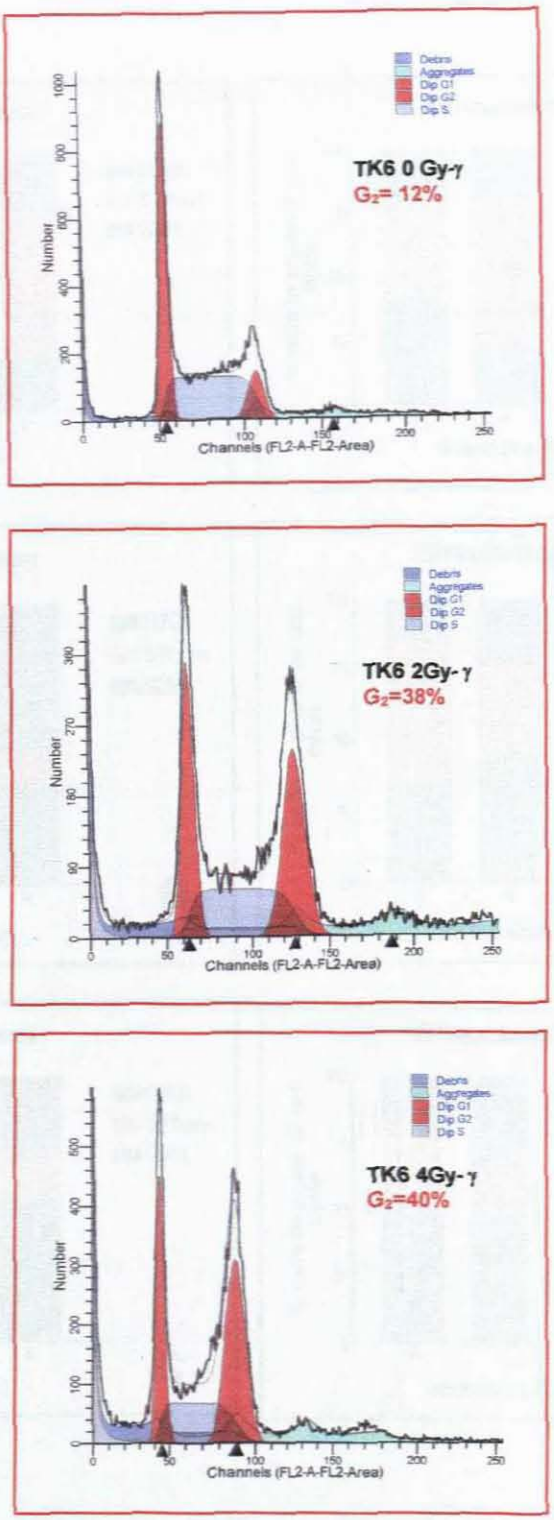

Figure 4.14 : *Histograms displaying redistribution of TK6 cells in the cell cycle indicating increased sensitivity to gamma radiation. A well-defined histogram is shown in the control sample with 12% of cells in G_2 progressing rapidly to a build up of 38% at 2 Gy, which increases to 40% at 4 Gy, 48 hours post γ-irradiation. The X-axis indicates DNA content.*

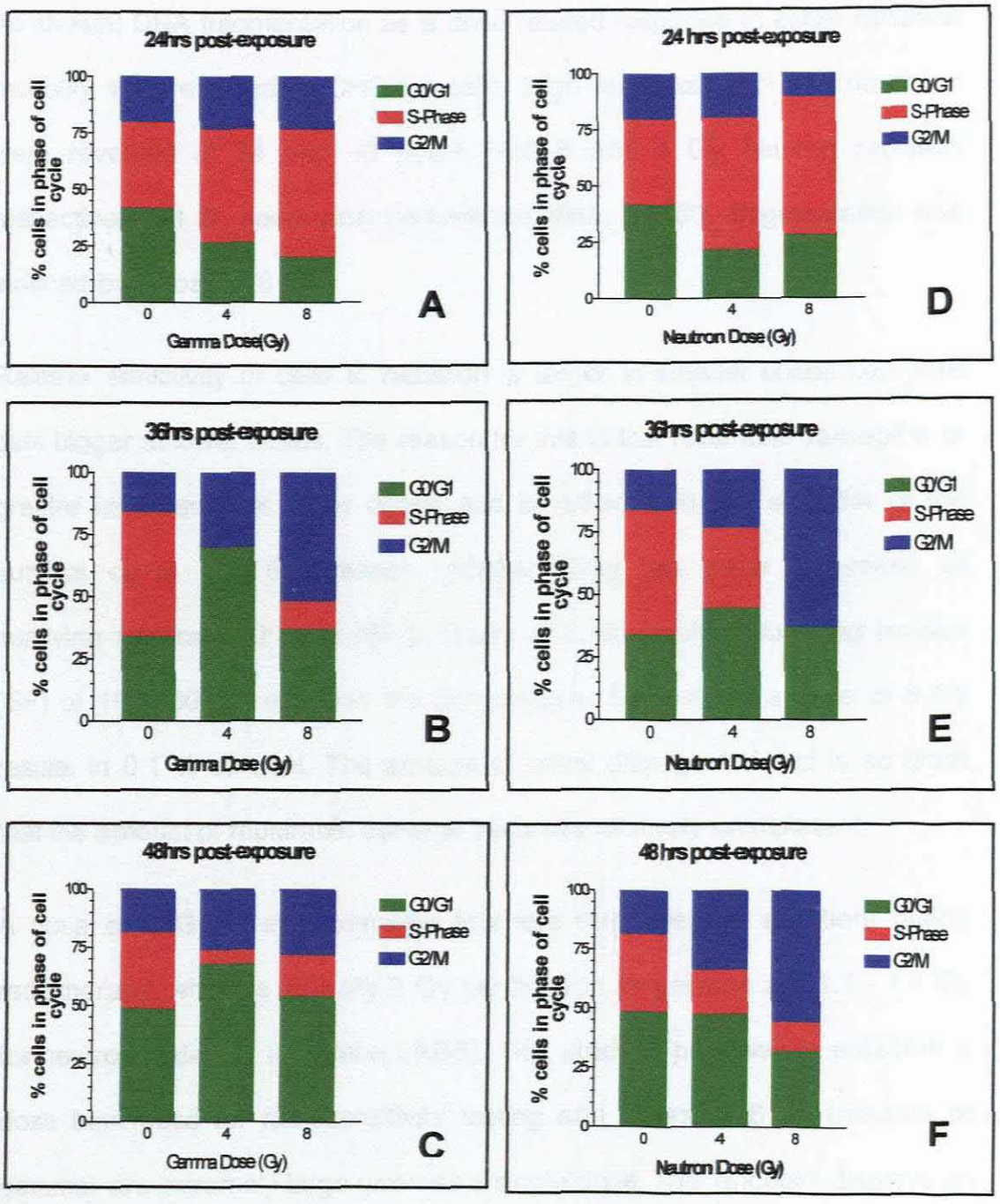

Figure 4.15: *Graphic representation of redistribution of cells in cell cycle of CHO-K1 cells as a function of $^{60}Co\gamma$- **(A-C)** and p(66/Be) neutron radiation **(D-F)** at 24, 36 and 48 hour post exposure. A build up of cells are seen at the G_2 phase of the cycle induced by both modalities at 36 and 48 hours post irradiation.*

4.3.4 Conclusion

As shown, DNA fragmentation as a dose related response to either radiation modality was reflected in CHO-K1 cells. High levels of DNA fragmentation were revealed at 24 and 48 hours post 8 and 4 Gy neutron radiation respectively. At 36 hours post gamma radiation, 13.76% fragmentation was induced by a dose of 8 Gy.

Relative sensitivity of cells to radiation is larger at smaller doses i.e., RBE gets bigger at lower doses. The reason for this is that reparable damage is of greater importance at lower doses and is reflected in the shoulder of the survival curve. For this reason radiosensitivity has been expressed as surviving fraction at 2 Gray (SF_2). Doses at 2 Gy result in surviving fraction (SF) of 10 – 80 % i.e. within the first decade. By contrast a dose of 8 Gy results in 0.1 % survival. The amount of lethal damage induced is so great that the amount of repairable damage becomes relatively unimportant.

A dose of 8 Gy is approximately four fold that given to a patient during radiotherapy, which is typically 2 Gy per fraction for gamma and 1.1 - 1.7 Gy for neutron radiation (iThemba LABS). This study in part was to establish a dose best used for radiosensitivity testing and doses of 8 Gy (neutron or gamma) are extremely large given as a single dose. This endpoint displays an insensitive response and limits the application as a biomarker as the large dose required effectively diminishes the quality of the damage. At lower doses the repairable damage is increased and the differences are larger allowing better differentiation.

Degradation of DNA is but one aspect of apoptosis and there is debate as to whether chromosomal DNA laddering together with nucleosomal DNA laddering should be regarded as the golden standard of apoptosis. Interestingly, certain cell types do not show nucleosomal DNA laddering even when there is morphological evidence of apoptosis (Lecoeur, 2002, Vinatier and Subtil, 1996, Ormerod, 2001). Certain cell types displayed high-order DNA fragments that did not proceed to nucleosomal levels of degradation. There is considerable variation in the DNA degradation phase of apoptosis and is dependent on cell type and toxic agent involved (Warrington *et al.,* 2003; Allen *et al.,* 1997).

Although flow cytometry is advantageous in that large numbers of cells can be analysed and evaluated, it is generally felt that biochemical identification of apoptosis cannot be used exclusive of morphological analysis (Ormerod, 2001).

4.3.5 Morphological Analysis of Apoptosis

The morphological appearance of cells undergoing apoptosis is specific and easily identified microscopically and is recommended in experimentation quantifying and qualifying apoptosis (Allen *et al.*, 1997). Microscopy is more definitive than all biochemical methods to differentiate the mode of cell death.

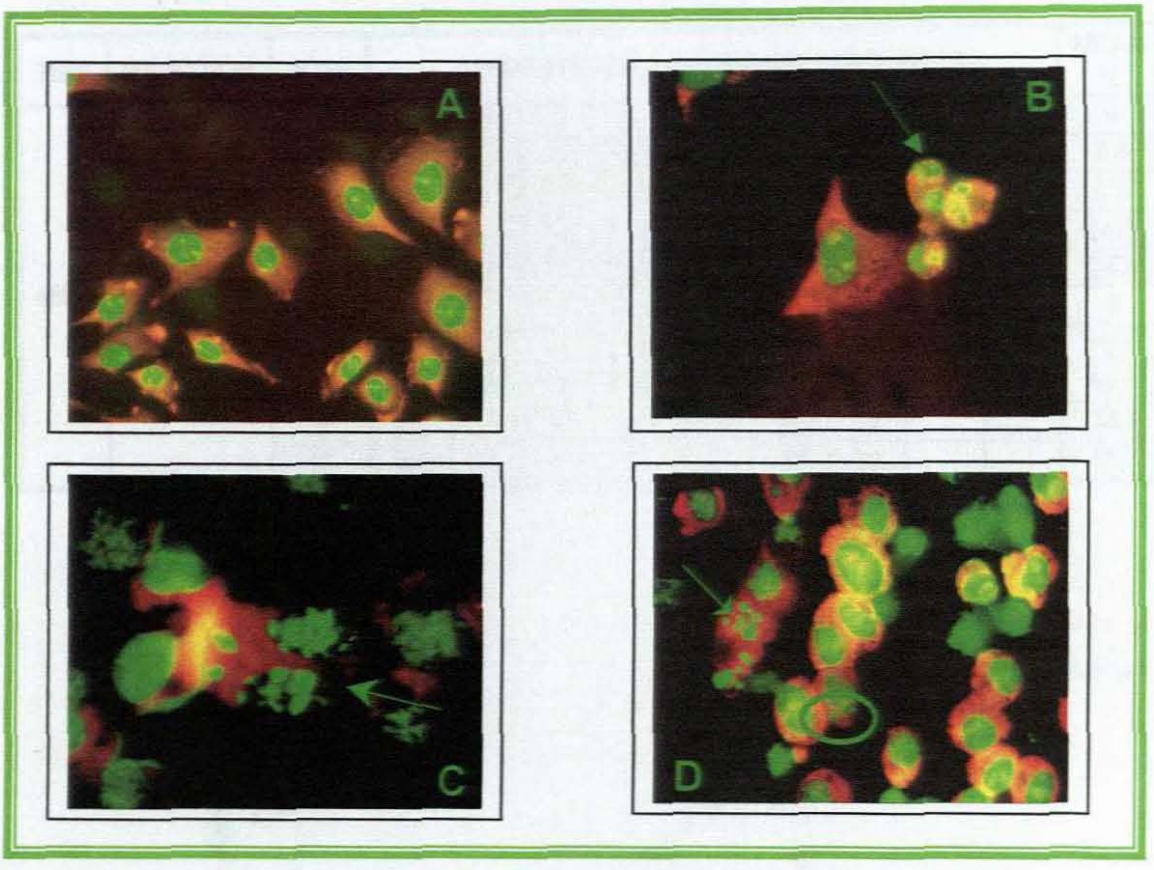

Figure 4.16: *Photomicrographs of CHO-K1 cells stained with Acridine Orange and visualised using a fluorescent microscope (x 400) equipped with a FITC filter set. The un-irradiated control sample* ***(A)*** *showing no fragmented nuclei while* ***(B-C)*** *displays DNA fragmentation (all arrows). Chromatin condensation* ***(C)*** *and cell shrinkage is clearly demonstrated* ***(B).*** *In the circle in* ***(D)*** *a micronucleus is demonstrated which is not to be confused with a fragmented nuclei (arrow).*

In this study it was demonstrated that CHO-K1 cells showed morphological characteristics of apoptosis following irradiation with low LET ^{60}Co γ- as well as high LET p(66/Be) neutron radiation. Apoptotic cells were visualised by fluorescence of fragmented nuclei and condensed chromatin and enumerated using a fluorescence microscope examples of which as shown in Figure 4.16. At least 500 cells per dose point were evaluated and the percentage of

apoptotic cells was calculated and shown in Table 4.9. The data is reflected in a dose response curve (Figure 4.17) and showed a gradual increase in apoptosis with escalating dose. Error bars estimated assuming a Poisson error based on mean apoptotic frequency and number of cells examined in a single experiment.

Table 4.9: *Percentage in vitro apoptosis enumerated per sample induced 48 hours post irradiation in CHO-K1 cells as a function of p(66/Be) neutron and ^{60}Co γ-radiation. Cells were visualised using a fluorescence microscope.*

TIME	RADIATION	DOSE	APOPTOTIC CELLS COUNTED PER SAMPLE									MEAN %
48hrs	Gamma	0	0	0	0	0	0	0	0	0	0	**0**
		4	2	5	2	1	2	10	5	7	6	**4.4**
		6	9	5	6	5	7	7	5	-	-	**6.3**
		8	9	12	14	18	16	17	18	-	-	**14.8**
		10	24	21	20	24	27	28	25	-	-	**24.3**
	Neutron	0	0	0	0	0	0	0	0	0	0	**0**
		4	14	15	14	18	11	11	16	13	11	**13.6**
		6	15	16	13	15	12	18	17	-	-	**15.1**
		8	22	22	23	25	28	22	29	-	-	**24.4**
		10	36	42	40	28	32	33	39	-	-	**35.7**

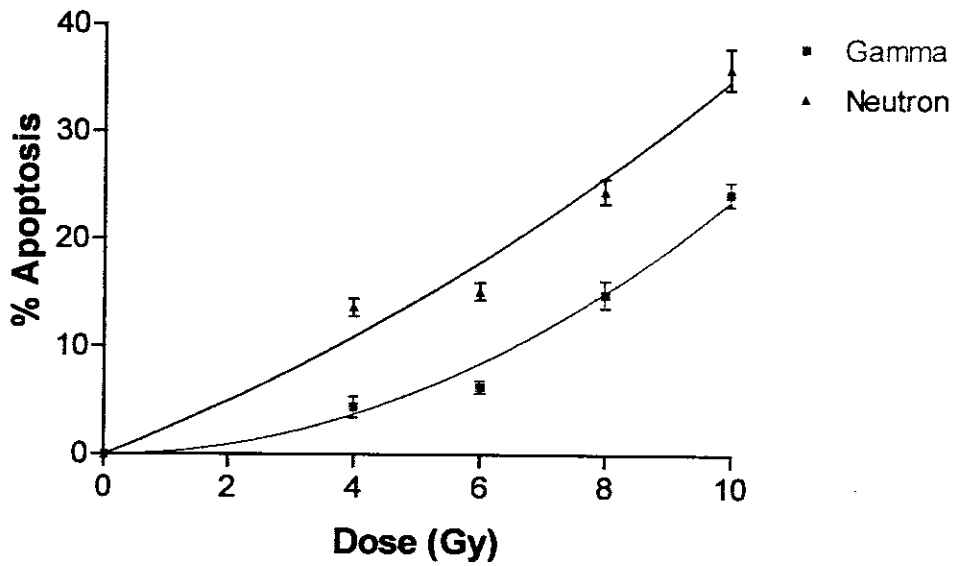

Figure 4.17: *Graphic representation of percentage in vitro apoptosis induced 48 hours post irradiation in CHO-K1 cells measured by fluorescent microscopy and plotted as a function of p(66/Be) neutron (▲) and ^{60}Co γ-radiation (■).*

Equivalent doses of 0; 4; 6; 8 and 10 Gy of p(66/Be) neutron radiation and ^{60}Co γ-radiation were administered. At 48hours post irradiation the percentage of apoptosis increased from 4.2% to 6%, to 14.6% and to 24.6%, for escalating doses of ^{60}Co γ-radiation while for the same doses of p(66)/Be neutron radiation the percentages ranged from 13.2% to 15%, to 24.4% and then to 35.4% at 10 Gy. There is an approximate 10% increase in apoptosis per dose point for neutron radiation compared to γ-radiation.

When the data for ^{60}Co γ-radiation was fitted to the linear-quadratic model the value of the initial slope (α coefficient) was not significantly different from zero. This reflects the relative insensitivity of the endpoint to reflect the cellular response. As the non-reparable component of radiation was not reflected in a statistically significant manner recalculation of the expression yielded a β-value of 0.234 ± 0.0075 Gy $^{-2}$ with a 95% confidence level of 0.219 – 0.25 (r^2 = 0.92).

By contrast the data fitted to the linear-quadratic model for induction of apoptosis by p(66)/Be neutron radiation reflected greater reparable and non-reparable damage. This was evident as a α-value of 2.25 ± 0.36 Gy^{-1} and a β-value of 0.12 ± 0.04 Gy $^{-2}$ was generated (r^2 = 0.93).

The relative biological effectiveness (RBE) was calculated as dose ratios to get approximately 15% apoptosis and found to be 1.5.

It is also noted that at approximate levels of iso-effect, i.e. at 8 Gy gamma and 4 Gy neutrons, the percentage of radiation-induced apoptosis is 14% and

13.6% respectively, indicating that these doses induced near equivalent levels of biological damage.

Giant Cell Formation

In this study photomicrographs taken at high doses of radiation revealed giant cells, aberrant mitosis and extensive micro-nucleation (Figure 4.18).

Chinese hamster cell lines are commonly used throughout the world in genotoxicity testing. Functioning of p53 is critical to how a cell responds to DNA damage. In this study the CHO-K1 cell line was used and has been reported to have mutant p53 sequence, mutant protein (high spontaneous levels that are non-inducible after X-irradiation) and mutant function (lack of G_1 checkpoint) (Hu *et al.,* 1999), explaining the presence of these cells in this study.

A factor determining a cells tendency to undergo apoptosis is its p53 status. Expression of p53 is known to be an important predictor of treatment outcome in haemopoietic tumours with its role in solid tumours more contentious. After irradiation cells undergo cell cycle arrest and p53 is pivotal in inducing arrest or apoptosis at the G_1 checkpoint. p53-Mutated lymphoma cells do not arrest at G_1 but do so at the G_2 checkpoint. Polyploid giant cell formation is enhanced in p53-mutated cells following irradiation (Illidge *et al.,* 2000). Delayed post-mitotic apoptosis is known to occur after one or more divisions. Micronucleation and nuclear sectioning can occur as part of mitotic death and micronucleation is thought of as an alternative to apoptosis. These nuclear segments and separated cells derived from giant cells appear viable but are

thought to undergo delayed apoptosis.

Giant cell formation occurs *in vivo* and *in vitro* in mammalian cells after exposure to high doses of ionising radiation similar to doses used in this study (Somosy, 2000, Olive and Durand, 1997). Lyng *et al.*, 1996 reported that morphological abnormalities induced by radiation persisted for several generations in the CHO-K1 hamster cell lines.

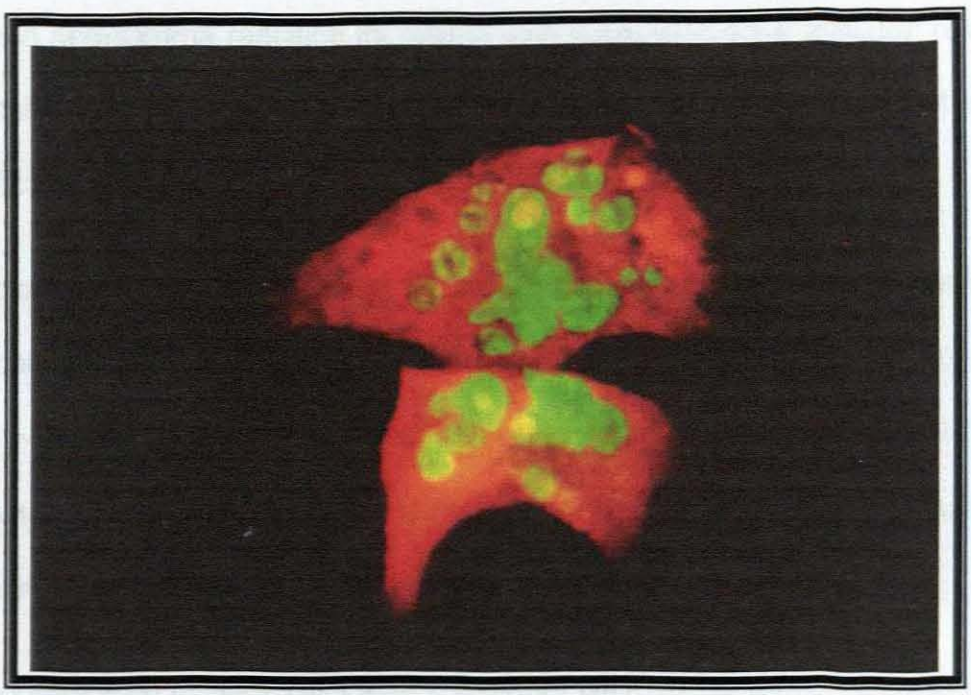

Figure 4.18: *Photomicrograph of CHO-K1 giant cells 48 hours post irradiation (10 Gy). Extensive micro- nucleation is evident.*

Illidge *et al.*, (2000) proposed that giant cells are not reproductively dead as previously thought and may be capable of releasing reproductive descendents and studied polyploid giant cell formation and delayed apoptosis in radioresistant p53-mutated lymphoma cells following a single 10 Gy dose. This formation may be a response and repair mechanism providing p53

mutated tumour cells with additional resistance and survival after radiation. Apoptosis, they suggest, could in fact in this context function not only in bringing about death but also in selecting for survival.

4.3.6 Conclusion

Although the response to dose is protracted, the percentage apoptosis does reflect the ionisation density of the radiation modality. The damage induced by neutron and gamma radiation increased with escalating dose although relative insensitivity to gamma radiation is noted as the initial slope did not differ significantly from zero.

Apoptosis as an endpoint showed little differentiation in the biological damage induced at doses of approximately iso-effective levels of (66/Be) neutron and ^{60}Co γ-radiation. The damage induced at equivalent doses however, was as expected increased by approximately 10%, indicating that cellular radiation sensitivity was represented by the endpoint.

The observation of giant cells was consistent with the literature (Nakano *et al.*, 1989) and do appear reproductively viable even after high doses (10Gy), 48 hours post neutron and gamma irradiation. Apoptosis evaluated at extended time intervals and ploidy in these cells warrants further study especially in p53-mutated cells to establish radiosensitivity or resistance.

4.4 Summary of Apoptotic Studies

Radiation-induced cellular death is due to apoptosis and mitosis-linked death as well as the loss of reproductive integrity (Cohen-Jonathan, 1999). The onset of apoptosis may occur immediately after irradiation (interphase death) at G_2 arrest, or after one or more mitosis. Studies conducted have attempted to correlate the extent of radiation-induced apoptosis to cellular radiosensitivity, some suggesting that the greater the propensity to undergo apoptosis the greater the radiosensitivity. Apoptosis is a dynamic process of events that can be followed using flow cytometery. These events however are not all suitable for the measurement of the number of apoptotic cells (Ormerod, 2002). Certain cell lines do not show classic DNA degradation and leads to the underestimation of the apoptotic population. In culture, cells may loose plasma membrane integrity referred to as secondary necrosis as observed in this study at 8 Gy neutron radiation. This results in cellular fragments containing small amounts of DNA that interfere with assays for apoptosis.

The assays validated in this study examined the apoptotic response in CHO-K1 cells induced by gamma and neutron radiation. The endpoints selected were representative of the earlier and late events in the apoptotic cascade. The presence of active caspase 3/7 in a cell sample is an event necessary for the cleavage of PARP leading to DNA fragmentation and ultimately leads to cellular death. The molecular mechanisms of detection vary and in this study detection of active caspase3/7 was done using a fluorometer that measured

the amount of fluorescence emitted by cell sample. Although caspase 3/7 activity was detected, inter- and intra- experimental variations were found. This made data inconsistent and incomparable rendering this assay unsuitable for reflecting radiosensitivity.

DNA fragmentation is a late event and the hallmark of apoptosis. The method of detection chosen by many authors is flow cytometry using the TUNEL assay enabling a quantitative evaluation of the population studied. In this study DNA fragmentation was measured at three-time intervals post gamma and neutron irradiation. Dose response was more marked at higher doses, which are not administered as single doses therapeutically, casting doubt on the use of this endpoint as a biomarker. However at 48 hours post radiation the mean fluorescence intensity channel shifted to the right and meaningful levels of FITC positive cells were quantified. This suggests that further time course studies should be conducted as some cells exhibit late radiation-induced apoptosis, reaching a maximum from 72 –96 hours (Yanagihara *et al.,* 1995).

Cell cycle analysis confirmed that CHO-K1 cells responded as expected to radiation exposure. These cells are p53-mutated and showed a build up in G_2 by 36 hours post irradiation. However by 48 hours post irradiation the cells appeared to recover returning to a near normal distribution throughout the cell cycle. The use of the TUNEL assay is beneficial when the time scale for apoptosis is protracted and information regarding the cell cycle is needed before the onset of apoptosis.

Biochemical methods are able to measure numerous features of the population studied but morphological examination of cells is recommended, as this allows visualisation of the characteristic fragmented nuclei and cell shrinkage, confirming apoptosis. In this study the morphological evaluation of apoptosis proved most valuable in defining apoptosis in CHO-K1 cells as well as reflecting radiosensitivity and displayed the ability to differentiate between the two radiation modalities.

Mutations of p53 are found in 50-60% of primary tumours. The observation of giant cell formation appears to be a feature of genomic instability in p53 mutant cells and is facilitated by radiation exposure (Olive and Durand, 1996). Polyploid giant cells arise by endo-reduplication after irradiation (10Gy) and instead of dying remain viable and begin to reconstruct, giving rise to secondary cells which continue the mitotic propagation. This process appears to provide a mechanism for double-strand DNA repair within the cells (Erenpreisa *et al.* 2000; Illidge *et al.* 2000). This provides an interesting alternative and may elucidate the path used by p53 mutant cells, including tumour cells, to survive high doses of radiation.

4.5 References

Akudugu, J.M. and Bohm L. 2001. Micronuclei and apoptosis in glioma and neuroblastoma cell lines and role of other lesions in the reconstruction of cellular radiosensitivity. **Radiat Environ. Biophys.** 40(4), 295-300

Allen, R.T., Hunter, W.J., Agrawal, D.K. 1997. Morphological and Biochemical Characterization and Analysis of Apoptosis. **J. Pharm. and Toxicol. Meth.** 37, 215-228

Al-Rubeai, M. and Singh, R.P. (1998) Apoptosis in cell culture. **Cur. Opin. Biotech.** 9, 152-156

Ashe, P.C. and Berry, M.D. 2003. Apoptotic signalling cascades. **Prog. in Neuro-Psychopharm. Biol. Psych.** 27, 199-214

Bernstein, C., Berstein, H., Payne, C.M., Garewal, H. 2002. DNA repair/pro-apoptotic dual-role proteins in five-major DNA repair pathways: fail-safe protection against carcinogenesis. **Mut. Res.** 511, 154-178

Blatt, N.B. and Glick, G.D. 2001. Review. Signalling Pathways and Effector Mechanisms Pre-Programmed Cell Death. **Bioorganic & Medicinal Chemistry.** 9, 1371-1384

Böhm, I., Schild, H. 2003. Review. Apoptosis: The Complex Scenario for a Silent Cell Death. **Mol. Imag. and Biol.** 5 (1), 2-14

Brauer, M. 2003. In Vivo monitoring of apoptosis. **Progress in Neuro-Psychopharm. Biol. Psychiatry.** 27, 323-331

Cohen-Jonathan,E., Bernhard,E.J. and McKenna,W.G. 1999. How dose radiation kill cells? **Curr. Opin. Cell Biol.** 3, 77-83

Crompton, N.E., Shi, Y., Emery, G.C., Wisser, L., Blattmann, H., Maier, A., Li, L., Schindler, D., Ozsahin, H. and Ozsahin, M. 2001.Sources of variation in patient response to radiation treatment. **Int. J. Radiat. Oncol. Biol. Phys.** 49(2), 547-54

Datta, R., Kojima, H., Banach, D., Bump, N.J., Talanian, R.V., Alnemri, E.S., Weichselbaum, R.R., Wong, W.W. and Kufe, D.W. 1997. Activation of a CrmA-insensitive, p35-sensitive pathway in ionising radiation-induced apoptosis. **Amer.Soc. Biochem.Molec.Biol.** 272 (3), 1965-1969

Erenpreisa, J.A., Cragg, M.S., Fringes, B., Sharakhov, I. and Illidge,T.M. 2000. Release of mitotic descendants by giant cells from irradiated Burkitt's lymphoma cell lines. **Cell Biol. Intenat.** 24(9), 635-648

Harms-Ringdahl, M., Nicotera, P. and Radford, I.R. 1996. Radiation induced apoptosis. **Mut. Res.** 366, 171-179

Hu, T., Miller, C.M., Ridder, G.M. and Aardema,M.J. 1999. Characterization of p53 in Chinese hamster cell lines CHO-K1, CHO-WBL and CHL: implications for genotoxicity testing. **Mut. Res.** 426, 51-62

Illidge, T.M., Cragg, M.S., Fringes, B., Olive, P. and Erenpreisa, J.A. (2000) Polyploid Giant Cells provide a survival mechanism for p53 mutant cells after DNA damage. **Cell Biol. Internat.** 24(9), 621-633

Keechle, F.L. and Zhang, X. 2002. Review. Apoptosis: Biochemical aspects and clinical implications. **Clinica Chimica Acta.** 326, 27-45

Kerr, J.F.R., Wyllie, A.H. and Currie, A.R. 1972. Apoptosis: A Basic biological Phenomenon with wide ranging implications in tissue kinetics. **Br.J.Cancer,** 26, 239-257

Kumar, V., Abbas, A.K. and Fausto, N. (2005). **Pathologic Basis of Disease,** 7th Edition, Philadelphia, Elsevier Saunders.

Lecoeur, H. 2002. Nuclear apoptosis detection by flow cytometry: influence of endogenous endonucleases. **Exp. Cell Res.** 277(1), 1-14

Lukovic, D., Komoriya, A., Packard, B.Z. and Ucker,D.S. 2003. Caspase activity is not sufficient to execute cell death. **Experi. Cell Res.** 289, 384-395

Lyng, F.M., O'Reily,S., Cottell, D.C., Seymour, C.B. and Mothersill, C. 1996. Persistent expression of morphological abnormalities in the distant progeny of irradiated cells. **Rad. Environ. Biophys.** 35, 273-283

Mirkovic N., Meyn R.E., Hunter N.R.and Milas L. 1994. Radiation-induced *apoptosis in a murine lymphoma in vivo*. **Radiother. Oncol.** 33 (1), 11-16

Mustonen, R., Bouvier, G., Wolber, G., Stohr, M., Peschke, P. and Bartsch, H. 1999. A comparison of gamma and neutron irradiation on Raji cells: effects on DNA damage, repair, cell cycle distribution and lethality. **Mutat. Res.** 429(2), 169-79.

Nakano, T., Oka, K., Arai, T., Morita, S. and Tsunemoto, H. 1989. Prognostic

significance of Langerhans' cell infiltration in radiation therapy for squamous cell carcinoma of the uterine cervix. **Arch. Path. Lab. Med.** 113, 507-511

Ng, W-K. 2003. Mini-symposium: Iatrogenic Pathology. Radiation-associated changes in tissues and tumours. **Curr. Diag.Path.** 9, 124-136

Nicholson, D.W., Ali, A., Thornberry, N.A,, Vaillancourt, J.P., Ding, C.K., Gallant, M., Gareau, Y., Griffin, P.R., Labelle, M. and Lazebnik, Y.A. 1995. Identification and inhibition of the ICE/CED-3 protease necessary for mammalian apoptosis. **Nature.** 376 (6535), 37-43.

Olive, P.L., Banath, J.P. and Durand, R.E. 1996. Development of apoptosis and polyploidy in human lymphoblast cells as a function of position in the cell cycle at the time of irradiation. **Radiat. Res.**146, 595-602

Olive, P.L. and Durand, R.E. 1997. Apoptosis: an indicator of radiosensitivity *in vitro*. **Int.J. Rad. Biol.** 71, 695-707

Ormerod, M.G. 2001. Review. Using flow cytometry to follow the apoptotic cascade. **Redox Report,** 6(5), 275-287

Ormerod,M.G. 2002. Investigating the relationship between the cell cycle and apoptosis using flow cytometry. **J. Immun. Meth.** 265, 73-80

Rossouw, M.S. 2004. Validation of Endpoints as biomarkers of low-dose radiation damage. **Thesis Mtech. Degree.** 81-120

Sgonc, R. and Gruber.J. 1998. Mini-Review. Apoptosis Detection: An Overview. **Exp. Gerontol.** 33(6), 525-533

Sheridan, M.T. and West, C.M. 2001. Ability to undergo apoptosis does not correlate with the intrinsic radiosensitivity (SF2) of human cervix tumor cell lines. **Int. J. Radiat. Oncol. Biol. Phys.** 50(2) ,503-9.

Shi, Y-Q., Wuergler, F.E., Blattmann, H., Crompton, N.E.A. 2001. Distinct apoptotic phenotypes induced by radiation and ceramide in both p53-wild-type and p53-mutated lymphoblastoid cells. **Radiat. Environ. Biophys.** 40, 301-308

Shinomiya, N. 2001. Invited Review. New concepts in radiation-induced apoptosis: 'premitotic apoptosis' and 'postmitotic apoptosis'. **J.Cell.Mol.Med.** 5(3), 240-253

Shinomiya, N., Kuno, Y., Yamamoto,F., Fukasawa,M., Okumura,A. Uefuji,M. and Rokutanda,M. 2000. Different mechanisms between premitotic apoptosis and postmitotic apoptosis in X-irradiated U937 cells. **Int. J. Radiat. Oncol. Biol. Phys.** 47(3), 767-777.

Singh, R., Al-Rubeai, M., Gregory, C. and Emery, A. 1994. A cell death in bioreactors – a role of apoptosis. **Biotechnol. Bioeng.** 44, 720-726

Somosy Z. 2000. Radiation response of cell organelles. **Micron.** 31(2), 165-81.

Suzuki, F., Akimoto, Y., Sasai, K. and Yajima, H. 2003. Cellular radiosensitivity and cell-type-specific activation of apoptosis signaling pathways. **Internat. Cong. Series.** 1258, 233-237

Testard. I., Dutrillaux, B. and Sabatier, L. 1997. Chromosomal aberrations induced in human lymphocytes by high-LET irradiation. **Int. J. Radiat. Biol.** 72(4), 423-33.

Vermes, I., Haanen, C. and Reutelingsperger, C. 2000. Flow cytometry of apoptotic cell death. **J. Immun. Meth.** 243, 167-190

Vinatier, D. and Subtil, D.D. 1996. Review article. Apoptosis: A programmed cell death involved in ovarian and uterine physiology. **Eur. J. Obst. Gyn. Repro. Biol.** 67, 85-102

Walker, N.P., Talanian, R.V., Brady, K.D., Dang, L.C., Bump, N.J., Ferenz, C.R., Franklin, S., Ghayur, T., Hackett, M.C., Hammill, L.D. 1994. Crystal structure of the cysteine protease interleucin-1β-converting enzyme: a (p20/p10)2 homodimer. **Cell.** 78, 343-352

Warrington,R.C., Norum,J.N., Hilchey,J.L., Watt,C., Fang,W.D. 2003. A simple, informative and quantitative flow cytometric method for assessing apoptosis in cultured cells, **Progress Neuro-Psychopharm. Biol. Psychiatry.** 27, 231-243

Weil, M.M., Amos, C.I., Mason, K. A. and Stephens, L.C. 1996. Genetic basis of strain variation in levels of radiation-induced apoptosis of thymocytes. **Radiat. Res.** 146(6), 646-651

Wyllie, A.H. 1980. Glucocorticoid-induced thymocyte apoptosis is associated with endogenous endonuclease. **Nature.** 284, 555-556

Yanagihara, K., Nii, M., Numoto, M., Kamiya, K., Tauchi, H., Sawada, S. and Seito T. 1995. Radiation-induced apoptotic cell death in human gastric epithelial tumour cells; correlation between mitotic death and apoptosis. **Int J Radiat Biol.** 67(6), 677-85.

Zhivotovsky, B., Joseph, B. and Orrenius, S. 1999. Minireview. Tumor Radiosensitivity and Apoptosis. **Exp. Cell. Res.** 248, 10-17

Chapter 5

Conclusion

and

Directions for Future Studies

To raise new questions, new possibilities, to regard old problems from a new angle requires creative imagination and marks real advances in science.

Albert Einstein

As is well known cells from tumors of the same origin and pathology can show a wide variation in response to radiation treatment (Bergqvist *et al.*, 1998; West *et al.*, 1995; Dickson *et al.*, 2002; Baumann *et al.*, 2003). Knowledge of the intrinsic radiosensitivity of a tumor could help produce and optimise radiotherapy protocols for individual patients. The focus of this study was to validate a variety of predictive assays in an effort to determine inherent radiosensitivity.

The clonogenic or colony-forming assay is a well-established method of determining the ability of a cell to retain reproductive integrity thereby establishing its sensitivity to radiation. If a cell were unable to reproduce this would translate into efficient tumour curability. In this study it was concluded that the sensitivity of CHO-K1 cells to ionising radiation could be estimated using both clonogenic survival and micronuclei formations. Both endpoints

yielded measurable data over a useful dose range and cellular damage was quantified with reasonable precision. A future assessment could be done by exposing cell lines varying in radiosensitivity to neutron and proton radiation, using these endpoints.

Cells taken from fresh specimens are often not clonogenic.In this study CHO-K1 cells were subjected to different qualities of radiation and DNA damaged was measured by single-cell gel electrophoresis. Different levels of cellular damage were reflected by the comet assay in a dose response manner expected form neutron and gamma radiation. The use of an assay in which cells do not need to be clonogenic as well as one that measures the cells response at the individual level provides an advantageous prospect. Future studies could concentrate on exposing cells of known radioresistance and sensitivity to the assay. Another future direction would be to use cells obtained from fine needle aspirates. This is can easily be achieved before the patient has undergone radiotherapy and after to assess radiation induced-damage *in-vivo*. The potential for introduction into the clinical setting where patient response to radiotherapy can be predicted remains an attractive option.

Apoptosis was evaluated in this study by assessing radiation-induced caspase activity, DNA fragmentation and cellular morphology. Caspase activity was measured using a fluorometer and cellular radiation sensitivity was poorly represented by an ineffectual response showing little

differentiation between damage induced by neutron and gamma radiation. Fluctuations in readings also led to high inter-experimental variation resulting in poor reproducibility. This technique showed an insensitivity to increase in dose, making it unsuitable for cellular radiosensitivity testing.

As biological systems differ in response to radiation it would be advantageous to evaluate additional time intervals to determine optimal caspase 3/7 activity in CHO-K1 cells.

DNA fragmentation as a result of radiation was assessed flow cytometrically using the TUNEL assay. A dose response was evident showing meaningful values at 48 hours post 4 and 8 Gy gamma and neutron irradiation. This study in part was to establish a dose best suited for radiosensitivity testing and doses of 8 Gy (neutron or gamma) are extremely large given as a single dose. This endpoint displays an insensitive response and limits the application as a biomarker as the large dose required effectively diminishes the quality of the damage. From this is would be valuable to conduct further time course studies as well as the use of a FLuorescent Inhibitor of CAspases (FLICA) as proposed by Smolewski *et al.* (2002). This technique proposes to estimate the cumulative apoptotic index (CAI) labelling the cell with FLICA and arresting the process of apoptosis, which would normally culminate in the disintegration of the cell. The CAI is then measured at predetermined time points by flow cytometry.

Apoptosis evaluation was concluded by morphological examination of CHO-K1 cells exposed to equivalent doses of gamma and neutron radiation. These results proved most valuable in defining apoptosis as well as reflecting

radiosensitivity and displayed the ability to differentiate between the two radiation modalities.

Treatments that induce apoptosis are cell cycle specific and will disrupt the cell cycle as reflected in this study by CHO-K1 cells displaying a build up in the G_2 phase after radiation exposure. An investigation into the relationship between radiation-induced apoptosis and the cell cycle would be most useful. Further the information revealed by the DNA histogram is static in that the percentage of cells in S phase can only be estimated (Ormerod, 2002). The use of BrdUTP can improve this measurement by incorporation into the apoptotic cells and followed by the addition of anti-BrdUrd-FITC can be evaluated by flow cytometry. On analysis, the cell cycle phase from which the apoptotic population was initiated would be revealed including an accurate measurement of the number of cells in the S-phase. Clinically this would be most helpful as the number of cells in S-phase is used as an indication of the nature of a tumour and potentially used for treatment planning.

The observation of viable giant cells after high doses of radiation was confirmed in the literature as a process by which p53 mutated cells may survive high doses of radiation. It would be most valuable if ploidy studies could be conducted on these cells as well as careful enumeration to establish a possible relation between giant cell formation and increasing dose.